ADAMA SCIENCE AND TECHNOLOGY UNIVERSITY

School of Mechanical Chemical and Materials Engineering

Designing Camshaft of Mechanical Continuously Variable Valve Timing (CVVT) Mechanism

A Thesis Submitted in Partial Fulfillment of the Requirements for the award of the Degree of Master of Science in Automotive Engineering

By

Semere Maschalu

Thesis Advisor

Ramesh Babu (Associate Professor)

September 2017

ADAMA, ETHIOPIA

CANDIDATE'S DECLARATION

I hereby declare that the work which is being presented in the thesis entitled "Designing Camshaft of Mechanical Continuously Variable Valve Timing (CVVT) Mechanism" in partial fulfillment of the requirements for the award of the degree of Master of Science in Automotive Engineering is an authentic record of my own work carried out from February 2017 to September 2017 under the supervision of N. RAMESH BABU Department of Mechanical and Vehicle Engineering, Adama Science and Technology University, Ethiopia.

The matter embodied in this thesis has not been submitted by me for the award of any other degree or diploma. All relevant resources of information used in this thesis have been duly acknowledged.

Name	Signature	Date
Semere Maschalu		2017-09-20-GC
Student		

This is to certify that the above statement made by the candidate is correct to the best of my knowledge and belief. This thesis has been submitted for examination with my approval.

Name	Signature	Date
N. Ramesh Babu		20/09/2017
Advisor		

School of Mechanical, Chemical and Materials Engineering
Mechanical Systems and Vehicle Engineering Program

ADAMA SCIENCE AND TECHNOLOGY UNIVERSITY

SCHOOL OF MECHANICAL, CHEMICAL AND MATERIALS ENGINEERING

Designing Camshaft of Mechanical Continuously Variable Valve Timing (CVVT) Mechanism

By

Semere Maschalu

Approved by Board of Examiners

Cherinet Girma	
Chairman, Department Graduate committee	Signature
Dr. Addisu Bekele	11/10/2017
Internal Examiner	Signature
Dr. Antenh M.T.	
External Examiner	Signature
N. Ramesh Babu	
Advisor	Signature

Mechanical Systems and Vehicle Engineering Program
School of Mechanical, Chemical and Materials Engineering

Table of Contents

AKNOWLEDGMENT

First, I would like to thank my advisor Ramesh Babu (Associate Professor) for his guidance, attention and constructive criticism. I would also like to thank my parents and my brother for their support and appreciation throughout the completion of this paper. Finally, I want to thank my friends for their idea sharing and emotional support. Glory to the creator of all!

LIST OF TABLES

LIST OF FIGURES

ABBREVIATIONS

VVT – Variable Valve Timing

VVA – Variable Valve Actuation

VTEC – Valve Timing Electronic Control

VTL – Variable Timing Lifter

LIVC – Late Intake Valve Closing

EVA – Electromagnetic Valve Actuator

CVVT – Continuous Variable Valve Timing

ICE – Internal Combustion Engine

EAP – Engine Analyzer Pro

CAD – Computer Aided Design

VE – Volumetric Efficiency

P_b– Brake Power

T_b – Brake Torque

BSFC/bsfc – Brake Specific Fuel Consumption

EVO/evo – Exhaust Valve Opening

EVC/evc – Exhaust Valve Closing

IVO/ivo – Intake Valve Opening

IVC/ivc – Intake Valve Closing

EVL/evl – Exhaust Valve Lift

IVL/ivl – Inlet Valve Lift

BDC/bdc – Bottom Dead Center

TDC/tdc – Top Dead Center

btdc – before top dead center

atdc – after top dead center

bbdc – before bottom dead center

abdc – after bottom dead center

EGR – Exhaust Gas Recirculation

ECU – Engine Control Unit

DOHC – Double Overhead Cam

F_{ce} – Fuel consumption of existing camshaft

F_{cn} – Fuel consumption of new camshaft

F_s– Fuel saved

R_a – Aerodynamic resistance

R_{rl}– Rolling resistance

CL – Carbon content of fossil fuels

OF – Oxidation factor for fossil fuels

IC1 – Intake Cam Profile 1

IC2 – Intake Cam Profile 2

IC3 – Intake Cam Profile 3

EC1 – Exhaust Cam Profile 1

EC2 – Exhaust Cam Profile 2

EC3 – Exhaust Cam Profile 3

ABSTRACT

In recent years, Co_2 emission from conventional fuel powered vehicles has become the major contributor to the overall global warming effect around the planet. Also, fuel prices have risen considerably due to several factors one of which is attributed to political instability in major fuel producing nations. As a result, vehicle manufacturers have made several attempts to reduce the fuel consumption of their engines which have proven very effective. One of the measures taken by manufacturers is the development of variable valve timing (VVT) systems. However the various VVT systems have their own shortcomings for the ideal engine operation which are briefly explained in this document. In this study, analysis, optimization and modification on mechanical continuously variable valve timing (CVVT) camshaft which has axially varying cam profile is made, with the aim of providing empirical relations for designers and students interested in the system for maximum fuel economy and performance for IC engines at any specific speed while minimizing Co_2 emission per kw.hr. The analysis is performed using a computer simulation program known as Engine Analyzer Pro V3.9**.** The study is focused only towards fuel efficiency and performance while other emission analysis such as CO, HC and No_x are not considered due to incapability of software at hand. While conducting the study, simulations were run at different engine speeds by tuning the valve opening and closing angles, and lift to get values for optimum operation. The tests were conducted on a range of speeds from idle to maximum speed with intervals of constant step and all the optimum values were recorded. Optimum values are selected based on better performance. Then, the performance of the optimum valve timing parameters has been compared with the performance of the original camshaft. The results have shown a maximum volumetric efficiency improvement of 19% and maximum percent improvement for brake torque is seen to be 30.82% while percent improvements for brake power are exactly the same as brake torque with negligible differences at some engine speeds. Also a maximum improvement of 8.5% is seen for BSFC. As for yearly fuel saving and Co_2 emission reduction per vehicle, a maximum fuel saving of 96.47kg/yr is achieved at 5500 rpm, and a maximum Co_2 emission reduction of 85.9kg/yr at a similar engine speed of 5500 rpm. However, higher percentages of fuel savings and Co_2 emission reductions are seen in the range between 2000 rpm and 6000 rpm.Afterwards, based on the finally obtained cam profiles, the camshaft has been modeled in a CAD program and a suitable operating mechanism has been proposed. Finally, empirical relations for important dimensions have been formulated. Finally a prototype of the cylinder head has been made from wood, cement and plastics.

Keywords: Variable valve timing, Engine performance, Three dimensional cam, CVVT actuation system

Chapter One

INTRODUCTION

1.1. Background

Resources of fossil fuels are finite and if they are to be used to provide energy for transport they must be used efficiently. There are also strong pressures to make automotive vehicles less environmentally polluting and one of the most important factors in reducing global warming is the increased use of vehicles with better fuel economy [1].

As early as a few decades ago, people recognized that despite the simple design and low cost of conventional crankshaft synchronized cam driven valve actuation, it can offer optimized engine performance at only one point on the engine torque speed operating map mainly due to the fixed valve timing with respect to the crank shaft angle under different operating conditions. On the other hand, research has shown that variable valve timing (VVT) can achieve higher fuel efficiency, lower emissions, larger torque output, and other possible benefits [2].

In conventional IC engines, the valves are actuated by cams that are located on a belt- or chain-driven camshaft. As a long developed valve drive, the system has a simple structure, low cost, and offers smooth valve motion. However, the valve timing of the traditional valve train is fixed with respect to the crankshaft angle because the position profile of the valve is determined purely by the shape of the cam. If instead the valve timing can be decoupled from the crankshaft angle and can be adjusted adaptively for different situations, then the engine performance can be optimized with respect to higher torque/power output, increased gas mileage, and reduced emissions, at any point of the engine map. This flexibly controlled valve timing is called variable valve timing (VVT) and the corresponding valve drive system is called variable valve actuation (VVA).

From the research of engine scientists, the main benefits from VVT can be summarized in specific numbers: a fuel economy improvement of approximately5~20%, a torque improvement of 5~13%, an emission reduction of 5 ~10% in HC, and 40~60% in NOx[2].

As discussed earlier the performance of an IC engine can be greatly improved via application of VVT over conventional valve actuation system. However, even with different VVT systems, optimum engine performance is difficult to achieve due to lack of simultaneous control of opening and closing angles, opening duration and lift of valves.

For instance, in cam changing systems, two cam profiles with different opening/closing angles, duration and lift are used for low and high speed operating ranges. In this case, only one specific speed for each ranges are optimally operated while the rest of the speed ranges are operated under close approximation.

And also for cam phasing systems the opening or closing angles can be controlled by rotating the camshaft forward or backward relative to its driving sprocket, but the duration of opening and lift are fixed.

There is however one promising and relatively new VVT system which is found on some Ferrari engines. This system uses only one cam for each inlet and exhaust valves. The profile of the cam varies axially, and the camshaft is moved axially to change the profile the follower moves along with as shown in figure 1.1.

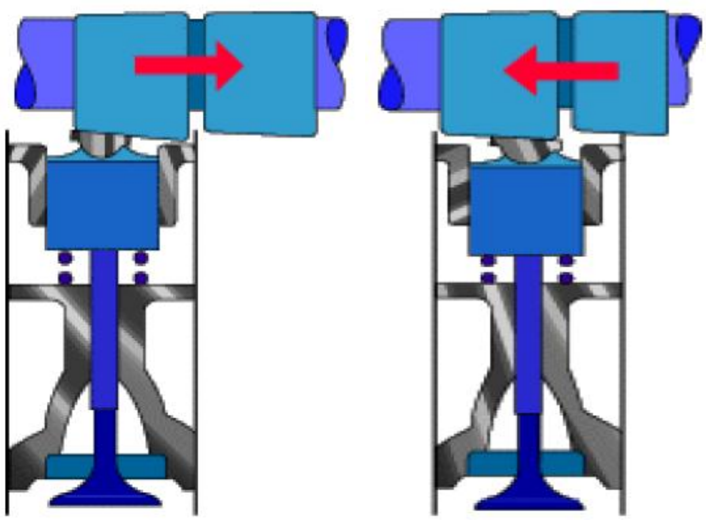

Figure 1.1 The variable cam system used on some Ferraris [3]

1.2. Statement of the problem

The CVVT shown in figure 1.1 above has the potential to be an effective valve actuation system since each operating speed can be assigned with its own valve lift profile suitable for maximum performance. However, the system does not control the opening and closing angles, andit controls only the lift of valves.

This study makes a slight modification to the cam lobe by giving it a twisted sense, and make it able to control lift, opening and closing angles independently according to engine rpm.

1.3. Objectives

1.3.1. General Objective

The objective of this study is to design a continuously variable valve timing system that gives better performance on all engine speeds, and formulate empirical relations for designing the continuously variable valve timing camshafts, which will improve fuel economy, performance and Co_2 emissions of conventional fuel powered reciprocating IC engines.

1.3.2. Specific Objectives

The specific objectives of the proposed project are as follows:

- To select one specific engine model for the study and test the performance of different cam profiles at various speeds at some steps using a computer simulation program (Engine Analyzer Pro V3.9).
- To summarize test results of power, torque, bsfc, volumetric efficiency and other relevant parameters obtained as output from software and to select optimum cam profiles for each of the test speeds and by assuming a linear relationship to fill in the ranges in between test speeds.
- To compare the performance of the new camshaft with the existing one with respect to power, torque, bsfc, volumetric efficiency, fuel consumption and Co2 emission at different engine speeds.
- Formulate empirical relations for all CVVT camshaft terminologies selected to completely describe the cam geometry based on optimum performance and model the camshaft using a CAD program.
- Suggest and design a mechanism to apply the designed camshaft to an IC engine.

1.4. Significance of the project

The significance of the proposed study is as follows:

- Introduce an idea for reduction of Co_2 emission by reducing fuel consumption, which helps to ease the impact of global warming.
- Provide a design reference on CVVT camshaft for students and designers.
- Introduce a computer aided study technique for the effect of cam/valve profiles on engine performance.
- Produce engines with better fuel economy, power, torque and overall performance over any range of speed.

1.5. Delimitation (scope)

This study is focusedon the estimation of improvements on engine performance parameters including fuel consumption and Co_2 emission that can be achieved,and designing a CVVT camshaft that yields the desired output to provide a design reference.

1.6. Limitations

The simulation program used in this study does not have an emission analysis tool, and it is not possible to fairly estimate all emissions using analytical method except for Co_2 emission. Another limitation faced in this study is the different valve timing characteristics of various engine assemblies such as, carbureted or injector; naturally aspirated or turbo/supercharged; gasoline or diesel and so on. Hence, this study is limitedto a naturally aspirated and carbureted gasoline engine.

Chapter Two

LITERATURE REVIEW

2.1. Impact of valve events on engine performance

2.1.1. Effects of Changes to Exhaust Valve Opening Timing - EVO

As the exhaust valve opens the pressure inside the cylinder resulting from combustion is allowed to escape into the exhaust system. In order to extract the maximum amount of work (hence efficiency) from the expansion of the gas in the cylinder, it would be desirable not to open the exhaust valve before the piston reaches Bottom Dead Centre (BDC). Unfortunately, it is also desirable for the pressure in the cylinder to drop to the lowest possible value, i.e. exhaust back pressure, before the piston starts to rise. This minimizes the work done by the piston in expelling the products of combustion (often referred to as blow down pumping work) prior to the intake of a fresh charge. These are two conflicting requirements, the first requiring EVO to be after BDC, the second requiring EVO to be before BDC [4].

The choice of EVO timing is therefore a trade-off between the work lost by allowing the combusted gas to escape before it is fully expanded, and the work required to raise the piston whilst the cylinder pressure is still above the exhaust back-pressure. With a conventional valve train, the valve lifts from its seat relatively slowly and provides a significant flow restriction for some time after it begins to lift and so valve lift tends to start some time before BDC. A typical EVO timing is in the region of 50-60° before BDC for a production engine.

The ideal timing of EVO to optimize these effects changes with engine speed and load as does the pressure of the gasses inside the cylinder. At part load conditions, it is generally beneficial if EVO moves closer to BDC as the cylinder pressure is much closer to the exhaust back pressure and takes less time to escape through the valve. Conversely, full load operation tends to result in an earlier EVO requirement because of the time taken for the cylinder pressure to drop to the exhaust back-pressure.

2.1.2. Effects of Changes to Exhaust Valve Closing Timing - EVC

The timing of EVC has a very significant effect on how much of the Exhaust gas is left in the cylinder at the start of the engine's intake stroke. EVC is also one of the parameters defining the valve overlap, which can also have a considerable effect on the contents of the cylinder at the start of the intake stroke.

For full load operation, it is desirable for the minimum possible quantity of exhaust gas to be retained in the cylinder as this allows the maximum volume of fresh air & fuel to enter during the Intake stroke. This requires EVC to be at, or shortly after TDC. In engines where the exhaust system is fairly active (i.e. Pressure waves are generated by exhaust gas flow from the different cylinders), the timing of EVC influences whether pressure waves in the exhaust are acting to draw gas out of the cylinder or push gas back into the cylinder. The timing of any pressure waves changes with engine speed and so a fixed EVC timing tends to be optimized for one speed and can be a liability at others [4].

For part load operation, it may be beneficial to retain some of the exhaust gasses, as this will tend to reduce the ability for the cylinder to intake fresh air & fuel. Retained exhaust gas thus reduces the need for the throttle plate to restrict the intake and results in lower pumping losses (see Appendix A) in the intake stroke. Moving EVC Timing further after TDC increases the level of internal EGR (Exhaust Gas Recirculation) with a corresponding reduction in exhaust emissions.

There is a limit to how much EGR the cylinder can tolerate before combustion becomes unstable and this limit tends to become lower as engine load and hence charge density reduces. The rate of combustion becomes increasingly slow as the EGR level increases, up to the point where the process is no longer stable. Whilst the ratio of fuel to oxygen may remain constant, EGR reduces the proportion of the cylinder contents as a whole that is made up of these two constituents. It is this reduction in the ratio of combustible to inert cylinder contents which causes combustion instability.

Typical EVC timings are in the range of 5-15° after TDC. This timing largely eliminates internal EGR so as not to detrimentally affect full load performance.

2.1.3. Effect of changes to Intake Valve Opening Timing – IVO

The opening of the intake valve allows air/fuel mixture to enter the cylinder from the intake manifold. (In the case of direct injection engines, only air enters the cylinder through the intake valve). The timing of IVO is the second parameter that defines the valve overlap and this is normally the dominant factor when considering which timing is appropriate for a given engine.

Opening the intake valve before TDC can result in exhaust gasses flowing into the intake manifold instead of leaving the cylinder through the exhaust valve. The resulting EGR will be detrimental to full load performance as it takes up space that could otherwise be taken by fresh charge. EGR may be beneficial at part load conditions in terms of efficiency and emissions as discussed above [4].

Later intake valve opening can restrict the entry of air/fuel from the manifold and cause in-cylinder pressure to drop as the piston starts to descend after TDC. This can result in EGR if the exhaust valve is still open as gasses may be drawn back into the cylinder with the same implications discussed above. If the exhaust valve is closed, the delay of IVO tends not to be particularly significant, as it does not directly influence the amount of fresh charge trapped in the cylinder.

Typical IVO timing is around 0-10° before TDC which results in the valve overlap being fairly symmetrical around TDC. This timing is generally set by full load optimization and, as such, is intended to avoid internal EGR.

2.1.4. Effect of changes to Intake Valve Closing Timing – IVC

The volumetric efficiency of any engine is heavily dependent on the timing of IVC at any given speed. The amount of fresh charge trapped in the cylinder is largely dictated by IVC and this will significantly affect engine performance and economy.

For maximum torque, the intake valve should close at the point where the greatest mass of fresh air/fuel mixture can be trapped in the cylinder. Pressure waves in the intake system normally result in airflow into the cylinder after BDC and consequently, the optimum IVC timing changes considerably with engine speed. As engine speed increases, the optimum IVC timing moves further after BDC to gain maximum benefit from the intake pressure waves.

Closing the intake valve either before or after the optimum timing for maximum torque results in a lower mass of air being trapped in the cylinder. Early intake closing reduces the mass of air able to flow into the cylinder whereas late intake closing allows air inside the cylinder to flow back into the intake manifold. In both cases, the part load efficiency can be improved due to a reduction in intake pumping losses.

A typical timing for IVC is in the range of 50-60° after BDC and results from a compromise between high and low speed requirements. At low engine speeds, there will tend to be some flow back into the intake manifold just prior to IVC whereas at higher speeds, there may still be a positive airflow into the cylinder as the intake valve closes.

2.1.5. Effects of Valve Overlap

As discussed previously, valve overlap is the time when both intake and exhaust valves are open. In simple terms, this provides an opportunity for the exhaust gas flow and intake flow to influence each other. Overlap can only be meaningfully assessed in conjunction with the pressure waves present in the intake and exhaust systems at any particular engine speed and load.

In an ideal situation, the valve overlap should allow the departing exhaust gas to draw the fresh intake charge into the cylinder without any of the intake gas passing straight into the exhaust system. This allows the exhaust gas in the combustion chamber at TDC to be replaced and therefore the amount of intake charge to exceed that which could be drawn into the cylinder by the swept volume of the piston alone.

A given amount of overlap unfortunately tends to be ideal for only a portion of engine speed and load conditions. Generally, the torque at higher engine speeds and loads can benefit from increased overlap due to pressure waves in the exhaust manifold aiding the intake of fresh charge. Large amounts of overlap tend to result in poor emissions at lower speeds as fuel from the intake charge can flow directly into the exhaust. High overlap can also result in EGR which, although beneficial to part load economy, reduces full load torque and can cause poor combustion stability especially under low load conditions such as idle. Poor idle quality can therefore result from too much overlap [4].

The valve overlap tends to be fairly symmetrical about TDC on most engines. The further away from TDC that valve overlap is present, the more effect the piston motion will have on the airflow. Early overlap may result in exhaust gasses being expelled into the intake manifold and late overlap may result in exhaust gasses being drawn back into the cylinder. Both of these situations result in internal EGR that can be beneficial to part load emissions and efficiency. As discussed earlier, internal EGR tends to be avoided due to the detrimental effect it has on full load torque.

2.1.6. Valve Peak Lift

Valve peak lift directly affects the ability for air to flow into the cylinder and exhaust to leave the cylinder and as a result it significantly influences engine performance. There are some practical limitations of peak lift in most engines that are dependent on the design of the particular engine:

- Normally the piston crown is profiled to maximize the clearance adjacent to the valves but there are limitations as to how much valve lift can be accommodated without unduly compromising the piston design.
- The duration of the valve lift imposes a restriction on valve lift due to the acceleration required to achieve a high lift with a short duration. The higher the running speed of the engine, the more the peak lift is restricted for a given valve lift duration.

Low values of valve peak lift will clearly restrict the ability of gas to flow into and out of the cylinder, effectively throttling the engine. Maximum engine power output will generally benefit from as much valve lift as possible up to the point where air flow becomes restricted by other features such as the manifold system or cylinder head porting.

It does not follow that engines should have the maximum possible valve lift as this can adversely affect low speed performance. Lower intake valve lifts result in higher gas velocity past the valve and this improves fuel mixing and combustion. For maximum torque at a given speed, lift should be kept as low as possible up to the point where the intake of fresh charge becomes restricted.

The chosen value of peak valve lift is therefore a compromise between low speed and high speed full load requirements. A typical value for a production engine is in the range of 8-10mm.

2.2. Variable valve timing

As technology has advanced, so too has the development of engine design and nowadays it is normal for modern vehicles to have multi-valve technology. Variable valve timing is seen as the next step to enhance engine efficiency.

Variable valve timing was first introduced as an innovative design that increased engine torque and output while addressing environmental issues, such as pollutants emitted from automotive engines. The variable valve timing system uses an electronic system, known as the engine control unit (ECU) to electronically control the operation of the engine valves [1].

The system is able to detect the engine speed and adjust the valve timing accordingly. As a consequence, more oxygen can be supplied through the air intake valve as more fuel is injected into the combustion chamber. Greater fuel and oxygen in the combustion chamber leads to increased power and torque.

Most variable valve timing systems are combined with lift control, which varies the lift intake and exhaust valves while the engine is operating at high speed. As the intake and exhaust valve lift increases, a larger volume of air/fuel mixture is introduced, along with ejection of a greater volume of exhaust gas. This results in the engine producing higher output power while operating at high speeds. The variable valve timing system allows the valve timing of an automotive engine to be ideally fixed by increasing the valve lift when the engine speed is high, which results in improved fuel economy [5].

In principle, variable valve timing improves fuel efficiency and performance because it adjusts the valve timing between high and low engine speeds for optimum performance, thus efficiency throughout the entire speed range can be improved.

Many mechanisms have been proposed to produce variable valve timing systems. Each mechanism varies the valve timing either in duration, phase, or both. There are numerous versions of VVT mechanisms in production today, and these VVT systems can be basically classified into seven VVT models, which are reviewed below.

2.2.1. Phase Changing

Cam phasing VVT is the simplest, cheapest and most common mechanism used presently. Basically, it varies the valve timing by shifting the phase angle of camshafts relative to the crankshaft. The phase angle can be shifted either by the use of a phasing actuator, whereby the phase angle is produced by adjusting the hydraulic flows in and out of the actuator chambers or with the camshaft drive being connected to the camshaft through a helical spline.

High performance double overhead cam (DOHC) engines had long valve open duration, high valve lift and produced maximum power output. However, the large valve overlap caused poor idle stability and also reduced engine torque at low speeds [6].

2.2.2. Cam Changing

Cam changing systems are the most efficient VVT systems in production presently, since they allow variability in the duration of valve opening as well as the lift of the valves. They can also switch between completely different cam profiles, unlike other systems which can only basically vary the timing by advancing and retarding a standard set of cams.

In 1989, the valve timing electronic control (VTEC) engine system was introduced, which was able to maintain a high output throughout the entire engine speed range, thus enabling the high speed performance of a racing engine without sacrificing low and medium speed performance [7].

To develop a high performance engine it is necessary to increase the volumetric efficiency and reduce friction. A racing engine requires wider valve overlap and increased valve lift to obtain optimum performance at high engine speed. However in a conventional engine, the valve timing and degree of valve lift is set for optimum performance at low and medium engine speeds [9].

By designing for higher valve lift, wider valve timing larger valve diameter; it was possible to obtain a higher volumetric efficiency to cope with high output engine speeds. With VTEC, the valve timing and lift can be adjusted at low engine rotation to increase torque and prevent air from being forced back through the intake [7].

2.2.3. Intake Valve Closing

Intake valve closing is a practical concept applicable to engines in which the intake can be phased relative to each other to extend the total intake opening period. Problem of pumping losses must be addressed, because as the engine was throttled, pumping losses progressively increased until no useful output was generated at idle speed [8].

Their proposed system consists of an intake camshaft, which causes late closing of the intake valve at all times. At high loads a reed valve situated in the intake manifold prevented the charge from being rejected from the cylinder. At low loads, the reed valve was deactivated to allow the charge to return to the inlet manifold. They asserted that the LIVC system allowed the engine to operate with wider than normal throttle settings at low speed, thus enabling the reduction of pumping losses.

2.2.4. Lost Motion Valves

Lost motion valves are operated directly by conventional cams and the timing variation is produced by varying the length of the pushrod to produce an adjustable lash in the valve mechanism. The rocker fulcrum or the camshaft is moved to vary the valve lash. Since these mechanisms convey output motion during only part of the cam lift, they are called "lostmotion" mechanisms. Lost motion mechanisms are very simple to implement and can be used to attain very ranges of valve opening. Systems can be designed that automatically vary duration with engine speed to provide near-optimum full throttle fuel efficiency and torque [1].

Lost motion mechanism, termed a variable timing lifter (VTL), can vary the timing of engine valve opening and closing, was durable and precise in its control. When applied to a high specific output engine, the mechanism allowed much lower idle speeds and reduced idle fuel consumption without compromising high speed power. The VTL can minimize the effects of fixed valve timing compromise by providing a reduction in valve open duration and valve overlap at low engine speeds to allow a slow and stable idle, which reduced idle fuel consumption. The device however, responds only to engine speed and cannot optimize valve timing for changes in load [10].

2.2.5. Electrically Actuated Valves

Electrically actuated valves are operated directly by electric actuators, usually solenoids. Varying the time of energizing and de-energizing the solenoids produces variation in the timing.

Schechter and Llevin (1996) introduced a camless engine with independent and continuously variable control of valve timing, lift and duration. The engine valve opening and closing was controlled by two solenoid valves that were connected to high and low pressure plenums. Valve opening was controlled by the solenoid valve connected to the high pressure plenum, while valve closing was controlled by the solenoid valve connected to the low pressure plenum [11].

The electromagnetic valve actuator (EVA) system that controls valves electronically, without the need for a camshaft, rocker assembly, and pulley or timing belt was introduced by Douglas in 1997 [10].

The EVA system had one actuator at each valve chamber with two opposing spring coils fitted at each valve chamber providing the necessary force to open and close the valves. The spring forces were supplemented by electromagnetic force from the EVA coils. The intake and exhaust valves were independently computer controlled and timed, making it possible to fine tune air/fuel and exhaust flows to engine needs.

2.2.6. Hydraulically Actuated Valves

Hydraulically actuated valves are operated directly by hydraulic actuators, usually hydraulic cylinders and the fluid is metered through either mechanical or solenoid valves.

The use of a hydraulically controlled variable valve system, which utilized a hydraulic mechanism to open and close the valve was investigated by Desantes in 1988. The system was based on an axial lifting of the intake valve by a hydraulic plunger. The degree of early intake valve closing depended on the engine running conditions, which were controlled by a microprocessor. The microprocessor controlled an electro valve, which discharged the oil stocked under the plunger through the driven valve. The plunger was located at one end of the rocker arm, which pivoted around the cam contact point as fixed center. The variable closing of the intake valve depended on the moment at which the microprocessor ordered the electro valve opening and closure [5].

2.2.7. Valves Actuated by Two Cams in Parallel

In these systems, the valves are operated by two cams in parallel in such a way that the displacement equals the larger effective displacement of either cam. Timing is varied by changing the phase angle between each cam and the crankshaft. The most common implementation of this concept employs a single cam profile, which is actually made up of two separate cams that can be rotationally shifted relative to each other. Two concentric shafts usually drive the two cams. The outer camshaft drives one set of cams while slots in it allow the second set of cams to project through from the inner shaft.

2.2.8. Three-dimensional Cam Mechanism

One of the problems of cam profile switching is that the valve motion is switched only between two specific cam profiles. However, the use of a three-dimensional cam design allows the engine to continuously change the valve timing, lift and duration over a wide range of engine operating conditions. In this mechanism, the cam profile continuously varies along the cam axis, and the axial movement of the camshaft with respect to follower brings a different profile of the cam into engagement with the follower, prompting a change in valve opening profile. A combination of three-dimensional cam mechanism and cam phaser has been also implemented to control both valve timing and valve lift independently [12].

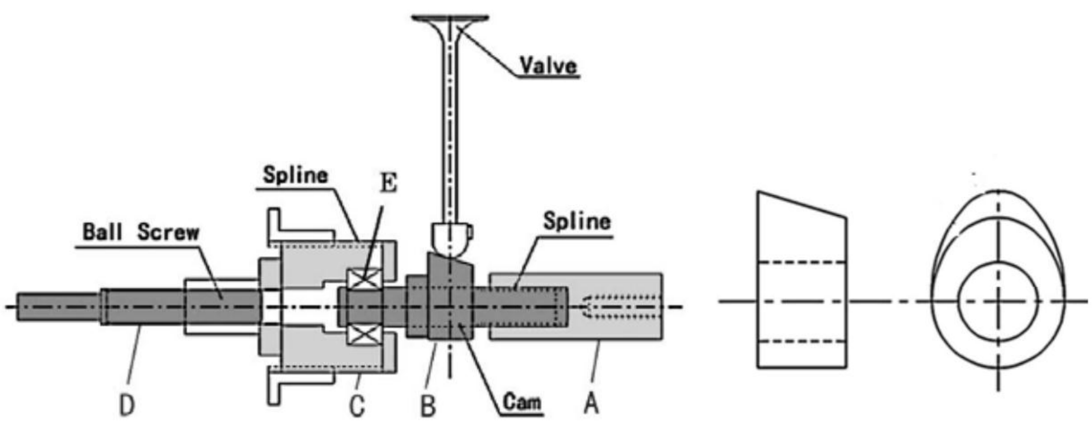

Figure 2.1 Three dimensional cam mechanism

2.3. Common valve timing diagrams

The valve timing of an engine is set to give the best possible performance. This means that the valves must be opened and closed at very precise times. The traditional way of showing exactly when the valve opens and closes is by the use of a valve-timing diagram (Figure 2.2). As can be seen the valves are opened and closed in relation to the number of degrees of movement of the crankshaft. When comparing the diagrams for the petrol engine of medium and high performance cars, it will be noticed that the high performance car has larger valve opening periods, especially the closing of the inlet valve which is later. This is so that at high operating speeds the increased lag allows as much pressure energy as possible to be generated in the cylinder by the incoming air and fuel charge, prior to its further compression by the rising piston. There is also an increase in the value of valve overlap for the high performance engine (Figure 2.3) [13].

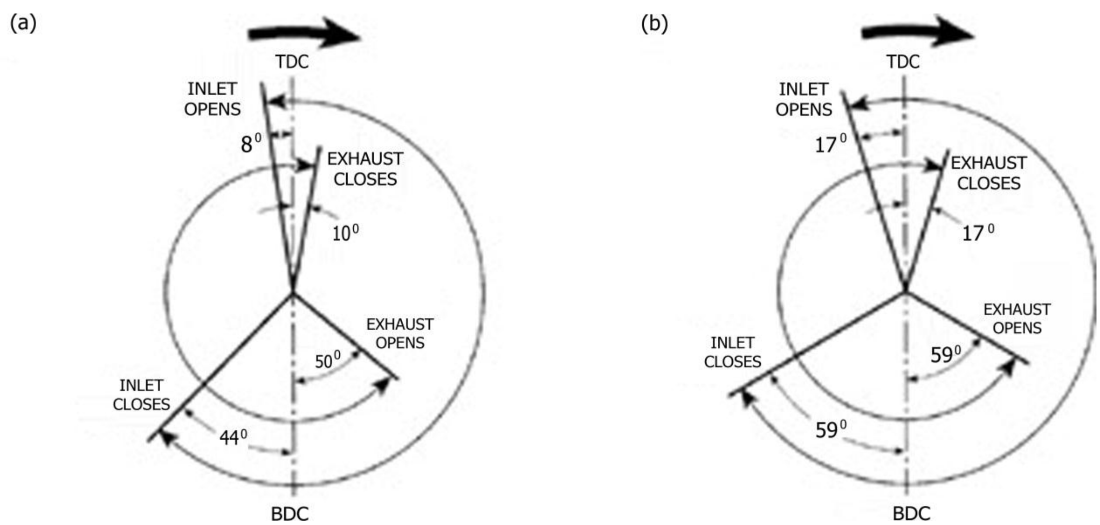

Figure 2.2 Valve-timing diagrams (a) medium-performance engine, (b) high-performance engine

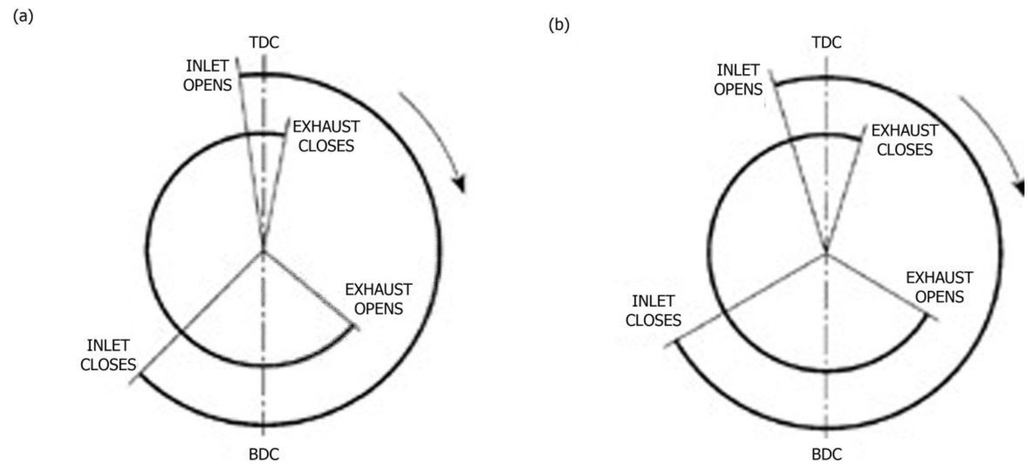

Figure 2.3 Valve-timing diagrams (a) four-cylinder OHV engine, (b) four-cylinder OHC engine

Some manufacturers use slightly different valve timing diagrams for high and low speed engines. For instance the diagram shown in fig below suggests larger intake closing and exhaust opening angles. Valve timing of 4-stroke and 2-stroke engine can be drawn into valve timing diagram as shown in the Figure 2.4 [14].

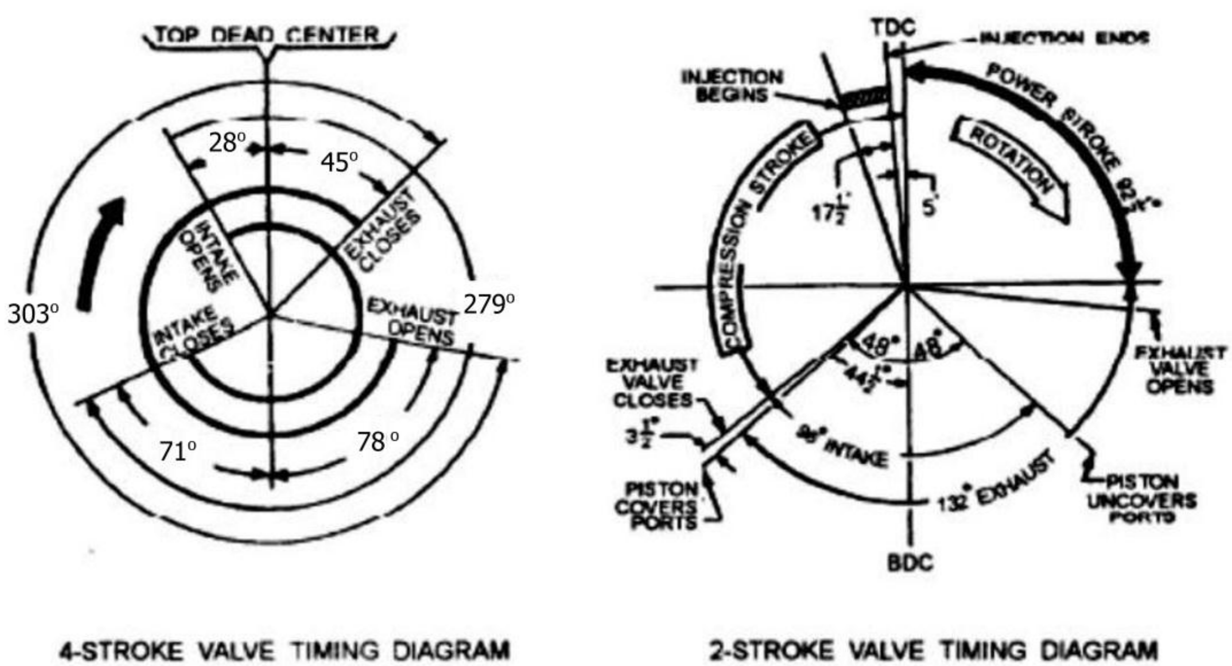

Figure 2.4 Typical valve timing diagram

2.4. Mathematical models and computer simulation

Many mathematical models have been developed to help understand, correlate, and analyze the operation of engine cycles. These include combustion models, models of physical properties, turbulence models, models of the flow of swirl, squish, and tumble in the cylinders, and fuel injection spray models, models of flow into, through, and out of the cylinders. Even though models often cannot represent processes and properties to the finest detail, they are a powerful tool in the understanding and development of engines and engine cycles [15].

Models range from simple and easy to use, to very complex and requiring major computer usage. In general, the more useful and accurate models are quite complex. Models to be used in engine analysis are developed using empirical relationships and approximations, and often treat cycles as quasi-steady-state processes.

Some models will treat the entire flow through the engine as one unit, some will divide the engine into sections, and some will subdivide each section (e.g., divide the combustion chamber into several zones-burned and unburned, boundary layer near the wall, etc.). Most models deal only with one cylinder, which eliminates any interaction from multi cylinders that can occur, mainly in the exhaust system.

2.4.1. Equations of State of the Working Gases

The equations of state of the unburned (subscript u) and burned (subscript b) are derived on the basis of combustion equilibrium chemistry and the coefficients of the thermodynamic properties. These two thermodynamic laws apply to the gaseous fuel-air mixture in the cylinder [15].

During the process of combustion the cylinder contains a mixture of the unburned and burned fuel-air. The mixture is quantified by the burned to total mass ratio $x=m_b/m$,

where$m=m_b+m_u$.

The equations of state for each of the gases is

$$PV_u=m_u\times R_u\times T\ u_u=Cv_u\times T+hf_u \quad \text{.............................(2.1)}$$

$$PV_b = m_b \times R_b \times T u_b = Cv_b \times T + hf_b \quad (2.2)$$

Then, if the gases are homogeneously mixed,

$$PV = m \times (xR_b + (1-x) R_u) \times T = mRT \quad (2.3)$$

And

$$U = m \times u = m \times (x \times Cv_b + (1-x) \times Cv_u) \times T + x \times hf_b + (1-x) \times hf_u \quad (2.4)$$

2.4.2. Heat transfer modeling

The differential heat transfer Q to the cylinder walls can be calculated if the instantaneous average cylinder heat transfer coefficient hg(θ) and engine speed N(=rpm) are known. The average heat transfer rate at any crank angle θ to the exposed cylinder wall at an engine speed N is determined with a Newtonian convection equation:

$$\hat{Q} = h_g(\theta) A_w(\theta)(T(\theta) - Tw)/N \quad (2.5)$$

The cylinder wall temperature $T_w$is the area-weighted mean of the temperatures of the exposed cylinder wall, the head, and the piston crown. The heat transfer coefficient $h_g(\theta)$ is the instantaneous averaged heat transfer coefficient. At this stage, the exposed cylinder area $A_w(\theta)$ is the sum of the cylinder bore area, the cylinder head area and the piston crown area, assuming a flat cylinder head. To compute the heat transfer coefficient an empirical equation is used [15].

$$h_g = 687 \times P^{0.75} \times U^{0.75} \times bo^{-0.25} \times T^{-0.465} \quad (2.6)$$

2.4.3. Combustion modeling

Under normal operating conditions, combustion is initiated towards the end of the compression stroke at the spark plug by an electric discharge. Following inflammation, a turbulent flame develops, propagates through this premixed fuel, air, burned gas mixture until it reaches the combustion chambers walls, and then extinguishes.

From this description it is plausible to divide the combustion process into three distinct phases:

(1) Spark ignition
(2) Combustion development
(3) Combustion termination

Spark ignition

Ignition is treated as an abrupt discontinuity between the compression and burn stages with the instantaneous conversion of a specified mass fraction f of the reactants to products. This produces the unburned and burned zone, each assumed to be homogeneous and hence characterized by its own single state.

Using the 1st law equation for burned gas,

$$M_b \times Cv_b \frac{dT_b}{dt} = \dot{Q}_b - P\frac{dV_b}{dt} + \dot{M}_b \times (Cp_u \times T_u - Cv_b \times T_b + hf_u - hf_b) \quad \text{………………(2.7)}$$

Integrating over a small time interval Δt,

$$\ddot{T}_b = \frac{1}{C_{vb}}(C_{pu} \times T_u + |(\Delta h_f)| - \frac{\ddot{P} \times \ddot{V}_b}{\ddot{M}_b}) \quad \text{……………………………(2.8)}$$

Where the “double dots” represent the moment right after the spark goes on, $\ddot{T}_b$ is the initial value of the temperature in the burned zone right after spark.

Combustion development

Assuming that the burned zone is a cylinder of height, h and radius, r at any instant of θ and using the model which consists in a two zone analysis of the combustion chamber which contains an unburned and burned gas region separated by a turbulent flame front in figure 2.5.

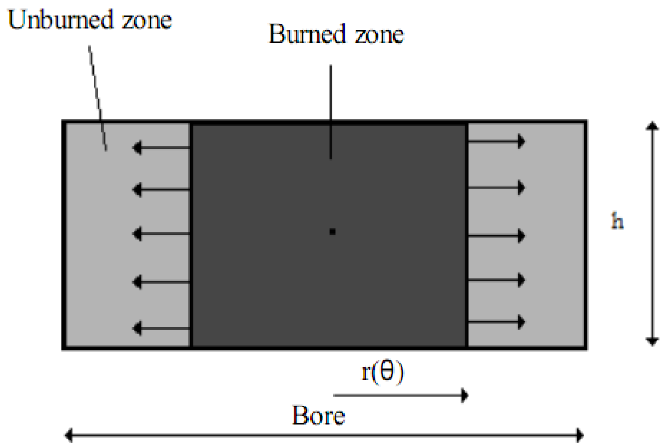

Figure 2.5 Combustion development

It is possible to predict how the radius, r is going to change during the flame travel, assuming a linear distribution. The variation of the burned radius due to the change of the crank angle can be expressed by the approximation in figure 2.6.

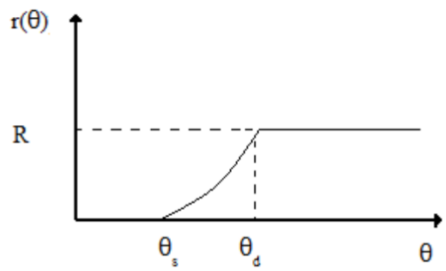

$$r = \frac{dr}{d\theta} = 0 \quad \text{for} \quad \theta < \theta_s$$

$$r = \hat{V}_f(\theta - \theta_s) \quad \text{and} \quad \frac{dr}{d\theta} = \hat{V}_f \quad \text{for} \quad \theta_s < \theta < \theta_d$$

$$r = R \quad \text{and} \quad \frac{dr}{d\theta} = 0 \quad \text{for} \quad \theta > \theta_d$$

Figure 2.6 Variation of burned radius

Being $h=h(\theta)$ the height from piston, at any instant of θ, to the top of the cylinder, comes

$$h = \frac{v}{(\pi \times R^2)} \qquad (2.9)$$

Where, v is the total volume of the cylinder.

The burned and unburned volume and mass are easy to predict, now that r and h are known.

The burned volume is,

$$V_b = \pi \times h \times r^2 \qquad (2.10)$$

$$V_b = \frac{1}{R^2} v \times r^2 \qquad (2.11)$$

And its derivative,

$$\frac{dV_b}{d\theta} = \frac{1}{R^2} r^2 \frac{dv}{d\theta} + \frac{2 \times v \times r}{R^2} \frac{dv}{d\theta} \qquad (2.12)$$

Combustion termination

The end of the combustion occurs when the flame front reaches the walls of the cylinder, $r=R$.

If the end of the combustion process is progressively delayed by retarding the spark timing, or decreasing the flame speed by decreasing the piston speed, the peak cylinder pressure occurs later in the expansion stroke and is reduced in magnitude. These changes reduce the expansion stroke work transfer from the cylinder gases to the piston.

2.4.4. Turbulence characteristics

The flow processes in the engine cylinder are turbulent. In turbulent flows, the rates of transfer and mixing are several times greater than the rates due to molecular diffusion. This turbulent flow is produced by the high shear flow set up during the intake process and modified during compression. It leads to increased rates of heat, mass transfer and flame propagation, so, is essential to the satisfactory operation of the ICE.

The turbulence kinetic energy per unit mass, k is described by,

$$\frac{dk}{dt} = P - D + \frac{1}{M_c}\left(I - E - k\frac{dM_c}{dt}\right) \qquad (2.13)$$

During the burn stage the turbulence energies of the burned and unburned gases are tracked together using the above equation with just the P and D terms, because during the combustion there is no mass transfer, so $dM_c/d_t=0$ and I and E are functions of dM_c/d_t.

$$\frac{dk}{dt}=P-D \qquad \text{..........(2.14)}$$

The term *P* is the turbulence energy production rate per unit mass and is modeled by,

$$P=F_p\frac{A_w}{v}\left|(U)^3\right|-\frac{2}{3}k\frac{1}{v}\frac{dv}{dt} \qquad \text{..........(2.15)}$$

D is the turbulence energy dissipation rate per unit mass and is modeled by,

$$D=F_d\frac{kV_t}{v^{(1/3)}} \qquad \text{..........(2.16)}$$

The coefficients F_p and F_d are parameters that can be set by reference to experiments.

2.4.5. Gas exchange cycle

This cycle deals with the fundamentals of the gas exchange process, intake and exhaust and the valves mechanism in a four stroke internal combustion engine, called the gas exchange cycle.

This cycle is called the gas exchange cycle because it is where the burned gases from the expansion stroke are expelled (exhaust stroke, $\theta = \theta_{evo} \approx 2\pi$ to $\theta=3\pi$) and fresh fuel-air is ingested (ingested stroke, $\theta_{ivo}$to $\theta = 4\pi$).

Valves allow the gas exchange to occur. Valve opening and closing control is called valve timing. The valves are driven by a cam that rotates at half the speed of the crankshaft. The valve flow area depends on valve lift and the geometric details of the valve head, seat and stem.

$$Port\ area=\frac{1}{4}\pi(D^2-d^2) \qquad \text{..........(2.17)}$$

Where $l=l(\theta)$ is the valve lift, *D* the port diameter and *d* the stem diameter.

It can be written mathematically as,

$$A_v=min\left(\pi D l(\theta),\frac{1}{4}\pi(D^2-d^2)\right) \qquad \text{..........(2.18)}$$

The valve lift, *l(θ)* is usually a curve that looks like figure below,

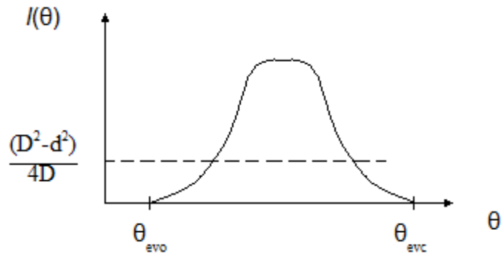

Figure 2.7 Valve lift diagram

Approximating this curve by the formula,

$$l(\theta)=\frac{l_m}{2}(1-\cos(\theta)) \quad \ldots\ldots(2.19)$$

Where, l_m is the maximum valve lift.

From the gas dynamics, the isentropic flow through an orifice is given by,

$$\tilde{m}=\rho_o\times C_f\times A_v\times c_o\times\left(\frac{2}{k-1}\left(\left(\frac{P_v}{P_o}\right)^{\left(\frac{2}{k}\right)}-\left(\frac{P_v}{P_o}\right)^{\left(\frac{k+1}{k}\right)}\right)\right)^{\left(\frac{1}{2}\right)} \quad \ldots\ldots(2.20)$$

As long as,

$$\frac{P_o}{P_v}<\left(\frac{P_o}{P_v}\right)_{cr}=\left(\frac{k+1}{2}\right)^{\left(\frac{k}{k+1}\right)} \quad \ldots\ldots(2.21)$$

If,

$$\frac{P_o}{P_v}\geq\left(\frac{P_o}{P_v}\right)_{cr} \quad \ldots\ldots(2.22)$$

Then,

$$\tilde{m}=\tilde{m}_{cr}=\rho_o\times C_f\times A_v\times c_o\times\left(\frac{2}{k+1}\right)^{\left(\frac{k+1}{2(k+1)}\right)} \quad \ldots\ldots(2.23)$$

When

$$\frac{P_o}{P_v} \leq \left(\frac{P_o}{P_v}\right)_{cr} \quad \text{...(2.24)}$$

the flow is “choked”. This means that the flow right at the orifice (the valve passage) is “sonic”. At this condition only $\tilde{m}_{cr}$ (=constant) can pass through the valve passage regardless of how small P_v/Po is. Note that P_o is the upstream pressure (stagnation pressure) and P_v is the downstream (static pressure just “behind” valve).

For an ideal gas,

$$\rho_o = \frac{P_o}{R \times T_o} \quad \text{..(2.25)}$$

andc_o is the speed of sound,

$$c_o = \sqrt{kRT_o} \quad \text{..(2.26)}$$

The non-ideal effects are accounted by introducing a flow coefficient C_f, which is assumed to be $C_f \approx 0.40$.

2.5. Performance calculations

2.5.1. Theoretical vs Empirical Models

An empirical model is based on past history, like the equations which predict HP per cylinder from intake valve air flow. These are based on experience with flow testing of cylinder heads and then dyno testing the engines [17].

Empirical models can be quite accurate if you are doing things similar to the developer of the model was doing (same fuel, same cam profile, same header design, etc.) However, if you want to simulate something which the developer of the model has not tried, you are basically "on your own" [17].

The Pro is mostly theoretical, which means it is based on numerous laws (equations) of basic physics, like Force = Mass x Acceleration. These equations are then "tuned" to better fit known engine data.

Accuracy and Assumptions

Iterations:

Before we talk about accuracy, it is important for you to understand the types of calculations going on inside the Engine Analyzer Pro and other sophisticated simulation programs. A simple engine program could involve calculating torque from volumetric efficiency [17].

Torque = K x engine displacement x volumetric efficiency

Where: K is a constant which includes many assumptions

However, lets look at a simplified version of the Pro's equation which calculates the temperature rise of intake air as it passes through the intake port.

You enter a volumetric efficiency and obtain a torque value. The answer you obtain on the left side of the equation has no effect on the inputs on the right side of the equations.

Final Temp = Intake Temp + K x (Final Temp + Intake Temp)

In this case the "Final Temp" answer you get on the left side has an effect on the inputs to the equation on the right. The only way to solve equations like this is through "iterations". Iteration is a process where you assume an answer, use that answer in the right side of the equation, calculate the actual answer and see if the actual answer is "close enough" to the answer you assumed.

2.5.2. Iteration Process

For this example, use above equation with K=.3, Intake Temp = 80

A. Assume Final Temp is 145 degrees
B. Calculate Final Temp: 80 + .3 x (145 + 80) = 147.5
C. Are assumed Final Temp and Calculated Final Temp Close Enough (within 1 degree)? No, so do again using new Final Temp answer

A. Assume Final Temp is 147.5 degrees
B. Calculate Final Temp: 80 + .3 x (147.5 + 80) = 148.25
C. Are assumed Final Temp and Calculated Final Temp Close Enough (within 1 degree)? Yes, so an approximate answer is:

Final Temp = 148.25 degrees

If "close enough" was 3 degrees, our first answer of 147.5 degrees would have been good enough. If "close enough" was .1 degree, it may require many more calculations to arrive at an answer which is "close enough". If the equation is very complex and the inputs are an unusual combination, no answer may be reached no matter how many times the calculation is performed. This is called "not converging on a solution". Making the tolerance "close enough" small will produce more exact answers but will require more calculation time.

Total Avg Flow Coef

This is the average flow coefficient for the port, valve and runner for the time the valve is open. It shows how well the port flows compared to a "perfectly" designed port with a "perfect" cam profile. A perfect profile is defined as one where the valve opens immediately to a lift which gives maximum valve flow, stays open the entire duration, and immediately snaps shut at closing. Figure 2.38 compares the actual flow curve with the theoretically "perfect" flow curves to illustrate Avg Flow Coef.

The Total Avg Flow Coef will compare head and camshaft combinations. An engine with a Total Avg Flow Coef of 1.0 is physically impossible to build. In reality, the Total Avg Flow Coef will be approximately .25 for production engines, .30 to .40 for race 2 valve engines, and up to .50 or more for high RPM, 4 valve race engines.

RPM Data

RPM Data looks much like a dynamometer data sheet which gives projected engine test results for each RPM tested.

Engine RPM

Is the engine crankshaft's rotational speed in revolutions per minute.

Brake Torque

Is the brake torque produced by the engine measured in ft.lbs. Brake torque is the usable net torque at the engine's flywheel. This is the same as the torque numbers you see in advertisements and in dynamometer torque and HP curves.

Brake Power

Is the Brake HP produced by the engine measured in horse power. Brake HP is the usable net HP at the engine's flywheel. This is the same as the HP numbers you see in advertisements and in dynamometer torque and HP curves.

2.6. Co_2 emission calculations

An engine with some brake power output P_b can make a vehicle of mass m travel at some specific velocity V.

$$P_b = F \times V \quad \text{(2.27)}$$

Where, F is the product of rolling resistance and weight of the vehicle

Rearranging the above equation,

$$V = \frac{P_b}{F} \quad \text{(2.28)}$$

It is possible to calculate the fuel consumption (kg/km) using the equation below.

$$Fuel\ consumption\ (kg/km) = \frac{bsfc\ (kg/kwhr) \times P_b(kw)}{V\ (km/hr)} \quad \text{(2.29)}$$

After calculating the difference in fuel consumptions between two cases using subtraction, Co_2 emission reduction can be calculated using the equation below [18].

$$Co_2\ reduced\ = \ Fuel\ saved \times CL \times OF \times 44/12 \quad \text{(2.30)}$$

Where

CL=carbon content of fossil fuels, 0.77ton/kl (fraction)

OF=oxidation factor for fossil fuels, 0.995 (fraction)

2.7. Cam profile construction

Cam is a machine element, which when rotated gives motion to its follower, in a desired manner. Its use can be seen in internal combustion engines for the operation of the inlet and exhaust valv. The motion may be linear or nonlinear. There are many types of cams and cam followers. The type of cam and its follower depends upon the requirement [19].

Types of cams

Cams can be classified according to the shape, and type of motion given by the cam. Various shapes of the cams are shown in figure 2.8. According to the shape, there are two main types: radial and cylindrical.

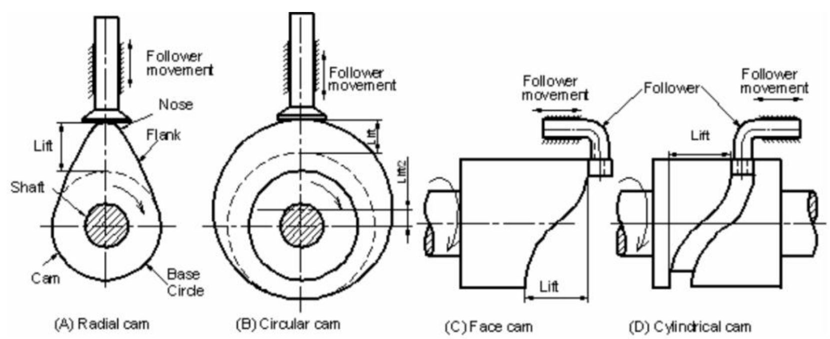

Figure 2.8 Types of cam

Radial cam

In the radial type, the follower moves perpendicular to the axis of rotation. The radius changes with change in angle. The peripheral face is used to drive the follower.

Figure 2.9 shows a generalized radial cam with the various periods of motion for the follower. At minimum radius (base circle), the follower is at the lowermost position. When the

cam rotates, it is moved radially outward during the lift period.
Then the follower remains at its highest position for the dwell period. It thendescends during the fall period back to the basecircle and remains at this position for the other dwell period.

A cam can have any value of these periods to give the desired type of motion.

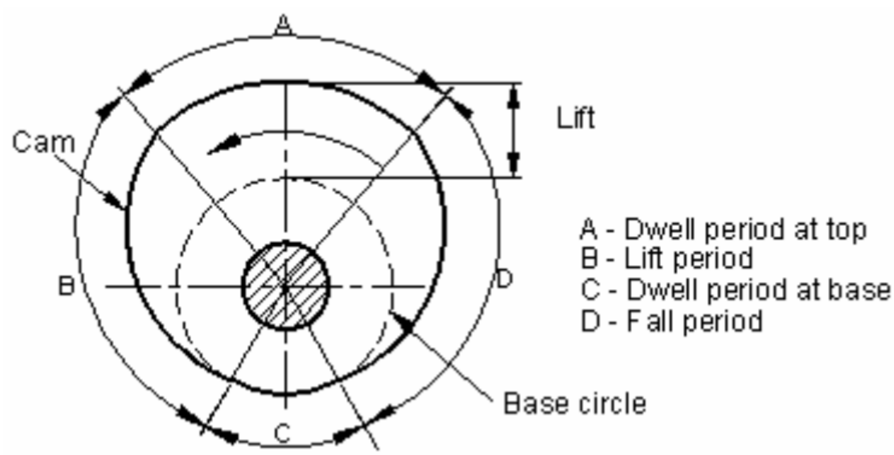

Figure 2.9 Radial cam periods of motion

Velocity during lift and fall period will depend upon the shape of the flank. Various shapes that a re commonly used are the following:

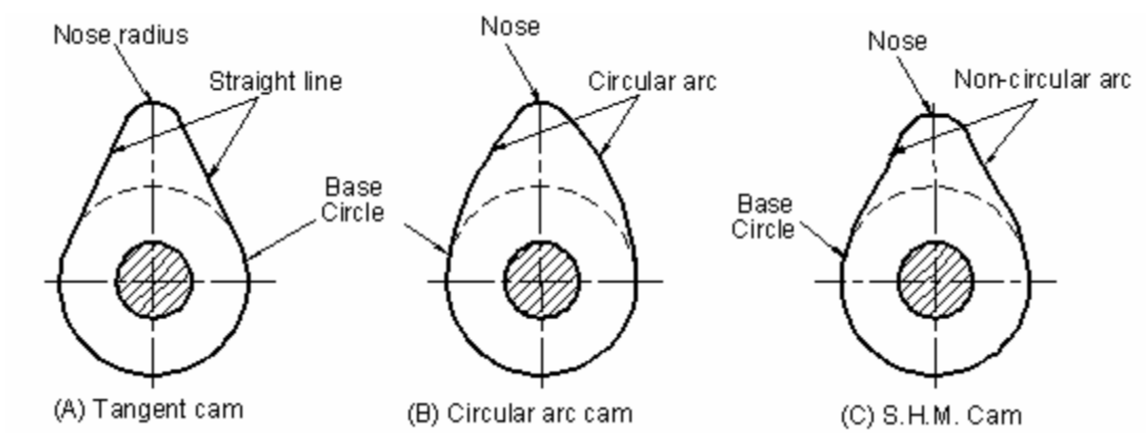

Figure 2.10 Types of radial cam

Lift diagram

Before drawing a cam profile, it is necessary to draw the lift diagram for the rise and fall period. It is nothing but an X-Y plot showing the movement of the follower on the Y-axis and rotation angle on the X-axis. It is needed for both radial and cylindrical cams. These diagrams are generally made full size so they could be directly measured and transferred to the drawing of the cam. The following information is necessary before the drawing:

- Lift period in degrees
- Rise period in degrees
- Types of motion like constant velocity or constant acceleration, etc. during rise period
- Fall period in degrees
- Type of motion during fall period
- Dwell period in degrees at base circle and nose

Drawing a radial cam

To draw a radial cam, the following data should be known:

- Lift diagram as drawn earlier
- Base diameter
- Width of cam
- Type of follower
- Diameter of follower

First, the displacement diagram, as shown in figure 2.11, is drawn as discussed in the following steps [31]:

1. Draw a horizontal line ANM such that AN represents the angular displacement when valve opens (i.e. 53.5º) to some suitable scale. The line NM represents the angular displacement of the cam when valve closes (i.e. 53.5º).
2. Divide AN and NM into any number of equal even parts (say six).
3. Draw vertical lines through points 0, 1, 2, 3 etc. equal to the lift of valve i.e. 16 mm.

4. Divide the vertical lines 3 – f and 3′ – f ′ into six equal parts as shown by points a, b, c ... and a′, b′, c′ ....in figure 2.11.
5. Since the valve moves with equal uniform acceleration and deceleration for each half of the lift, therefore, valve displacement diagram for opening and closing of valve consists of double parabola.
6. Join Aa, Ab , Ac intersecting the vertical lines through 1, 2, 3 at B, C, D respectively.
7. Join the points B, C, D with a smooth curve. This is the required parabola for the half of valve opening. Similarly other curves may be drawn as shown in figure 2.11.
8. The curve A, B, C, ..., G, K, L, M is the required displacement diagram.

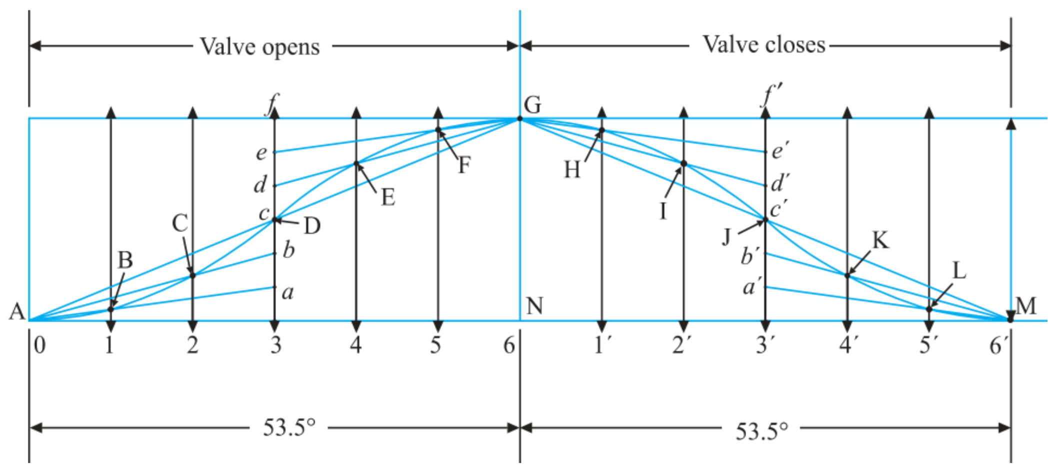

Figure 2.11 Radial cam lift diagram

Now the profile of the cam, as shown in figure 2.11, is drawn as discussed in the following steps:

1. Draw a base circle with center O and diameter.
2. Draw a prime circle with center O and radius, OA= Min. radius of cam + ½(Diameter of roller)
3. Draw angle AOG to represent opening of valve and angle GOM to represent closing of valve.
4. Divide the angular displacement of the cam during opening and closing of the valve (i.e. Angle AOG and GOM) into same number of equal even parts as in displacement diagram.
5. Join the points 1, 2, 3, etc. with the center O and produce the lines beyond prime circle as

shown in figure 2.12.

6. Set off points 1B, 2C, 3D, etc. equal to the displacements from displacement diagram.
7. Join the points A, B, C, ...L, M, A. The curve drawn through these points is known as pitch curve.
8. From the points A, B, C, ...K, L, draw circles of radius equal to the radius of the roller.
9. Join the bottoms of the circle with a smooth curve as shown.

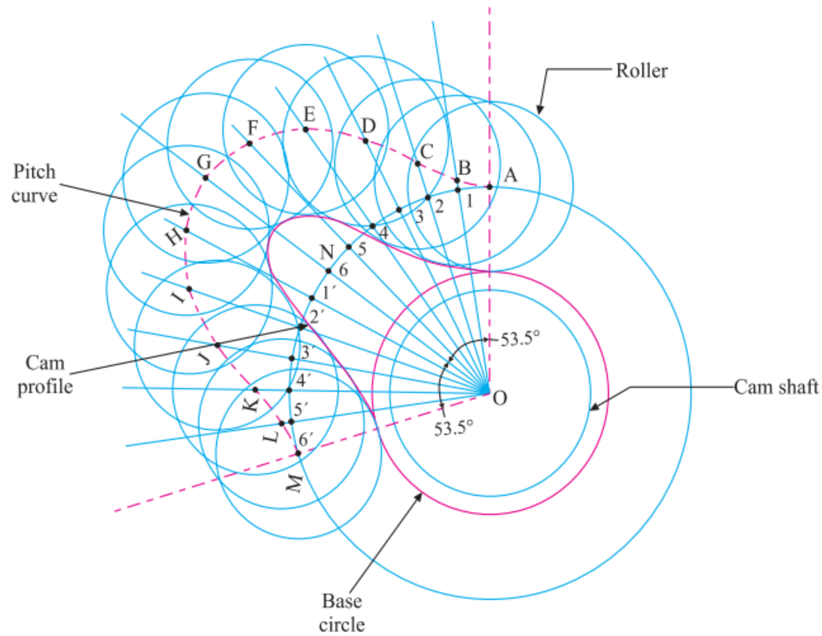

Figure 2.12 Radial cam profile construction

2.8. Linear Data Fitting

Given data points $(t_1, y_1), \ldots, (t_m, y_m)$, which are assumed to satisfy

$$y_i = Y(t_i) + e_i$$

Y is the so-called background function and the $\{e_i\}$ are (measurement) errors, often referred to as "noise". We wish to find an approximation to $Y(t)$ in the domain $[a, b]$ spanned by the data abscissas. To do that we are given (or we choose) a fitting model $M(x, t)$ with arguments t and the parameters $x = (x_1, \ldots, x_n)^T$. We seek $\hat{x}$ such that $M(\hat{x}, t)$ is the "best possible" approximation to

$Y(t)$for $t \in [a, b]$. In all data fitting problems the number of parameters is smaller than the number of data points, $n<m$ [20].

As a simple example consider the data

t_i	y_i
−1.5	0.80
−0.5	1.23
0.5	1.15
1.5	1.48
2.5	2.17

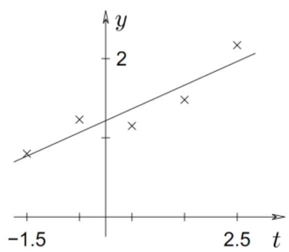

Figure 2.13 Linear data fitting

Figure above shows the data points and the model $M(x, t) = x_1 t + x_2$ with the parameter values $x_1 = 0.2990, x_2 = 1.2165.$

In the next case 45 data points shown by dots in Figure below can be fitted with the model

$$M(x, t) = x_1 e^{-x3t} + x_2 e^{-x4t}$$

In the figure two different choices of the parameters are used,

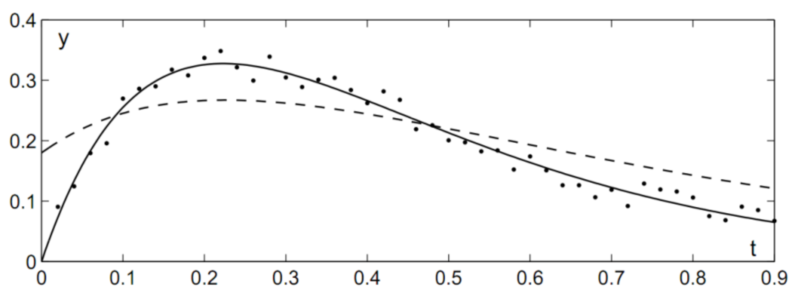

Figure 2.14 Polynomial curve fitting

Full line: $\tilde{x}$= (4.00, −4.00, 4, 5)^{T}Dashed line: $\check{x}$= (0.84, −0.66, 2, 4)^T

The first choice of parameters seems to be better than the other. Actually, the data points were computed by adding noise to the values given by$Y(t_i) = M(\tilde{x},t_i)$, so in this case $Y(t) = M(\hat{x},t)$ with $\hat{x} = \tilde{x}$.

Chapter Three

METHODOLOGY

Several steps have been followed while conducting the study from start to end. After reviewing previous works on related subjects, an engine model with complete specification was selected and modeled in a simulation program known as ENGINE ANALYZER PRO.

Several literature have been reviewed in the areas of the current states and developments and difficulties in CVVT systems; studies conducted on VVT systems using computer simulation programs; data optimization techniques to linearize fluctuating data; hydraulic actuation systems and mechanisms; the workings, algorithms and degrees of reliability behind Engine simulation programs.

Different input categories were required to be filled into the program to conduct the simulation. These input categories are cylinder head specification; engine block specification; intake and exhaust system specification; valve/cam train specification; charging system specification and simulation condition specification.

Characteristics such as intake and exhaust valve diameters, port diameter and average port length are included in the cylinder head specification, and cylinder diameter, stroke, connecting rod length; number of cylinders and compression ratio are included in the engine block specification. The parameters under the intake and exhaust system specification are design and type of the manifold; runner length, runner flow coefficient and if it is whether injection or carburation. The charging system specification allows choosing whether it is naturally aspirated or otherwise. Also, under the simulation condition specification, type of fuel and atmospheric conditions; engine rpm to start running simulation and the intervals of speed with the final speed are stated.

While these parameters are filled with careful considerations, the category given the most emphasis in this study is the valve/cam train specification which allowed varying the valve opening angles; closing angles and valve lift for both intake and exhaust cams. Other parameters such as rocker arm ratio and degree of asymmetry for the cam profile are available under this category. Using this category, valve timing angles and lift were tuned with the intension of finding optimum values for better performance at selected engine speeds.

General steps followedin this study aresummarized and shown in the work flow chart figure3.1 below.

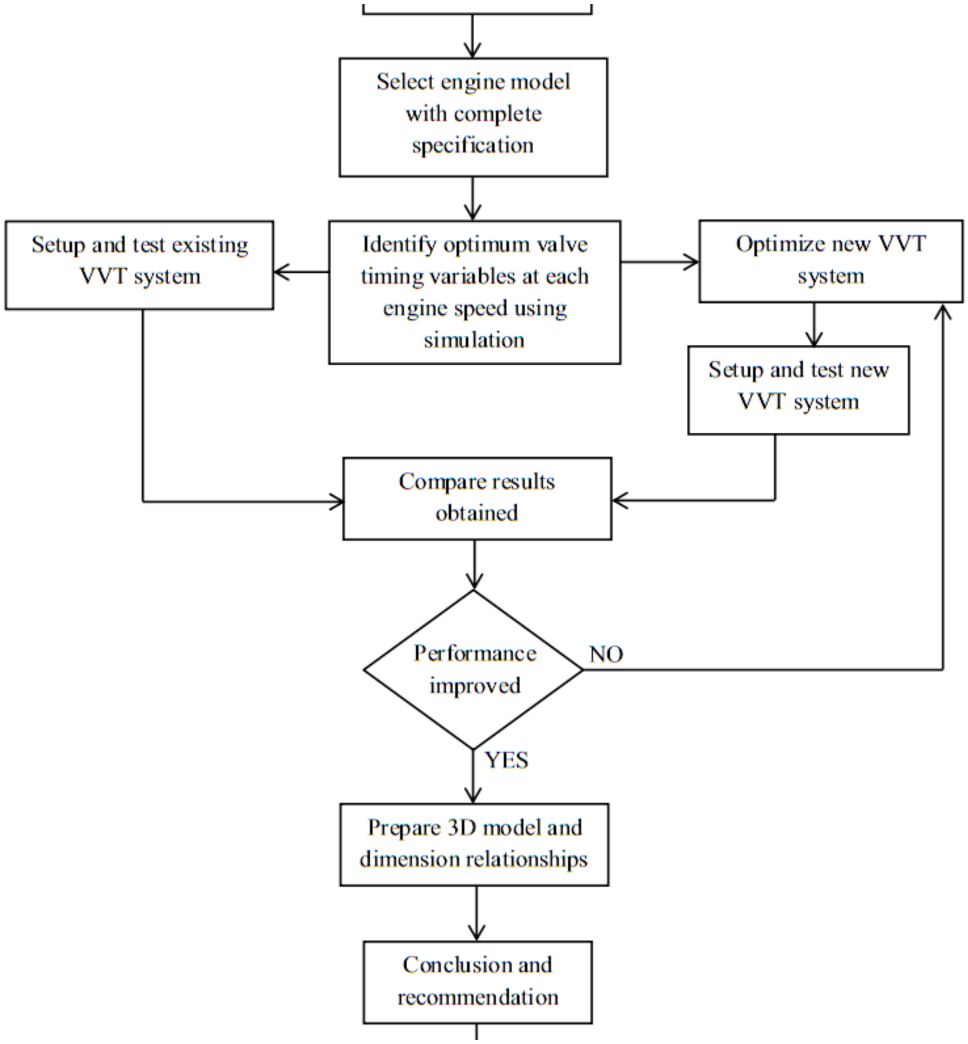

Figure 3.1 Work flow chart

The 2001 **NISSAN X-TRAIL** Engine model is selected for this study due to its relatively more complete specification when compared to other models. This specific engine model is 1997cc, naturally aspirated, carbureted and no VVT system with four valves per cylinder giving an output of 102 KW maximum power at 5200 rpm and 198 Nm of maximum torque at 4400 rpm.

In order to find the optimum valve timing parameters at a specific engine speed, each parameter was independently varied and simulations were run for each variations of for instance ivo, to observe the performance until maximum possible values are obtained. Then the same step is followed for the rest of the parameters namely ivc, evo, evc, ivl and evl. After the test at one specific speed is completed, the simulation speed is changed and the procedure is repeated for all the fourteen sample speed up to 7000 rpm.

The optimum valve timing and lift values obtained from the simulation are slightly fluctuating, which makes construction and operation of the camshaft difficult. Even if the camshaft could be constructed with such a complex shape, it will become impossible to develop a suitable follower system to smoothly work with the camshaft. Hence, these results have been modified into linear functions that best approximate the fluctuating values. While doing this, trying to represent all fourteen values with only one linear function reduces the effectiveness of representation, so two linear functions are applied with different slops where the last function continues from the first one.

Performances of the existing system and the new CVVT system obtained in the simulation have been exported and analyzed in MS EXCEL. After analyzing the results, fuel consumption and Co_2 emissions are calculated and compared to estimate improvements on volumetric efficiency, power, torque, bsfc, fuel saving and Co_2 emission reduction. The values have also been plotted and analyzed using MS EXCEL.

The new CVVT camshaft has been modeled in SOLIDWORKS along with suggestion of operating mechanism that only involves the cylinder head. The suggested actuation and operation mechanism tries to reduce problems arising with complexity and friction.

Relationships of dimensions relative to cylinder bore have been derived for all variables that describe the size and shape of the camshaft. These dimensions include the lift values of the six cam profiles; angles of opening duration and the angular shift of the centerline of the cam profiles from the center angle between TDC and BDC; and the axial distance between consecutive cam profiles.

Chapter Four

RESULT AND ANALYSIS

4.1. Engine setup

In this section an engine model with complete specification is selected and the parameters are setup on the simulation program to analyze its performance. Due to numerous data availability than most manufacturers provide, the **NISSAN X-TRAIL ST 2.0L** is selected for this study.

4.1.1. Engine specification

Table 4.1 summarizes most important dimensions required for program input. Other parameters which are not provided by the manufacturer are taken from previously conducted design exercise.

Table 4.1 Engine specification

Model	ST 2.0
Number of cylinders	4
Engine capacity	2 liter
Displacement(cc)	1997
Bore(mm)	84
Stroke(mm)	90.1
Compression ratio	10.1
Maximum power(Kw@rpm)	102@5200
Maximum torque(Nm@rpm)	198@4400
Number of valves/cylinder	4

This engine is not fitted with any form of VVT system, and is also naturally aspirated, which means no turbo or supercharging system is available.

4.2. Software input

Setting up the study is conducted in seven steps starting with filling the basic engine parameters listed in table under *short block specs*, except power and torque, which will be determined after running the simulation.

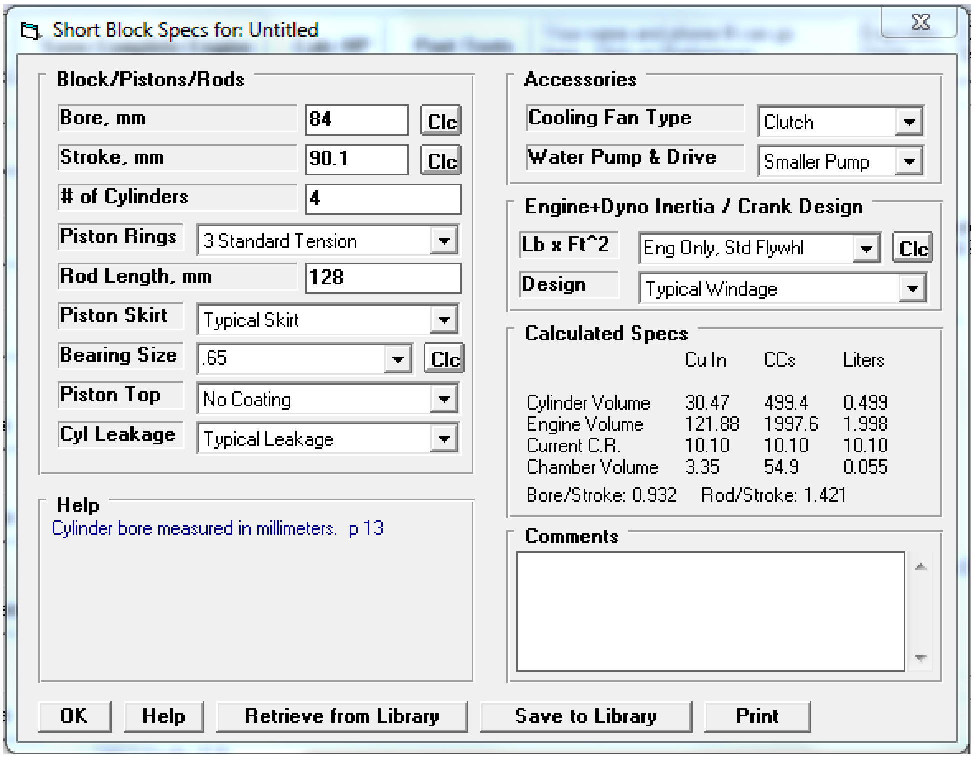

Figure 4.1 Engine block condition setup

The next step is to setup the cylinder head parameters under *Head Specs.* Some of the terminologies for this section are not available in the manufacturer's specification; hence values are taken form a similar sized engine example file in the simulation program except for valve diameter and average port diameter.

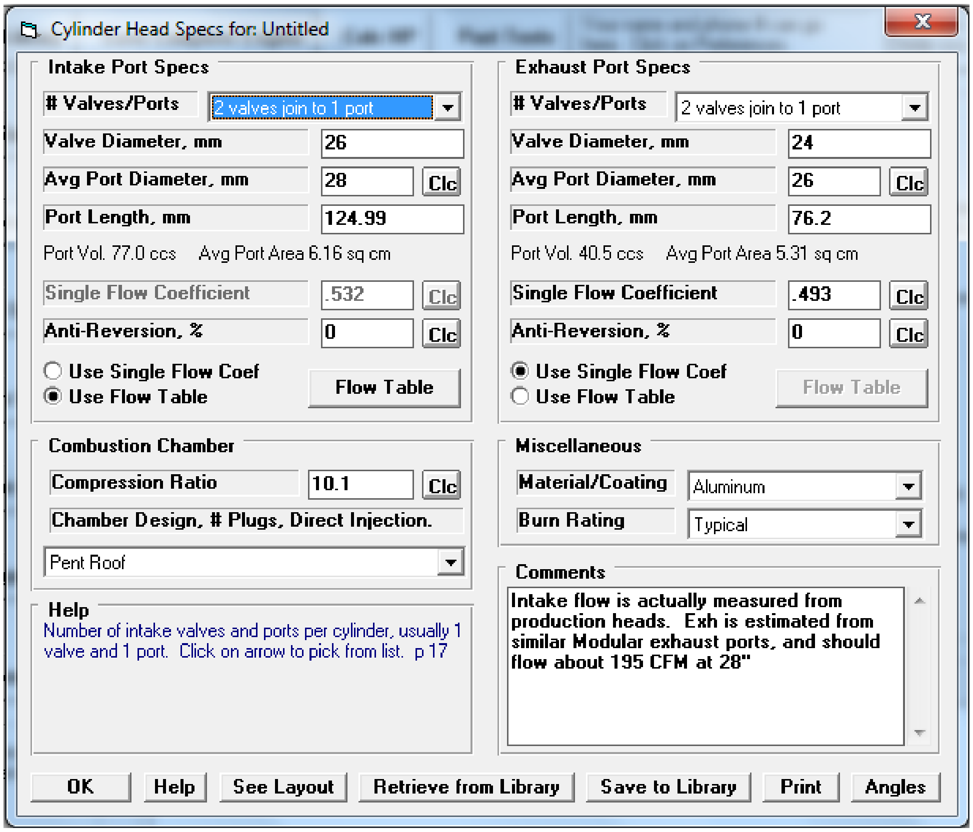

Figure 4.2 Cylinder head condition setup

The intake system parameters are also setup in the same manner. Here also there are parameters which are not provided by the manufacturer, so similar process as head specificationsis taken.

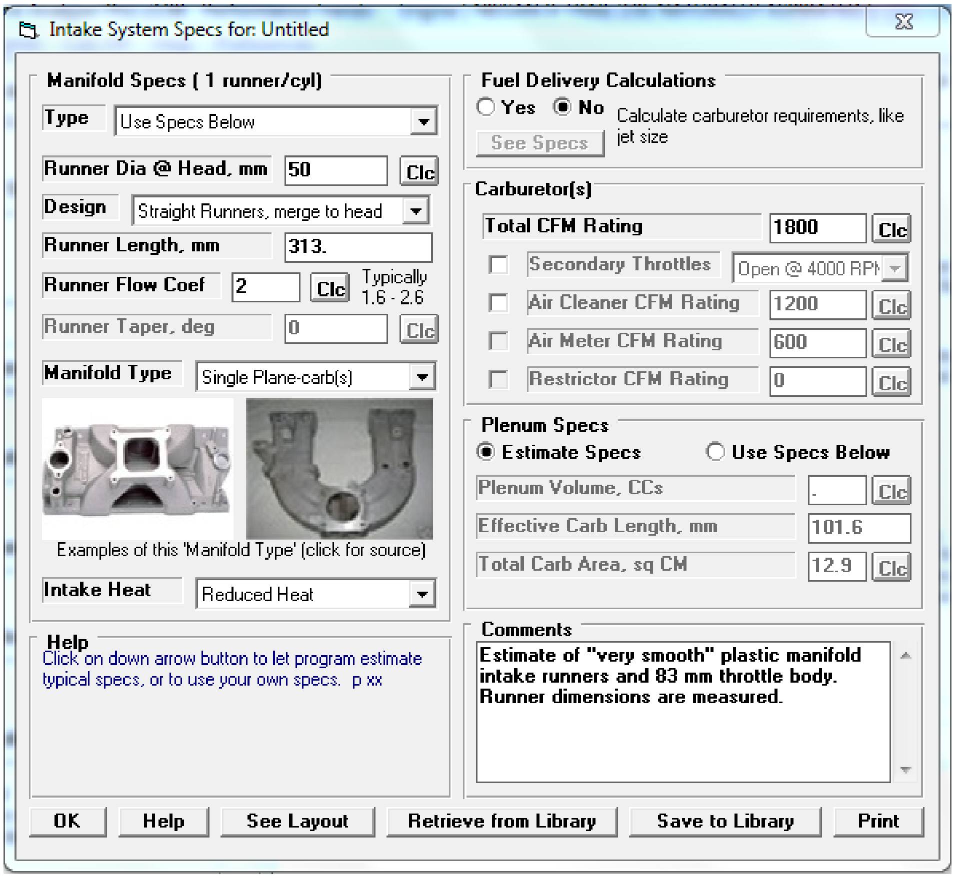

Figure 4.3 Intake system condition setup

The exhaust system specs are then setup with the same process as before.

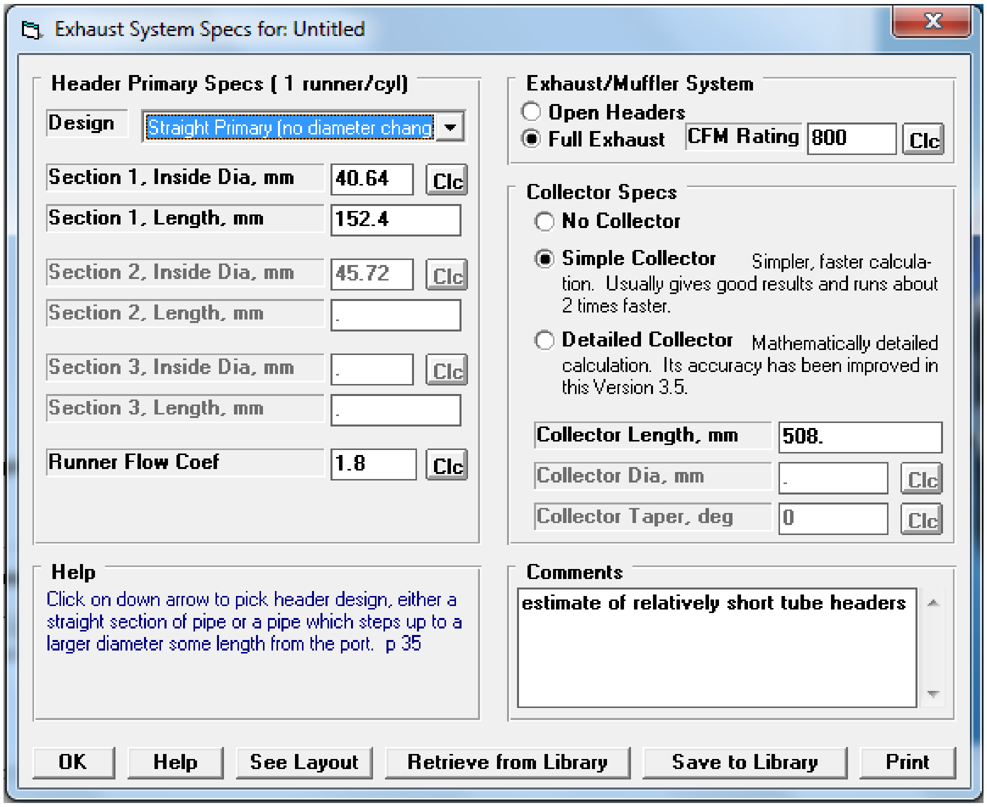

Figure 4.4 Exhaust system condition setup

Some unknown parameters are taken from a similar sized engine file while setting up the above sections, but also fair values are taken and are the same for all tests to be conducted ahead. The main focus of this study being to find the optimum valve events for different engine speeds, other engine parameters will not have much effect on the results.

4.2.1. Cam/Valve Train Specs

The main concern of this simulation lies in this section, which allows varying the valve profile.

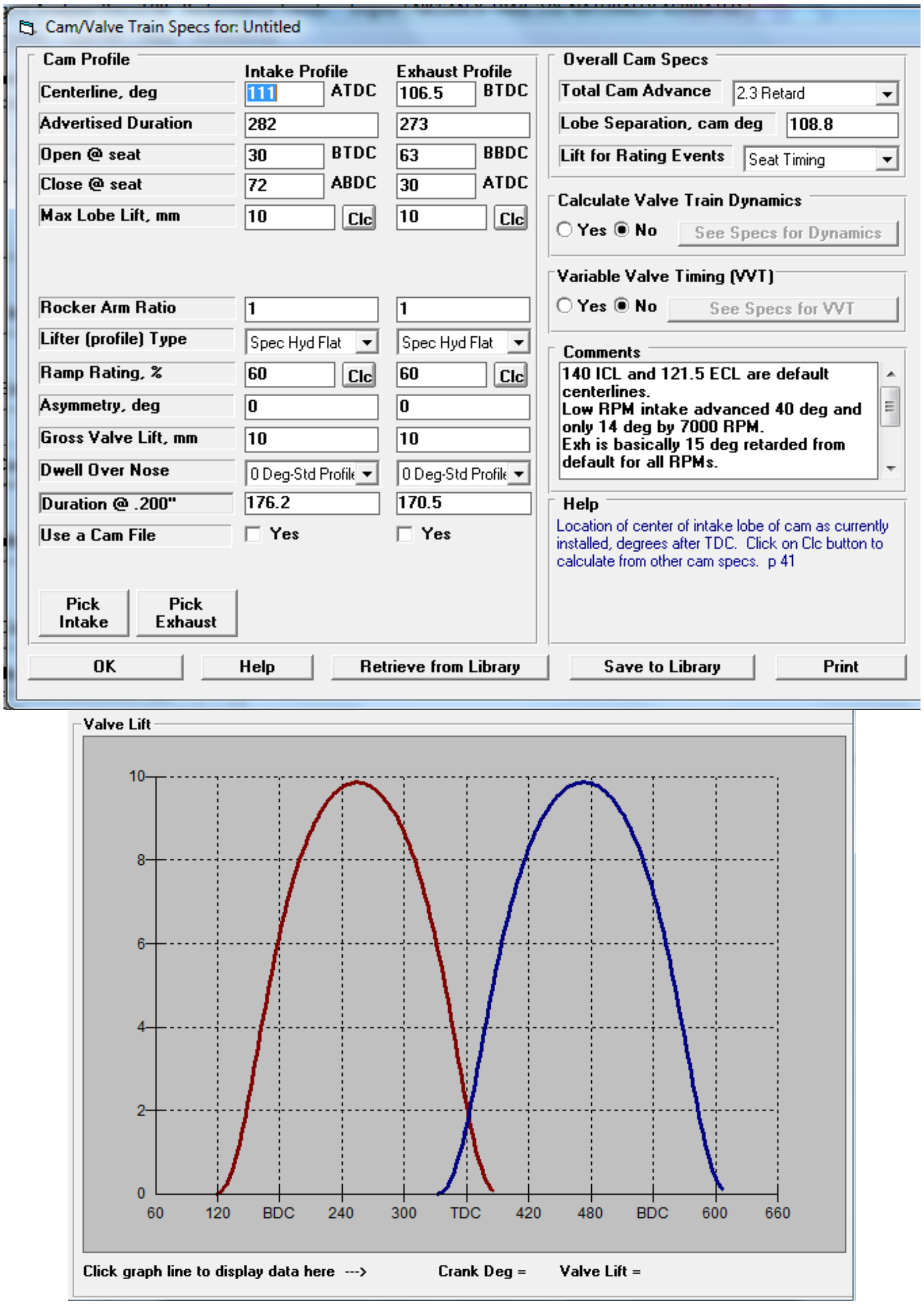

Figure 4.5 Cam/valve train condition setup

In this interface any valve profile can be setup and tested for performance. Parameters such as opening angle, closing angle, lift and centerline angle can be independently varied.

Finally under *Turbo/Supercharger Specs* Naturally Aspirated is selected.

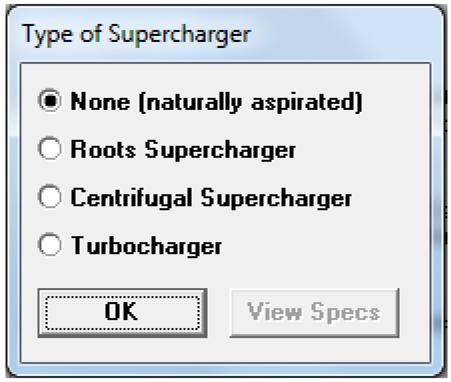

4.2.2. Running Simulation

Before running the simulation, it is necessary to specify the environmental condition (weather) for engine operation, type of fuel, type of cooling system and the engine speed of interest. It is also possible to select a range of speed with a fixed interval.

At completion of the simulation process, the engine performance parameters are displayed in a tabulated manner with a plot option for visual analysis. The tabulated parameters can also be exported and saved for reference and comparison on a later time using other programs such as *excel*.

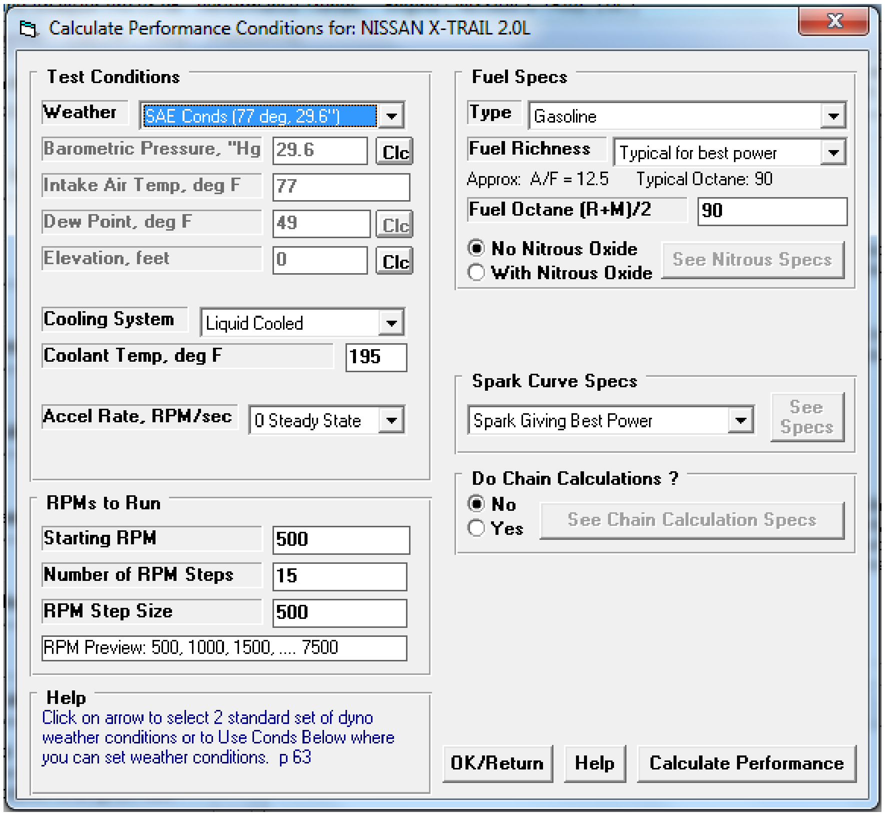

Figure 4.6 Simulation condition setup

4.3. Tuning process

The tuning process is the most important part of this study since it aims at finding the optimum valve timings for all the speed ranges from 500-7000 rpm with intervals of 500. Starting from 500 rpm, the three main valve profile parameters namely, opening angle, closing angle and lift are changed in a progressive manner while recording and observing their performance. Finally the values with better performance are selected and recorded for further optimization that might be needed.

As a way of comparing the valve profiles, four performance parameters are selected which are*Volumetric efficiency, Brake Torque, Brake Power and Brake Specific fuel consumption.* In this way, if one parameter tends to give an unexpected value, another parameter can give additional information.

To make things more clear, while tuning EVC/ATDC at 1000 rpm, starting from 5^0 and increasing the value, the volumetric efficiency and power or torque increases. However at some point the volumetric efficiency,torque and power start to reduce after 11^0, so it is selected as a better value. Sometimes volumetric efficiency,torque and power keep increasing while bsfc also starts to increase at some point. This can be seen for IVO/BTDC, while changing the value from 16 to 18, bsfc starts to increase. In such cases the bsfc value is used as a limiting factor.

Also for IVL value at 6000 rpm table shown in appendix section A, while changing value from 14.5 to 15, volumetric efficiency increases, but power and torque reduce while bsfc increases. This mainly happens because of too much air/fuel mixture in the cylinder and not enough time to burn completely. In some similar cases, the increase in bsfcmay not be clearly seen at the results of bsfc due to only three decimal places allowed by the program.

To show how the valve timings are selected for each sample speeds, tuning process for 1000 rpm is presented in table 4.2. The order of the valve timing parameters in the tables is in the sequence of which was tested first, second and so on.

Table 4.2 Tuning process at 1000 rpm

1000 rpm test result					
	degree	VE(%)	T_b(Nm)	P_b(Kw)	bsfc(kg/Kwhr)
ivo/btdc(deg)	10	81.6	180.41	18.9	0.273
	12	81.6	180.69	18.93	0.273
	14	81.8	180.92	18.95	0.273
	16	81.9	181.11	18.96	0.273
	18	82	181.48	19.01	0.274
ivc/abdc(deg)	10	81.9	181.11	18.96	0.273
	12	81.89	180.96	18.95	0.274
	8	81.87	181.12	18.97	0.273
evo/bbdc(deg)	25	81.9	181.11	18.96	0.273
	27	81.87	180.89	18.94	0.273
	23	81.77	181.12	18.97	0.273
evc/atdc(deg)	5	81.9	181.11	18.96	0.273
	7	81.9	181.35	18.99	0.273

	9	82.25	181.91	19.05	0.273
	11	82.51	182.37	19.1	0.273
	13	82.23	179.89	18.84	0.273
ivo/btdc(deg)	16	82.51	182.37	19.1	0.273
	17	82.66	183.02	19.16	0.273
	18	82.71	182.9	19.15	0.273
	19	82.88	183.18	19.19	0.273
	20	83.09	183.52	19.22	0.274
ivc/abdc(deg)	8	82.88	183.18	19.19	0.273
	9	82.9	183.23	19.19	0.273
	10	82.89	183.18	19.19	0.273
evo/bbdc(deg)	25	82.9	183.23	19.19	0.273
	26	83.05	183.37	19.2	0.274
	24	82.98	183.39	19.2	0.273
	23	82.78	183.12	19.18	0.273
evc/atdc(deg)	11	82.98	183.39	19.2	0.273
	12	83.08	183.75	19.24	0.273
	13	83.36	184.16	19.28	0.274
ivl(mm)	11	83.08	183.75	19.28	0.273
	12	83.24	184.01	19.27	0.273
	13	81.06	179.29	18.78	0.273
	12.5	83.28	184.07	19.28	0.273
evl(mm)	11	83.28	184.07	19.28	0.273
	11.5	83.38	184.11	19.28	0.274
	12	83.33	184.07	19.28	0.274

As can be seen from the table, ivo was initially set at 10^0 and after running the simulation, the four selected parameters are recorded. Then ivo is increased with steps of two degrees. While changing ivo from 16^0 to 18^0, the volumetric efficiency increased by only 0.1%, but the bsfc also started to increase. At this point the optimum ivo angle is decided to be 16^0, and is highlighted for ease of observation.

This step is repeated for ivc, evo and evc after which it is repeated with a step of 1^0. This gives more accurate values and also uses as a checking mechanism if the later tuned values affect the earlier ones. Finally lift is independently tuned for both intake and exhaust valves.

After conducting this process for all the selected speeds, the optimum valve profile parameters are summarized and presented in table 4.3.

Table 4.3 Simulation result for optimum valve timing parameters

rpm	ivo/btdc	ivc/abdc	evo/bbdc	evc/atdc	ivl	evl
500	9	8	24	5	11	11
1000	19	9	24	12	12.5	11
1500	26	11	28	16	13	12.5
2000	28	9	28	14	13	13
2500	28	21	36	20	13	12.5
3000	31	31	37	19	13.5	13.5
3500	34	41	35	24	13	13
4000	29	26	30	21	13	13
4500	42	35	36	22	14	13
5000	37	37	48	21	14	13
5500	32	49	55	26	15	13
6000	28	59	63	22	14.5	13.5
6500	20	72	62	19	14.5	14
7000	16	76	59	21	14.5	13

As shown in table, 14 sample speeds are tested and their optimum valve timing parameters show a slightly fluctuating but somewhat continuously increasing or increasing and decreasing at the same time. Among the 14 sample points, three or four points are seen to be out of the acceptable trend line. For instance, in figure below, the ivo angle shows an increasing behavior up to 3500 rpm, and starts to reduce in a fairly linear manner.

It was difficult to justify the reduction of ivo after 3500 rpm and the analysis was repeated with slightly higher atmospheric pressure, but a similar result was obtained. But another analysis done on the same engine fitted with a turbo charger showed characteristics that was initially expected and ivo angle continued to increase up to 7000 rpm.This is an obvious reason to believe the valve timings for naturally aspirated and turbo/super charged engines are very different. This also justifies the reduction of ivo after 3500 rpm is due to the induction system of the engine. In the case of a naturally aspirated engine, if intake valve opening is large at high speeds, more air might be admitted into the cylinder, but lack of resistance in the exhaust manifold due to no work to be done on turbocharger turbine will allow some portion of the air fuel mixture to escape. This reduces the power and torque, and increases BSFC.

Here it is clearly seen that the sample point at 4000 rpm is out of the trend line and such errors are common in computer simulations. Also, since the rest 13 sample points fairly conform to a second order polynomial function, the sample point with an exaggerated error is ignored. This assumption is also made for all the parameters unless points with error exceed a number of 4, in which case the analysis is repeated with some adjustment to the assumed input variables.

A second order polynomial curve fittings are plottedand their equations are also shown for all the parameters while y represents the angles for opening and closing of valves and x represents the engine rpm. For lift values, y represents valve lift in mm.

The average error values for these functions are given below each graph calculated by summing up all error values of each data point and dividing by the total number of data points in equation (4.1).

$$e = \frac{\sum_{i=1}^{n} e_i}{n} \qquad (4.1)$$

Summary table of error values is given in appendix A2 and A3 for thepolynomial curve fittings and the linear data fittings.

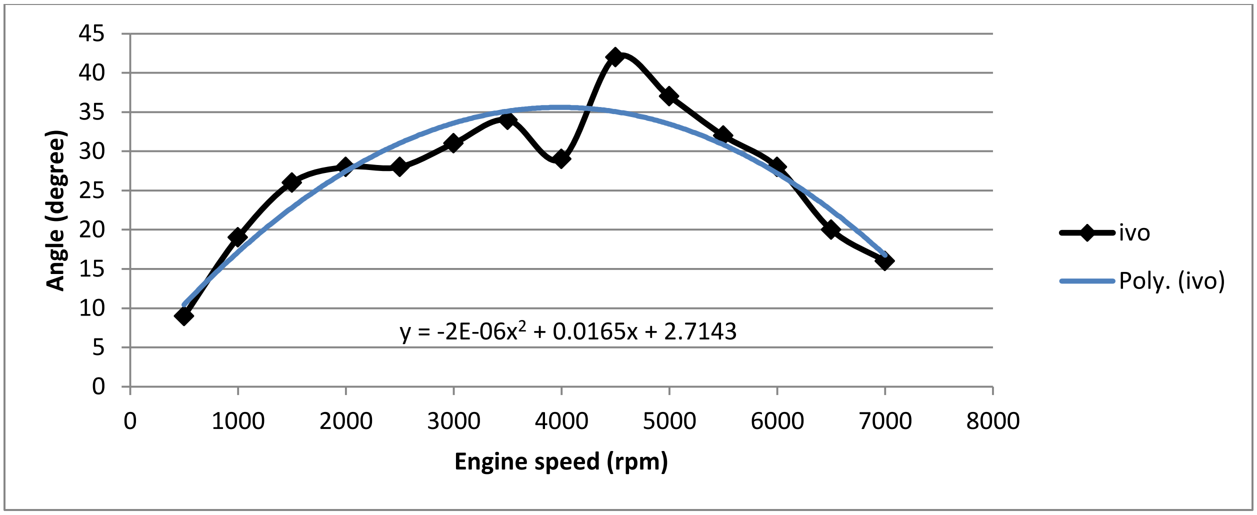

Figure 4.7 Intake valve opening angles

e = 0.124

In the optimization section of this paper, it is clearly discussed how the sample points are approximated to two linear functions. Figure 4.8 shows the optimum ivc angles at each sample engine speeds. Here also fluctuating results are observed, but 11 out of 14 sample points are seen to be fairly continuous.

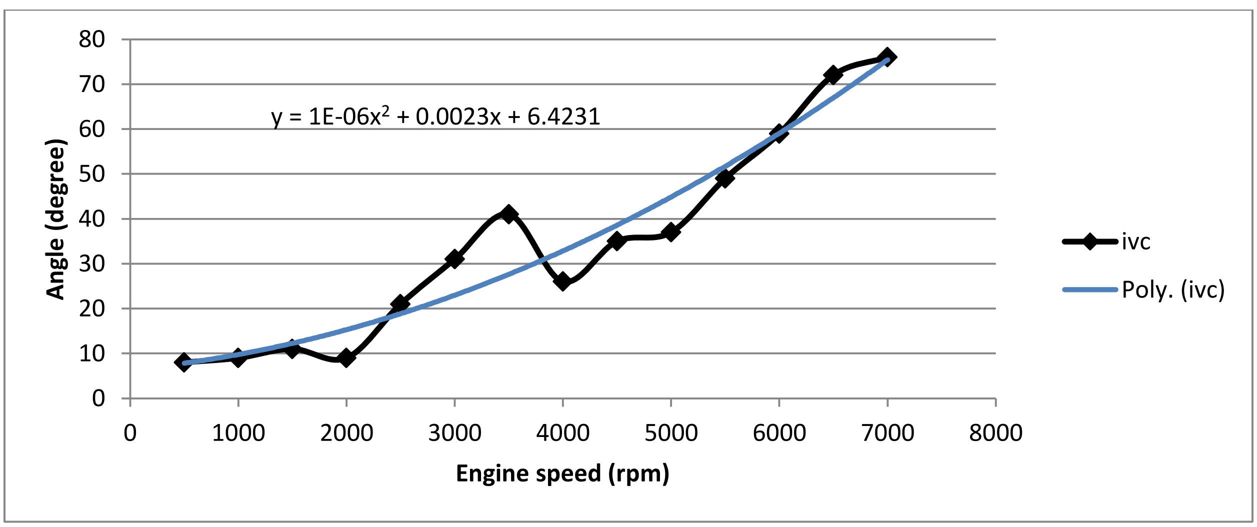

Figure 4.8 Intake valve closing angles

e = 0.163

Exhaust valve variables are where the most fluctuating results are seen. As shown in figure 4.9, evo angles tend to increase up to 3000 rpm and then decrease up to 4000 rpm, then increase again upto 6000 rpm and slightly decrease up to 7000 rpm. However these sample points can also be fairly approximated to two linear functions.

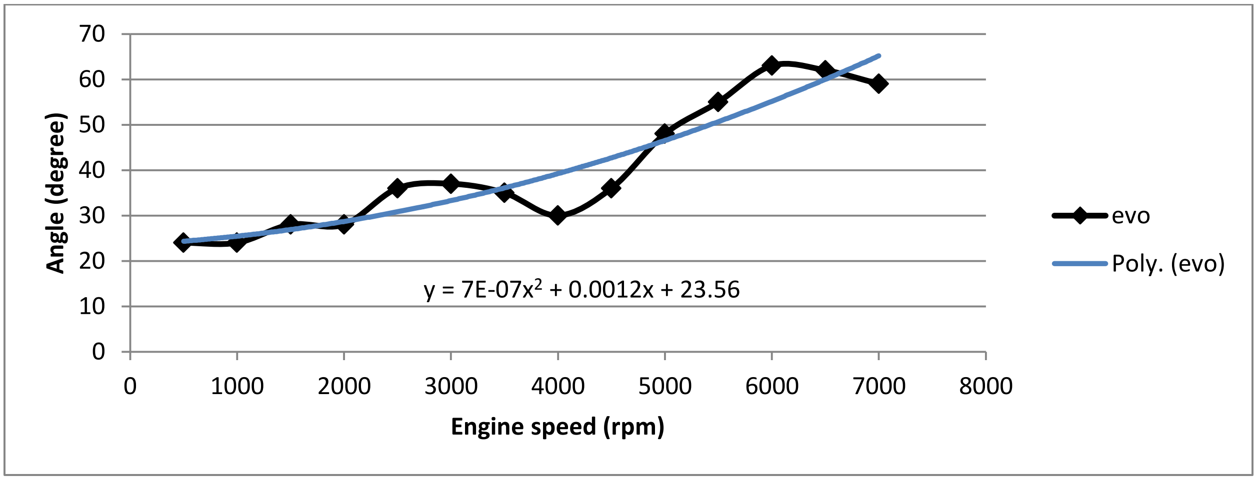

Figure 4.9 Exhaust valve opening angles

e = 0.09

For evc angles shown in figure 4.10, the sample point at 5500 is slightly out of the trend line. However, the rest 12 sample points can also be easily approximated to two linear functions, which will be discussed in detail in the optimization section.

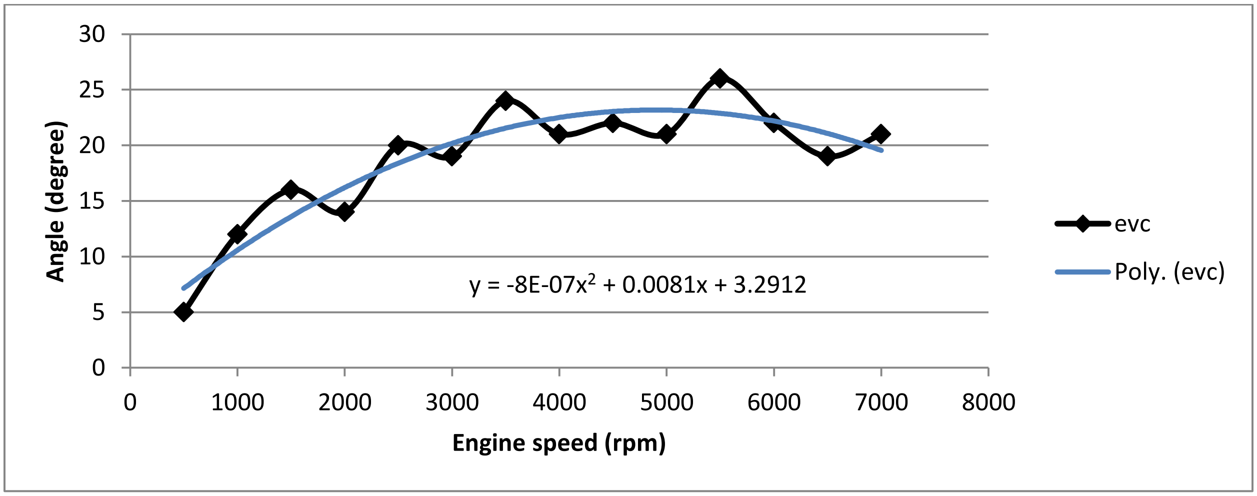

Figure 4.10 Exhaust valve closing angles

e = 0.12

Valve lifts for both intake and exhaust valves show a generally increasing trend with increasing engine speed, and also with relatively less fluctuation. Here the sample points can easily be approximated to a single linear function.

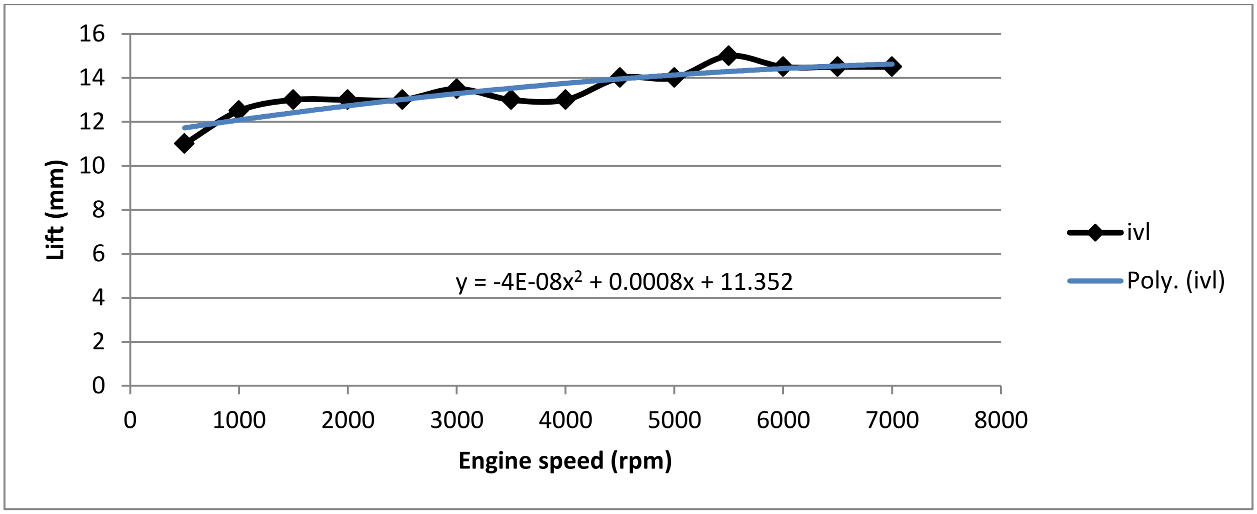

Figure 4.11 Intake valve lift values

e = 0.03

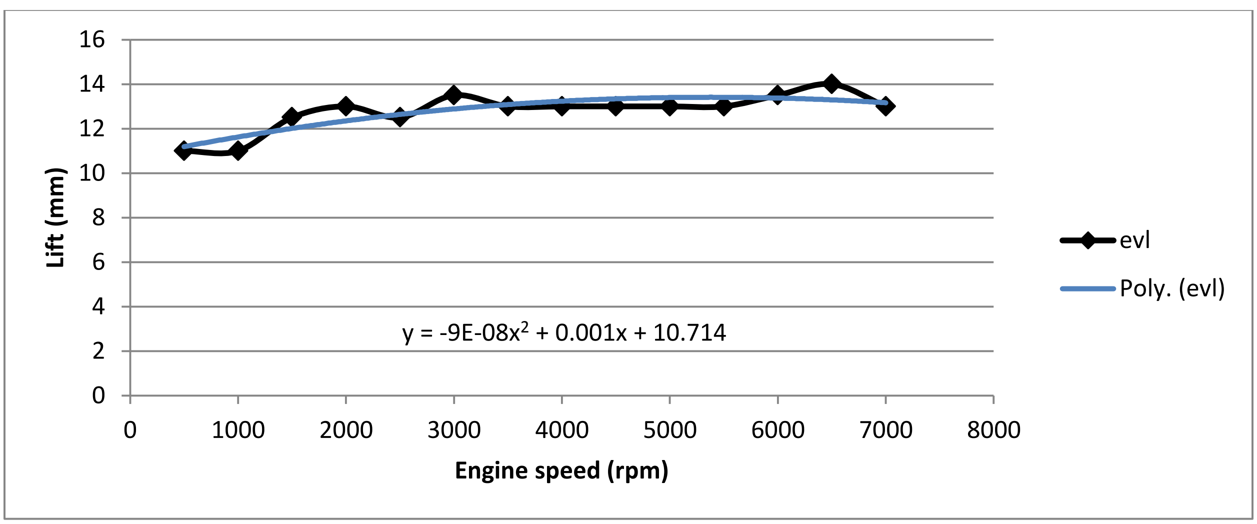

Figure 4.12 Exhaust valve lift values

e = 0.03

4.4. Modification of cam profile

As has been seen in previous section, all the cam profile variables have fluctuating values. In this condition, it is not possible to design and apply a camshaft with such shape. Even if the camshaft could be designed, it would be hard to develop a practical follower system to go with this camshaft. This problem is avoided by using one or two linear functions that can fairly describe the trend of the variables.

Linear function approximations of the cam profile variables are presented in table 4.4. Here the functions are drawn in a way to match the values of the variables obtained from the simulation as closely as possible.Diamondshapes are used to mark the simulated results and squareshapes connected with straight lines are used for the modified values.

Table 4.4 Modified valve timing parameters

rpm	ivo	ivc	evo	evc	ivl	evl
500	15.00	6.00	24.00	10.00	12.00	11.50
1000	18.13	10.00	25.71	11.86	12.23	11.69
1500	21.25	14.00	27.43	13.71	12.46	11.88
2000	24.38	18.00	29.14	15.57	12.69	12.08
2500	27.50	22.00	30.86	17.43	12.92	12.27
3000	30.63	26.00	32.57	19.29	13.15	12.46
3500	33.75	30.00	34.29	21.14	13.38	12.65
4000	36.88	34.00	36.00	23.00	13.61	12.85
4500	40.00	38.00	40.83	22.67	13.85	13.04
5000	35.40	45.40	45.67	22.33	14.08	13.23
5500	30.80	52.80	50.50	22.00	14.31	13.42
6000	26.20	60.20	55.33	21.67	14.54	13.62
6500	21.60	67.60	60.17	21.34	14.77	13.81
7000	17.00	75.00	65.00	21.00	15.00	14.00

For ivo angles shown in figure 4.13, two linear functions are used one going continuously up to 4500 rpm and the second one up to the 7000 rpm. It can be seen that two of the sample points at

500 rpm and 4000 rpm are far out of the trend line. Also the points at 1500 and 2000 rpm are slightly out of the trend line, but the rest 10 sample points are very closely represented.

Error values obtained with equation 4.1 and the equations describing the functions are given below the graphs for all parameters.

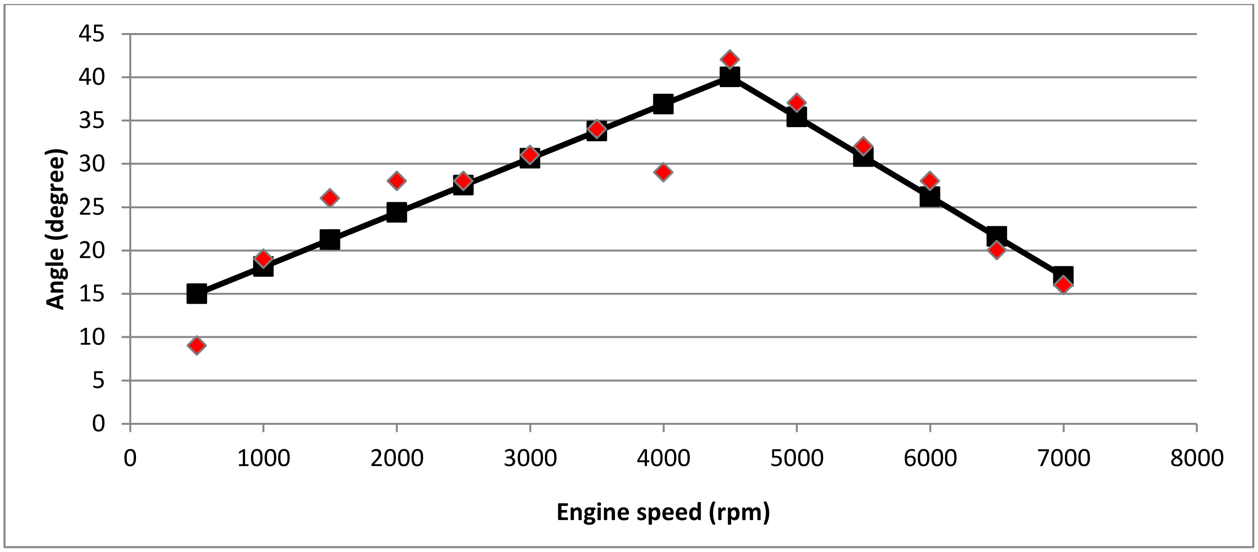

Figure 4.13 Modified intake valve opening angles

$IVO/BTDC = (0.00625 \times RPM) + 11.875$*For : 500*$\leq RPM \leq 4500$

$IVO/BTDC = (-0.0092 \times RPM) + 81.4$*For :4500*$\leq RPM \leq 7000$

e = 0.119

Similarly for ivc angles, three sample points at 2000 rpm, 3500 rpm and 4000 rpm are seen to be slightly far out of the trend line, but the rest 11 sample points fairly conform to the modified function. It should also be noted that the two linear functions intersect at 4500 rpm, which is similar to the functions for ivo angles. This is because both ivo and ivc angles are supposed to be modeled on the same cam, and can be made by linearly connecting three cam profiles at 500 rpm, 4500 rpm and 7000 rpm.

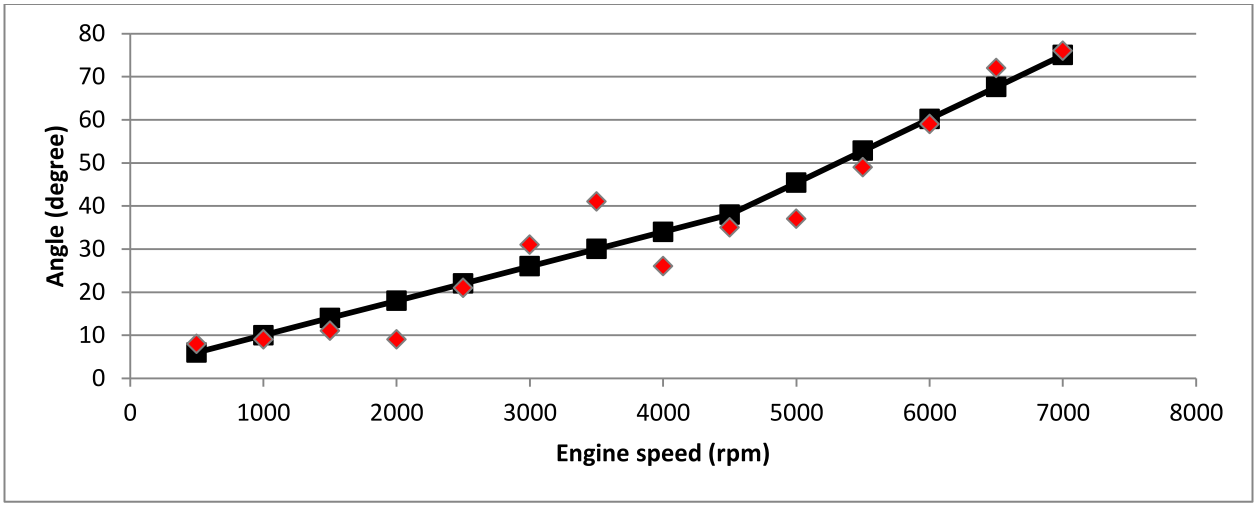

Figure 4.14 Modified intake valve closing angles

$IVC/ABDC = (0.008 \times RPM) + 2$*For : 500 ≤ RPM ≤ 4500*

$IVC/ABDC = (0.0148 \times RPM) - 28.6$*For :4500 ≤ RPM ≤ 7000*

e = 0.207

When coming to evo angles, almost all sample points conform to the trend line except two points at 4000 rpm and 6000 rpm that are slightly out of the trend line. As shown in figure 4.15 below, the two modified functions intersect at 4000 rpm, which means the functions for evc should also intersect at 4000 rpm.

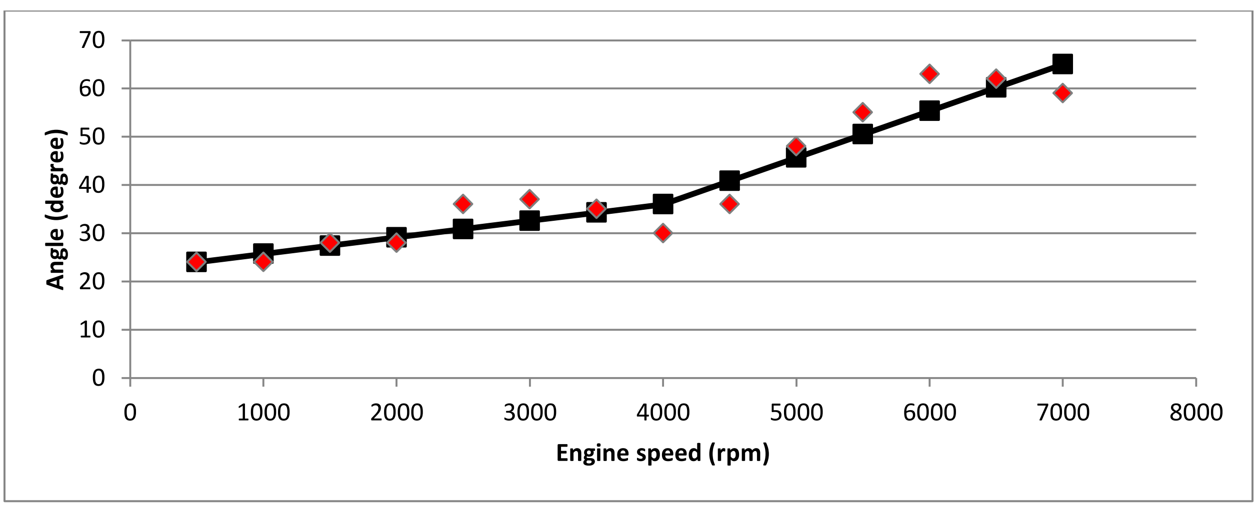

Figure 4.15 Modified exhaust valve opening angles

$EVO/BBDC = (0.00343 \times RPM) + 22.286$ *For : 500 ≤ RPM ≤ 4000*

$EVO/BBDC = (0.00966 \times RPM) - 2.667$ *For : 4000 ≤ RPM ≤ 7000*

e = 0.081

Figure 4.16 shows evc angles which and slightly out at 500 rpm and 5500 rpms. The rest 12 sample points fairly conform to the two linear function approximations that intersect at 4000 rpm, which is same intersection point as the functions of evo angles.

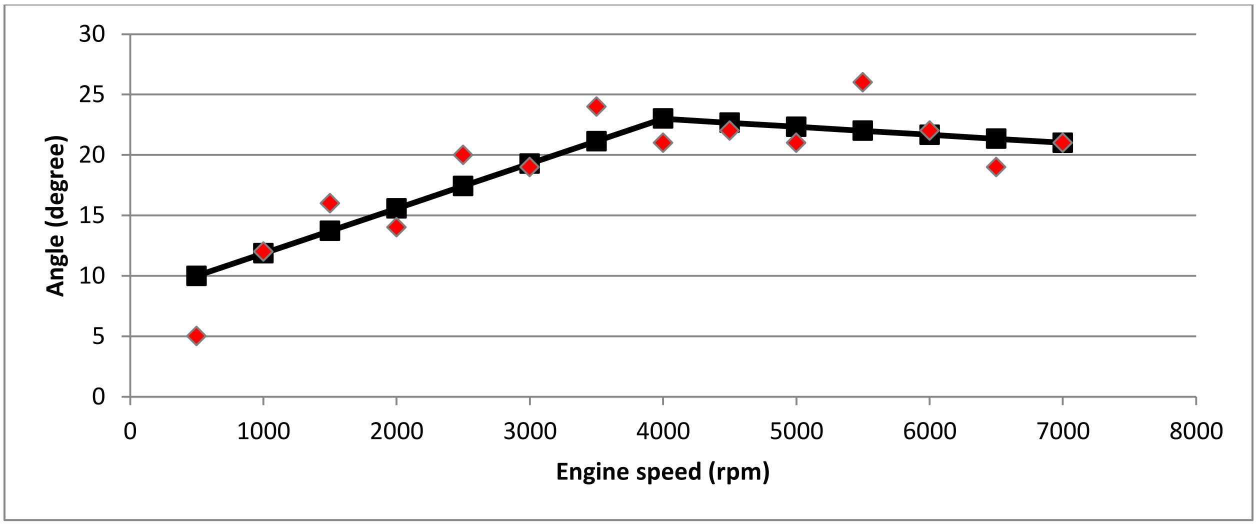

Figure 4.16 Modified exhaust valve closing angles

$EVC/ATDC = (0.00371 \times RPM) + 8.145$ *For : 500 ≤ RPM ≤ 4000*

$EVC/ATDC = (0.00066 \times RPM) + 25.64$ *For : 4000 ≤ RPM ≤ 7000*

e = 0.143

Lift values for both intake and exhaust valves are each represented by single linear functions with increasing trends from start to end as shown in figures 4.17 and 4.18.

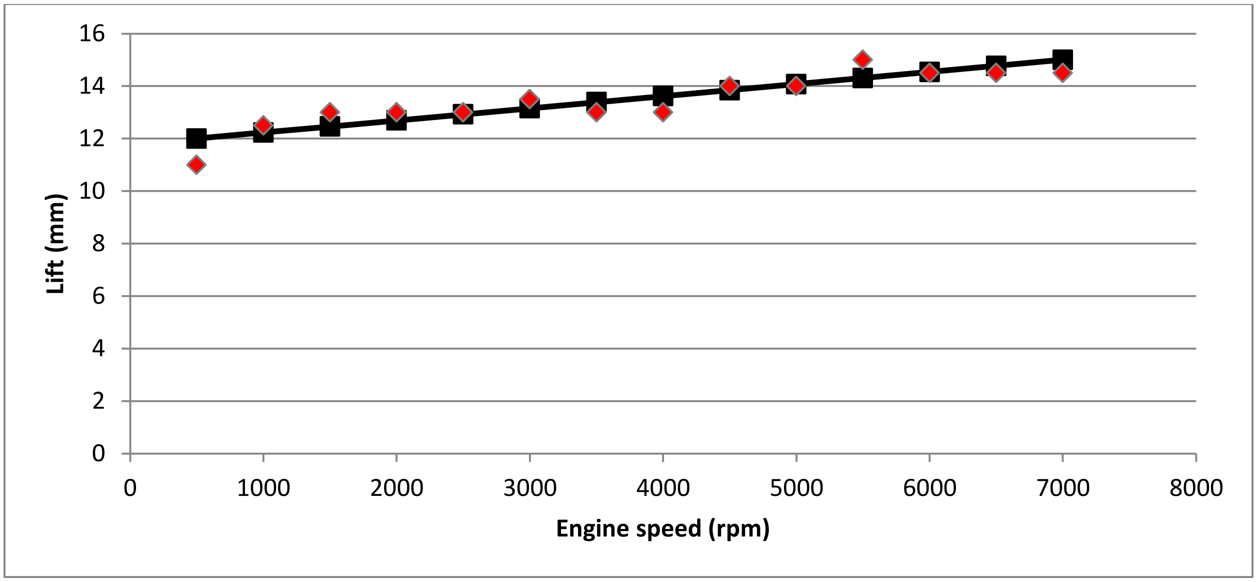

Figure 4.17 Modified intake valve lift values

$$IVL = (0.00046 \times RPM) + 11.76$$

e = 0.029

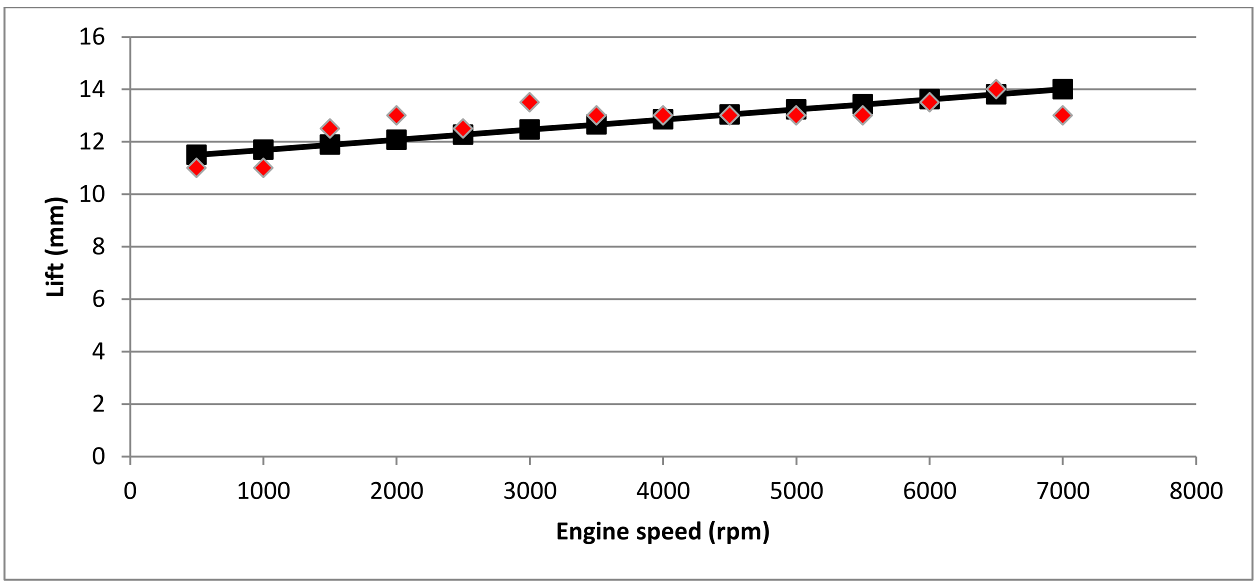

Figure 4.18 Modified exhaust valve lift values

$$EVL = (0.00038 \times RPM) + 11.308$$

e = 0.036

When comparing the average error factors of the second order polynomial curve fitting and the linear data fitting, the linear data fitting has higher error for IVC, EVC and EVL while it has lesser error for IVO, EVO and IVL.

4.4.1. Major cam profile variables

The major cam profiles define the shape of the cam when the axial distance between them is clearly known, which will be discussed in detail in the modeling section of this paper. But first these major cam profiles are summarized in table 4.5. For intake cam profile, the three defining points at 500 rpm, 4500 rpm and 7000 rpm are given the name IC1 , IC2 and IC3 respectively. Similarly the defining points for exhaust cam at 500 rpm, 4000 rpm and 7000 rpm are given the name EC1, EC2 and EC3 respectively.

Table 4.5 Major cam profile variables

	obtdc	cabdc	lift
IC1	15	6	12
IC2	40	38	13.846
IC3	17	75	15
	obbdc	catdc	lift
EC1	24	10	11.5
EC2	36	23	12.846
EC3	65	21	14

4.5. Performance of original engine camshaft

To estimate the performance of the original camshaft of the engine in this study, it is necessary to have a complete cam profile variable values. But this was not possible because such data for this engine model is not provided by the manufacturer and such type of information is not commonly provided by most manufacturers.

The second best option is to select a cam profile from those obtained in the simulation that better meets manufacturer power and torque specification, and at the same time gives better performance for all speed ranges. In this regard, the 3000 rpm cam is selected to be the original camshaft on this engine and its performance estimation obtained from conducted simulation is presented in table 4.6.

Table 4.6 Performance of existing camshaft

Engine RPM	VolEff	Brake Tq	Brake Kw	BSFC
500	69.232	130.36	6.82	0.321
1000	79.974	175.57	18.39	0.276
1500	84.248	197.9	31.09	0.257
2000	100.48	232.2	48.63	0.262
2500	104.938	243.04	63.63	0.261
3000	96.275	226.15	71.05	0.257
3500	86.283	197.22	72.29	0.265
4000	86.998	195.1	81.73	0.269
4500	90.166	199.2	93.88	0.274
5000	90.382	195.05	102.13	0.28
5500	89.871	187.25	107.85	0.29
6000	87.114	174.7	109.77	0.301
6500	79.382	151.38	103.04	0.317
7000	74.568	131.42	96.34	0.343

For more clear observation, each performance parameter is plotted with respect to engine speed. Figure 4.19 shows the volumetric efficiency characteristics of the camshaft. From the figure, it is seen that better volumetric efficiency is attained at around 2500 rpm, and most optimum cam profiles show the same behavior even if they improve the volumetric efficiency at their respective engine speeds.

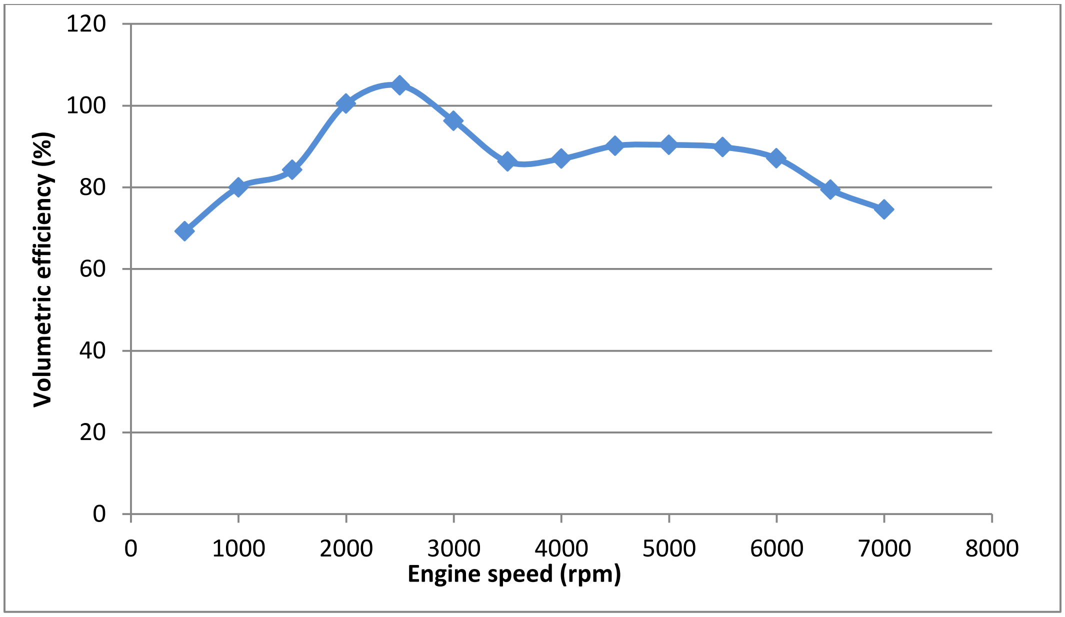

Figure 4.19 Existing camshaft volumetric efficiency

As for brake torque, maximum value is shown to be 243 Nm at 2500 rpm according to simulation result, but manufacturer specification states maximum torque is 198 Nm at 4400 rpm. Even though the maximum torque and the engine speeds for maximum torque are different, the simulation result shows a brake torque of 199.2 Nm at 4500 rpm which is almost the same as the specification for that speed.

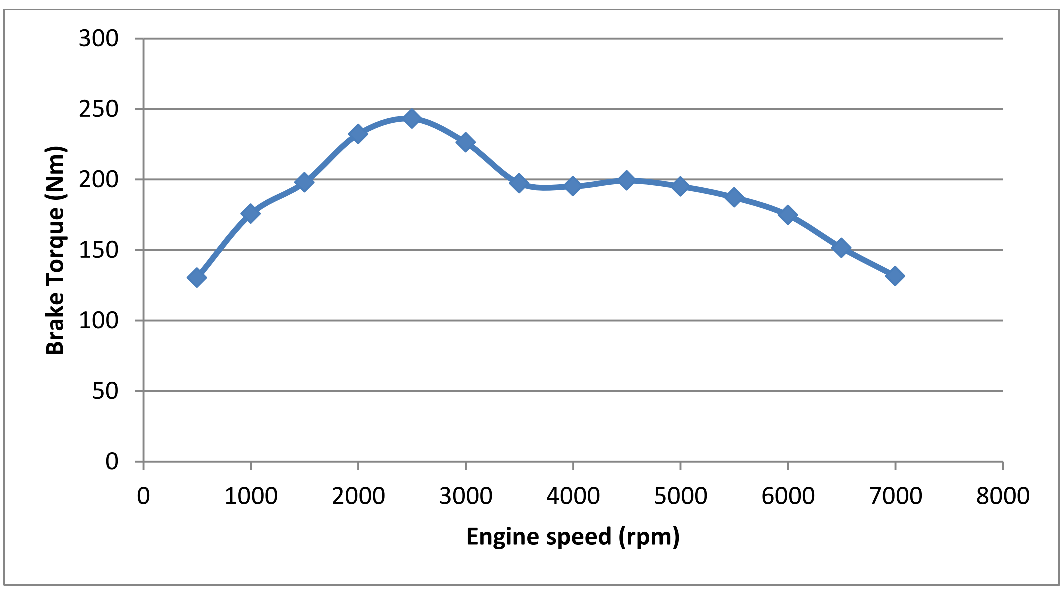

Figure 4.20 Existing camshaft brake torque

The engine is also said to have a maximum brake power of 102 kw at 5200 rpm, while the simulation shows also a similar brake power of 102.13 kw at 5000 rpm. However, according to the simulation, maximum brake power is seen to be 109.77 kw at 6000 rpm.

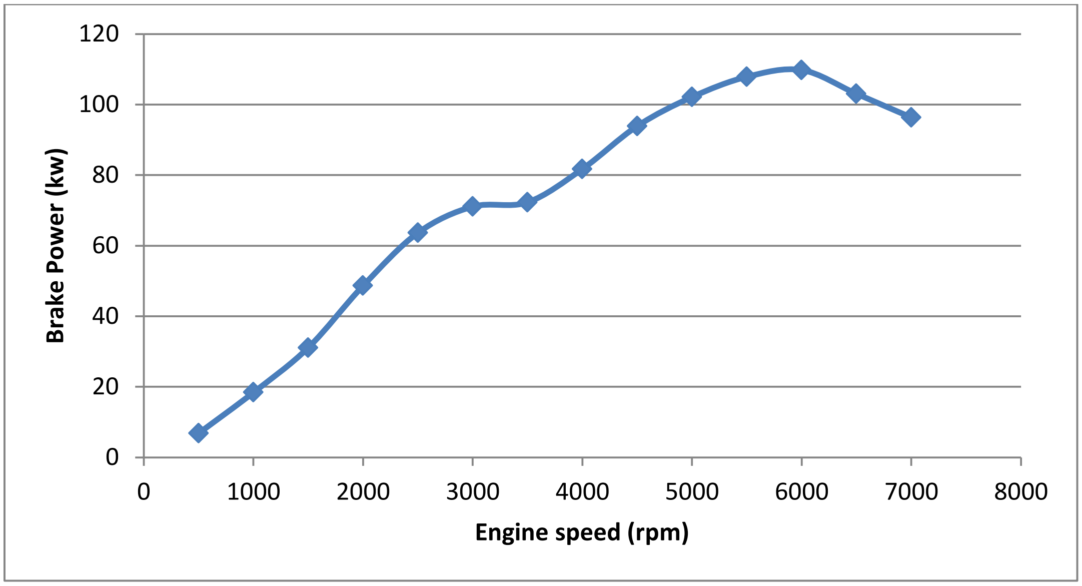

Figure 4.21 Existing camshaft brake power

Brake specific fuel consumption shown in figure below has a minimum value of 0.257 kg/kw.hr at 1500 rpm and 3000 rpm increases for both higher and lower engine speeds.

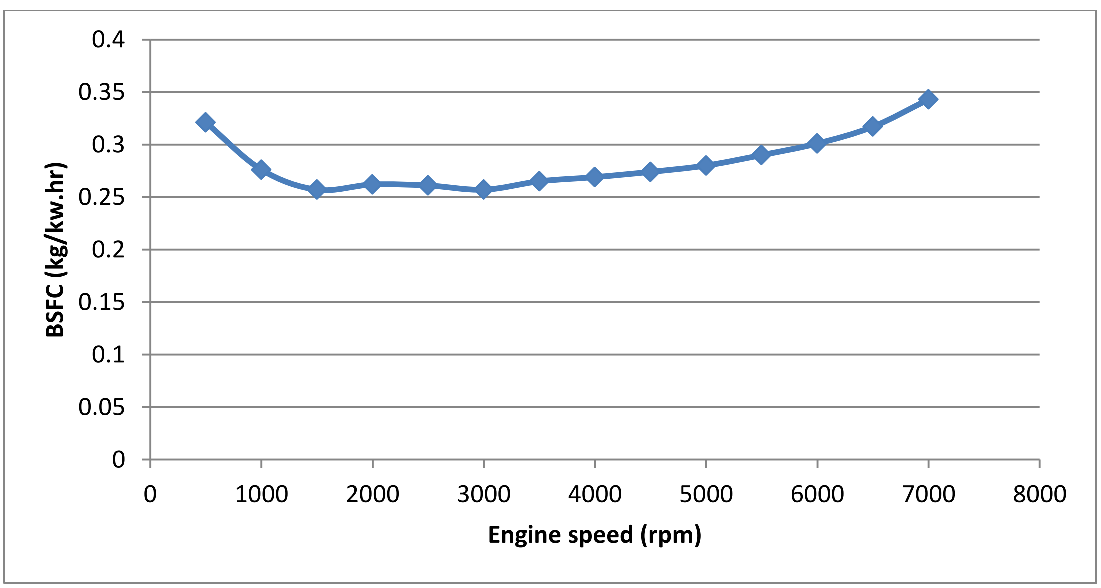

Figure 4.22 Existing camshaft brake specific fuel consumption

The engine performance parameters discussed above clearly show some variations from the specification data, especially for brake torque values at lower speeds. However, these variations are a matter of exact camshaft variables identification, and to some extent the equations and algorithm employed in the simulation program. That been said, the variations are not that much considerable. Since the study is focused at improving the performance of the engine, improvement shown is assumed to happen in reality only with similarly small variations.

4.6. Performance of new CVVT camshaft

The new CVVT camshaft is just a combination of 14 different cam profiles, each tuned to give optimum performance at specific engine speeds aligned and linearly connected in an axial manner. Their linear connection gives infinite number of cam profiles to operate from low to high speed ranges.

Volumetric efficiency characteristics of all cam profiles are presented in figure 4.23. All 14 cam profiles are designated C1 to C14 respectively. From the figure, it is seen that cam profiles with higher volumetric efficiency at lower speeds have lower volumetric efficiency at higher speeds and vice versa. Also volumetric efficiencies of slightly higher than 100% are seen at around 2500 rpm and are higher for most cam profiles at these speeds. This is also the reason for higher torque at these engine speeds.

With proper tuning, volumetric efficiencies above 100% canalso be reached by naturally aspirated engines. The limit for naturally aspirated engines is about 130%. VE's of up to 130% havebeen reported in various experimental studies [21].

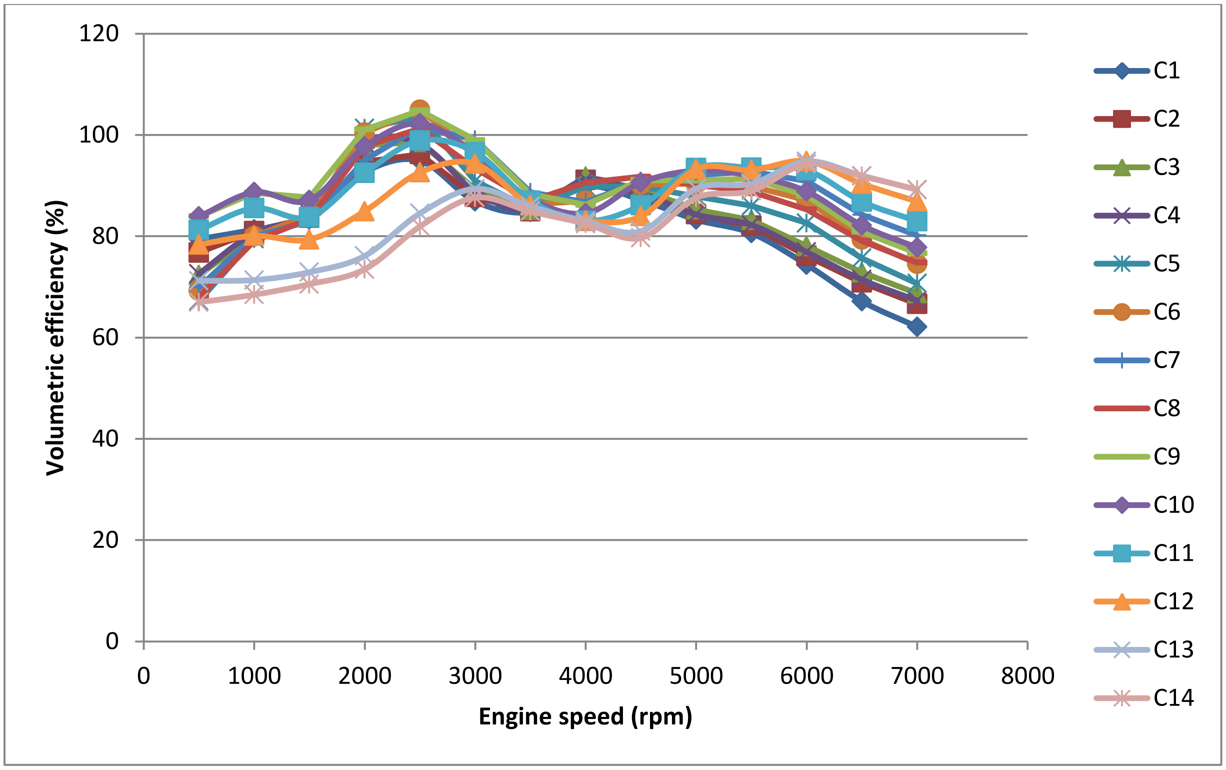

Figure 4.23 Optimum cam profiles volumetric efficiency

Simulation results of brake torque for the new CVVT camshaft is presented in figure 4.24 for all 14 cam profiles. Just like for volumetric efficiency, the cam profiles with higher brake torque at low speeds have lower torque values at high speeds and vice versa.

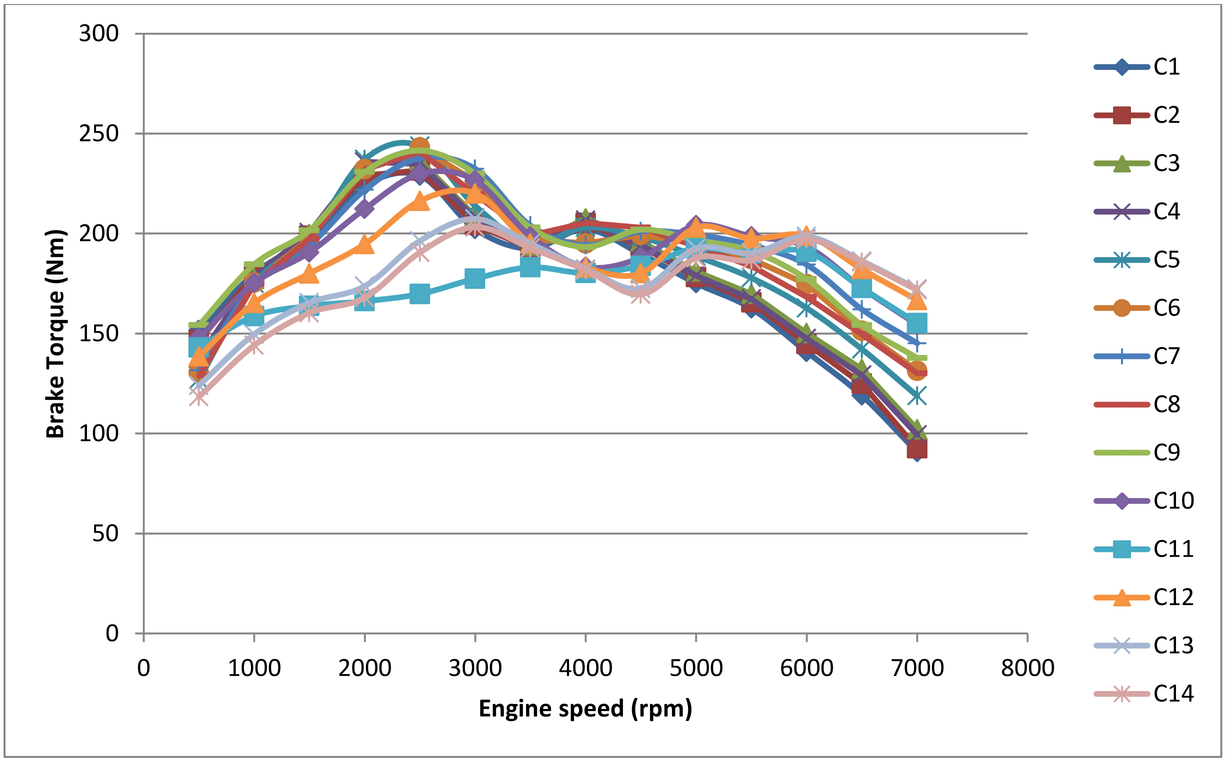

Figure 4.24 Optimum cam profiles brake torque

Brake power values of the CVVT camshaft are shown in figure 4.25 for all optimum cam profiles. As can be seen in the figure, larger differences in brake power are observed at higher engine speeds, especially above 5000 rpm. However, the spark advance setup in the simulation could have been the reason, and with appropriate spark control, it is possible to improve low speed power as well. It is important to give more emphasis to volumetric efficiency which is directly related to, but not only valve events. The other parameters directly relate to volumetric efficiency, but also depend on spark timing, air/fuel ratio and many more factors.

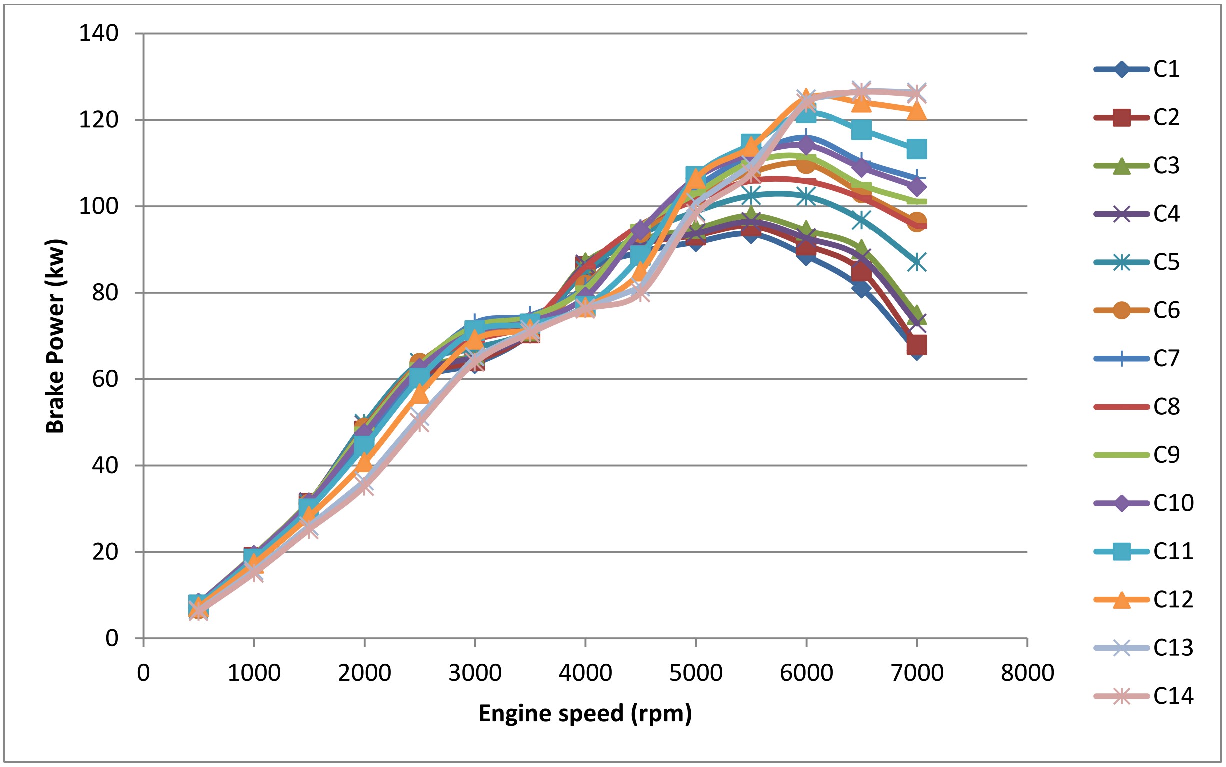

Figure 4.25 Optimum cam profiles brake power

Brake specific fuel consumption values are shown in figure 4.26, in which all cam profiles tend to show lower values at the lower end of mid-range speeds. The behaviors of low speed and high speed cam profiles discussed in volumetric efficiency and brake torque are also similarly observed in BSFC values.

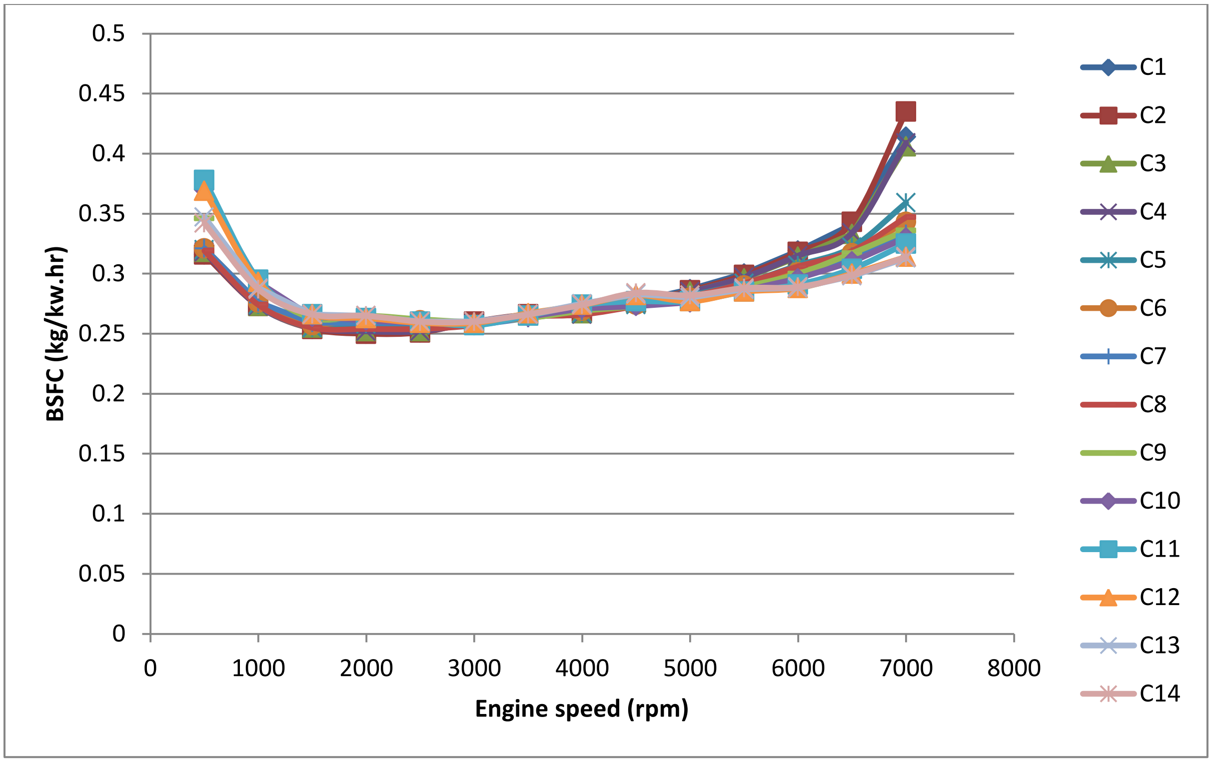

Figure 4.26 Optimum cam profiles brake specific fuel consumption

4.7. Performance improvement with new CVVT camshaft

The original engine camshaft and the new CVVT camshaft performance parameters are plotted with respect to engine speed to assess their difference. In figure below, volumetric efficiencies of both camshafts are shown with diamond markers for CVVT and triangle markers for the original camshafts. As can be seen from the figure, large improvements in volumetric efficiencies are obtained at higher speeds of above 5500 rpm and lower speeds below 1500 rpm. Also minimum improvements are shown around 1500 to 3500 rpm.

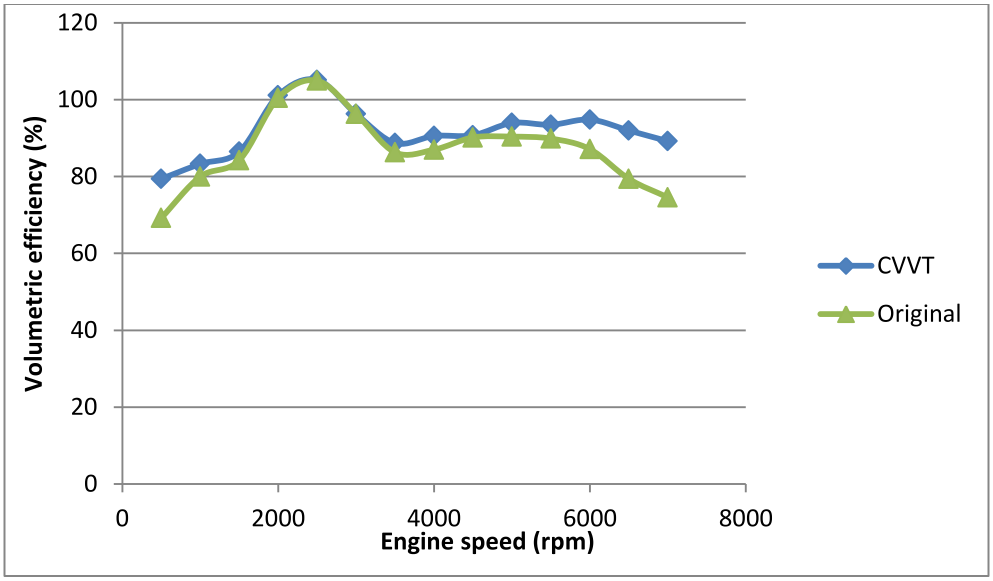

Figure 4.27 CVVT and existing camshaft volumetric efficiency

Similarly, larger improvements are observed at very low speeds below 1000 rpm and at higher speeds above 5000 rpm. This is because the default camshaft optimized for 3000 rpm performs better at medium speeds of around 3000 rpm.

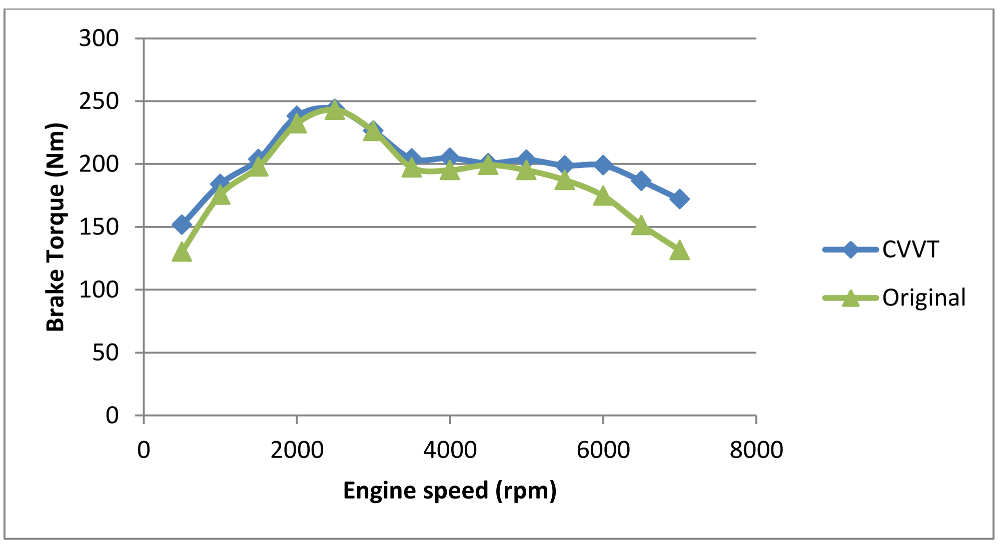

Figure 4.28 CVVT and existing camshaft brake torque

For brake power, larger improvements are seen at higher speeds above 5000 rpm. However, there are small improvements in the rest of the speed ranges, especially at speeds of below 1500 rpm. It should also be noted that the percent improvement shown in table 4.7 for power is similar to that of toque for all speed ranges, but since brake power is lower at lower speeds, the changes are difficult to detect.

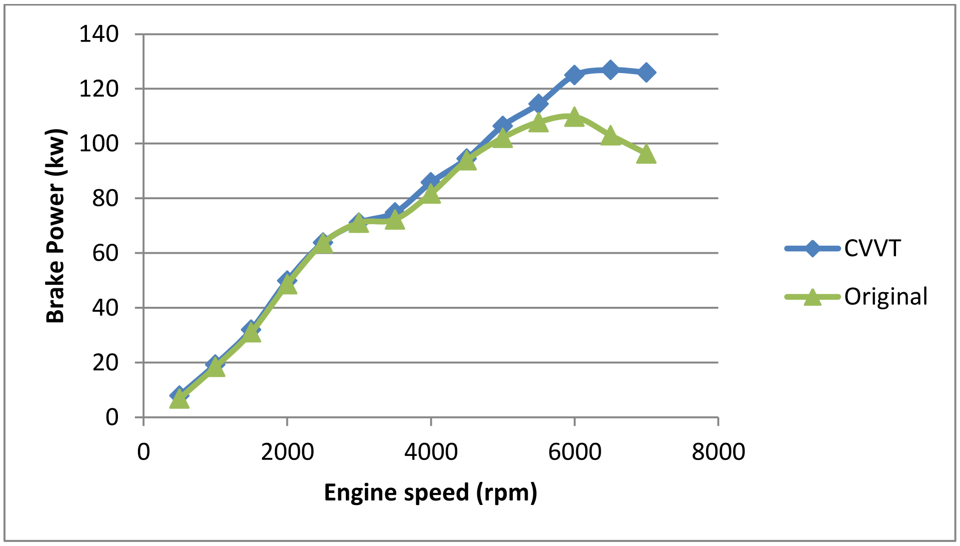

Figure 4.29 CVVT and existing camshaft brake power

Better improvements in BSFC are also shown at speeds above 5000 rpm, while the changes are lower than 5% for most of the rest speed range.

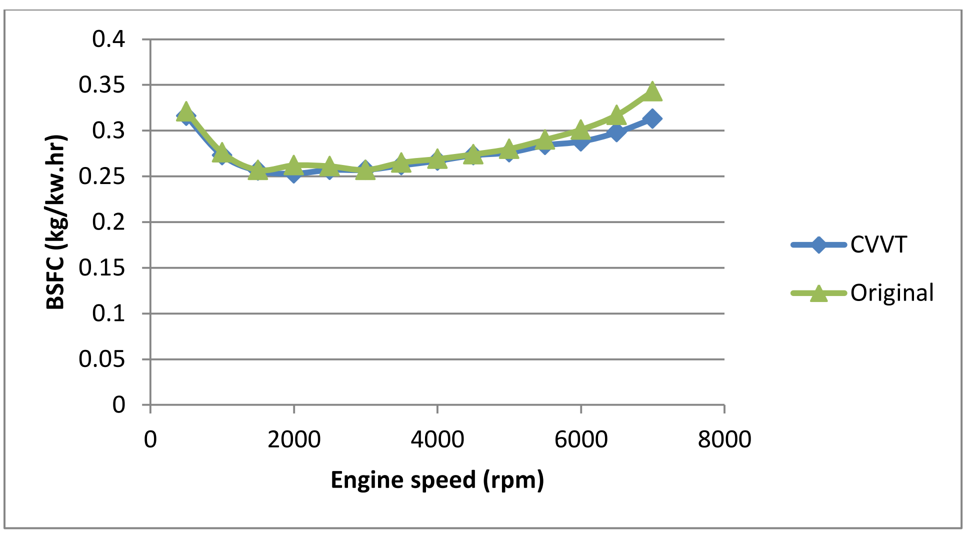

Figure 4.30 CVVT and existing camshaft brake specific fuel consumption

Percent improvements on the engine performance parameters of interest at each sample speed are listed in table 4.7.

Table 4.7 CVVT camshaft performance percent improvement

Engine RPM	Vol Eff (%)	Brake Tq (%)	Brake Kw (%)	BSFC (%)
500	14.69	16.31	16.42	1.56
1000	4.13	4.84	4.84	1.09
1500	2.61	2.99	2.96	0.39
2000	0.71	2.53	2.53	3.44
2500	0.05	0.29	0.30	1.53
3000	0.00	0.00	0.00	0.00
3500	2.81	3.54	3.54	1.13
4000	4.09	4.97	4.97	0.74
4500	0.64	0.70	0.68	0.36
5000	3.94	4.25	4.25	1.43
5500	4.00	6.17	6.17	2.07
6000	8.83	13.86	13.86	4.32
6500	15.86	23.13	23.14	5.99
7000	19.62	30.82	30.81	8.75

Results in table above are plotted with respect to engine speed in upcoming figures. Figure below shows the percent improvements for volumetric efficiency at different engine speeds. Here it is seen that larger volumetric efficiency improvements are attained at high engine speeds of above 5500 rpm, and a maximum value of 19.62% at7000 rpm. Also a large value of 14.69% is seen at 500 rpm.

At 2000 and 2500 rpm reductions in volumetric efficiency of 0.71% and 0.05% respectively are observed. However, it is also seen in the coming figure that the BSFC values at these speeds are reduced by 3.4% and 1.5% respectively. This is mainly the result of the less emphasis given to spark timing in this study. If more air fuel mixture is inducted into combustion chamber, and spark timing is the same, some fraction of mixture will be left unburned, increasing fuel wastage. Since the tuning process is done in a way to increase volumetric efficiency, and also reduce fuel consumption, the 3000 rpm cam profile has a slightly higher volumetric efficiency, but also a slightly lower BSFC and higher torque and power for this specific engine spark timing setup.

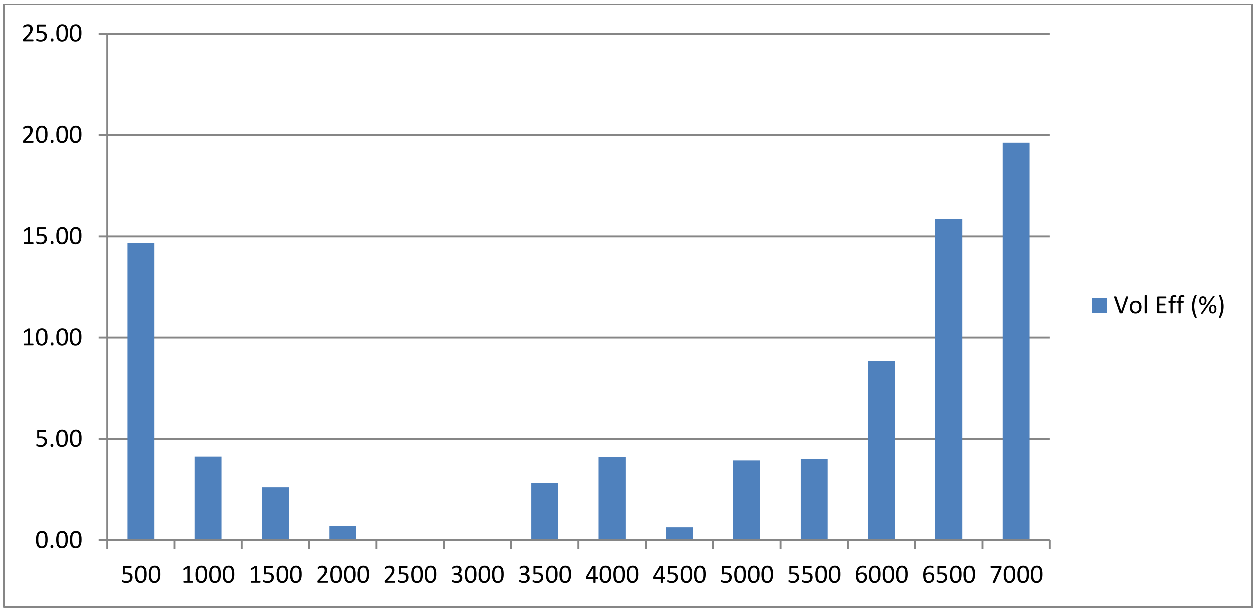

Figure 4.31 CVVT camshaft percent improvements in volumetric efficiency

Maximum percent improvement for brake torque is 30.82% at 7000 rpm and a minimum percent improvement is 0.0% at 3000 rpm. As seen in figure 4.32, larger improvements are seen at engine speeds of above 5500 rpm and at low speeds below 1000 rpm.

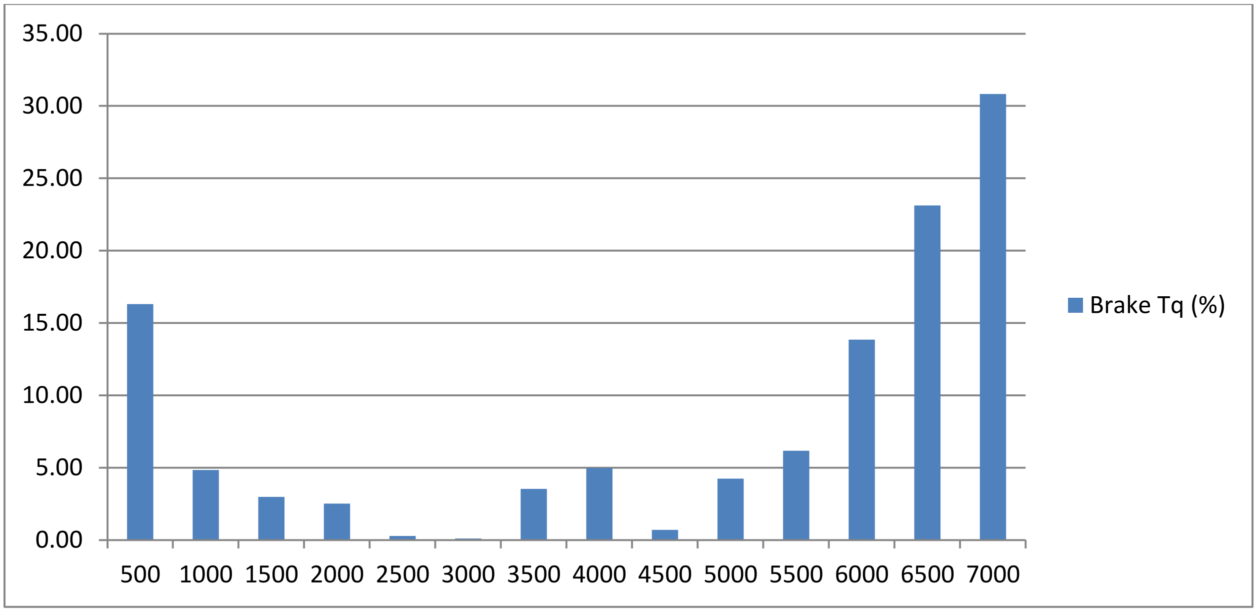

Figure 4.32 CVVT camshaft percent improvements in brake torque

Percent improvements for brake power are exactly the same as brake torque with negligible differences at some engine speeds.

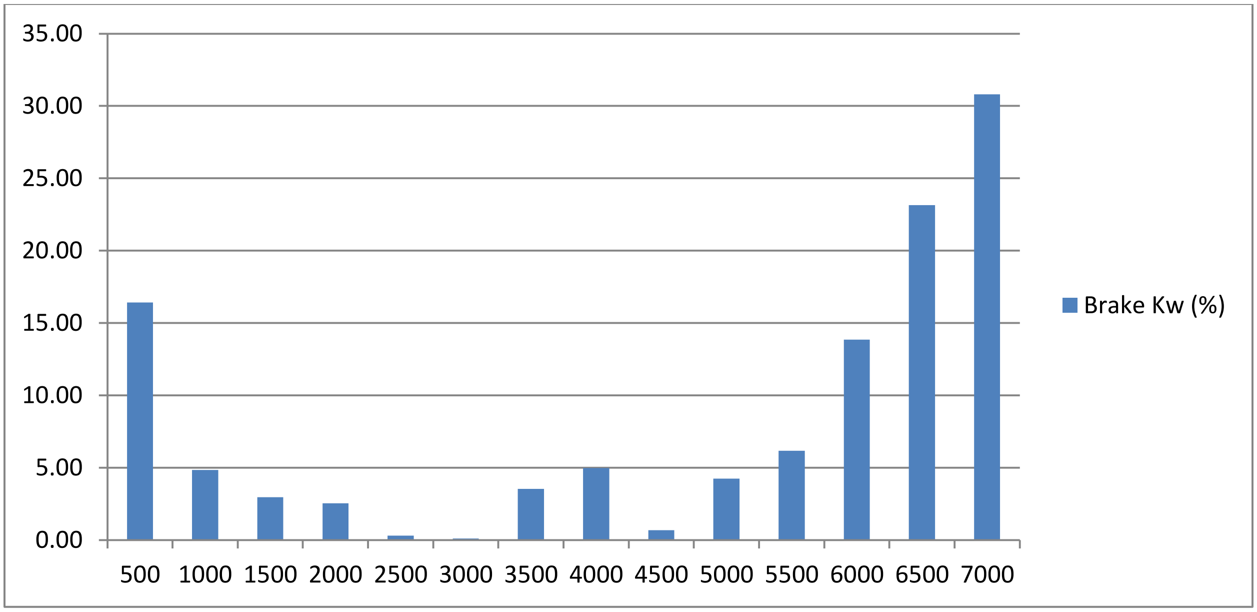

Figure 4.33 CVVT camshaft percent improvements in brake power

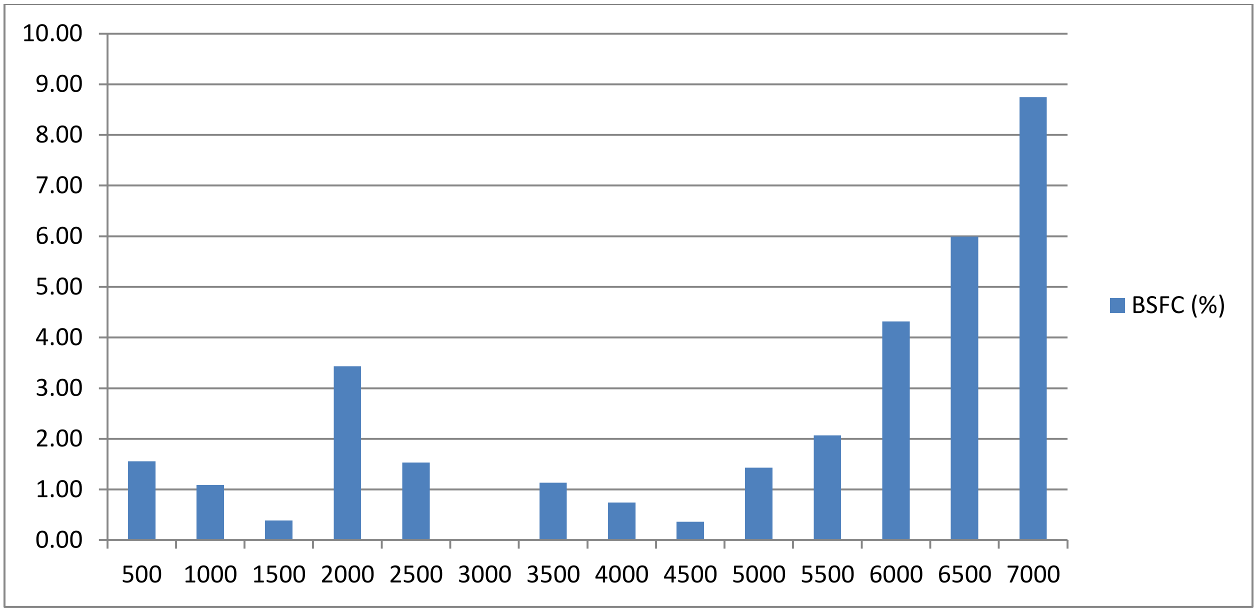

Figure 4.34 CVVT camshaft percent improvements in brake specific fuel consumption

4.8. Fuel saving and Co$_2$ emission reduction

Carbon dioxide emissions are calculated at the same rpm for both the existing and new camshaft and compared to determine the difference. Multiplying bsfc by brake power gives the fuel consumption in kg/hr.

To illustrate this, at 2000 rpm, the existing camshaft has a bsfc of 0.262kg/kw.kr and a brake power of 48.63kw, while the new camshaft has a bsfc of 0.253kg/kw.kr and a brake power of 49.86kw. The fuel consumptions in kg/hr are calculated as shown below.

$$F_C(kg/hr) = bsfc \times P_b \ldots\ldots\ldots\ldots\ldots\ldots\ldots\ldots\ldots\ldots\ldots (4.2)$$

$$F_{Ce}(kg/hr) = 0.262kg/kw.hr \times 48.63kw = \mathbf{12.74kg/hr}$$

$$F_{Cn}(kg/hr) = 0.253kg/kw.hr \times 49.86kw = \mathbf{12.61kg/hr}$$

The difference in fuel consumption is calculated by subtraction to be ***0.13 kg/hr.*** Assuming both vehicles are operated 8 hours per day, the daily fuel saving will be

$$Daily\ fuel\ saving = 0.13kg/hr \times 8hr/day = \mathbf{1.04kg/day}$$

However, this calculation method does not give accurate estimations of fuel savings since the vehicles will not operate for the same amount of time to cover a specific distance due to their difference in power output. To make the estimations more accurate, maximum possible speeds of vehicles should be determined at this rpm in km/hr, while taking aerodynamic drag into consideration.

$$R_a = \frac{1}{2} \times \rho_a \times C_D \times A_f \times V^2 \qquad (4.3)$$

$$R_{rl} = \mu \times W_v \qquad (4.4)$$

where., $\mu = 0.015 + (0.00016 \times v)$ ...... 'v' is 'km/h

or $\mu \approx 0.028$

Total vehicle resistance can be calculated as,

$$R_t = R_a + R_{rl} \qquad (4.5)$$

Maximum possible speed

$$V = \frac{P_b}{R_t} = \frac{P_b}{R_a + R_{rl}} \qquad (4.6)$$

$$P_b = V \times (\mu \times W_v + \frac{1}{2} \times \rho_a \times C_D \times A_f \times V^2)$$

$$P_b = V \times (0.028 \times 19620N + \frac{1}{2} \times 1.05kg/m^2 \times 0.3 \times 3.06m^2 \times V^2)$$

$$P_b = 549V + 0.48V^3$$

Substituting brake power for both new and existing camshaft and calculating velocity,

$$V_e = 38.54m/s = \mathbf{138.74km/hr}$$

$$V_n = 38.99m/s = \mathbf{143.17km/hr}$$

Now, fuel consumption can be calculated in kg/km as,

$$F_c(kg/km) = \frac{F_c(kg/hr)}{V(km/hr)}$$

$$F_{ce}(kg/km) = 0.092kg/km$$

$$F_{cn}(kg/km) = 0.088kg/km$$

Assuming both the vehicles are driven 100km/day, the existing engine fuel consumption will be **9.2 kg/day** while that of the new one will be **8.8kg/day.** This means **0.4kg** of fuel can be saved daily.

If the vehicles are operated for 100 days in a year, the yearly fuel saving can be calculated as,

$$Fuel\ saving_{annual} = Fuel\ saving_{daily} \times 100$$

$$Fuel\ saving_{annual} = 0.4kg/day \times 100day/year = \mathbf{40kg/year}$$

In this same manner, the fuel saving estimations for all rpms is calculated and analyzed.

Table 4.8 Fuel saving calculations summary

	Existing Camshaft			CVVT Camshaft			Fuel Saving	
RPM	F_c(kg/hr)	V(km/hr)	F_c(kg/km)	F_c(kg/hr)	V(km/hr)	F_c(kg/km)	F_s(kg/km)	F_s(kg/yr)
500	2.19	40.32	0.05	2.51	46.63	0.05	0.000494	4.94
1000	5.08	82.58	0.06	5.26	86.70	0.06	0.000749	7.49
1500	7.99	111.17	0.07	8.19	115.15	0.07	0.000713	7.13
2000	12.74	138.74	0.09	12.61	143.17	0.09	0.003999	39.99
2500	16.61	156.85	0.11	16.40	160.21	0.10	0.003503	35.03
3000	18.26	164.66	0.11	18.28	168.07	0.11	0.002139	21.39
3500	19.16	165.92	0.12	19.61	176.87	0.11	0.004577	45.77
4000	21.99	174.92	0.13	22.91	187.45	0.12	0.003488	34.88
4500	25.72	185.44	0.14	25.80	195.27	0.13	0.006575	65.75
5000	28.60	192.02	0.15	29.39	205.10	0.14	0.005648	56.48
5500	31.28	196.38	0.16	32.52	217.34	0.15	0.009647	96.47
6000	33.04	197.78	0.17	35.99	225.12	0.16	0.007162	71.62
6500	32.66	192.74	0.17	37.81	226.44	0.17	0.002488	24.88
7000	33.04	187.45	0.18	39.44	225.89	0.17	0.001668	16.68

Now Co2 emission can be calculated as,

$$Co_2\ reduced\ =\ Fuel\ saved \times CL \times OF$$

Where

CL=carbon content of fossil fuels, 0.77ton/kl (fraction)

OF=oxidation factor for fossil fuels, 0.995 (fraction)

At 2000 rpm, fuel saving is seen to be 40 kg/year

$$Co_2\, reduced\ =\ 40kg/yr \times 0.77kg/lit \times 0.995 \times \frac{1}{0.86kg/lit}$$

$$Co_2\, reduced\ = \mathbf{35.6 kg/yr}$$

Similarly, fuel savings at all rpm are calculated including their percentages and summarized in table 4.9.

Table 4.9 Annual Co_2 reduction

RPM	Fs(kg/yr)	Co_2(kg/yr)	Percentage
500	4.94	4.40	0.91
1000	7.49	6.67	1.22
1500	7.13	6.35	0.99
2000	39.99	35.63	4.05
2500	35.03	31.20	3.31
3000	21.39	19.05	1.93
3500	45.77	40.77	3.96
4000	34.88	31.07	2.78
4500	65.75	58.58	4.74
5000	56.48	50.32	3.79
5500	96.47	85.94	6.06
6000	71.62	63.81	4.29
6500	24.88	22.16	1.47
7000	16.68	14.86	0.95

As can be seen in figure 4.35, a maximum fuel saving of 96.47kg/yr is achieved at 5500 rpm. Also figure 4.36 shows a maximum Co2 emission reduction of 85.9kg/yr at a similar engine speed of 5500 rpm.

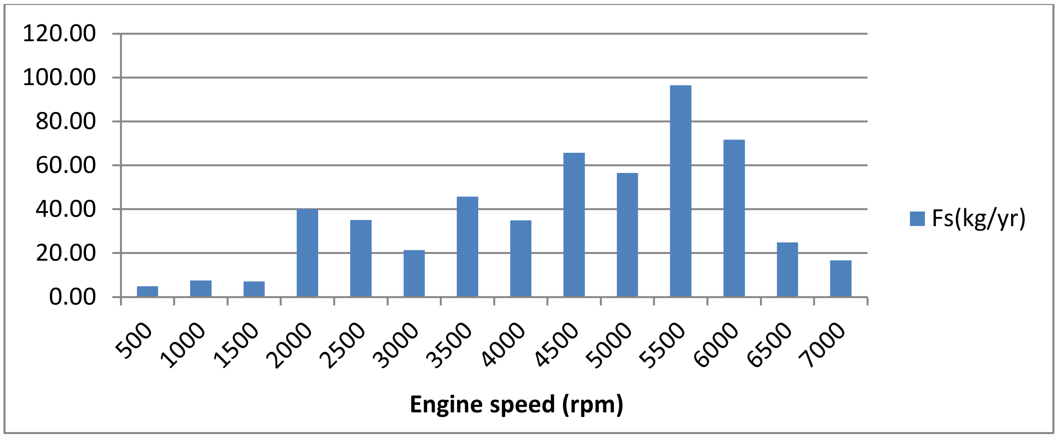

Figure 4.35 Annual fuel savings

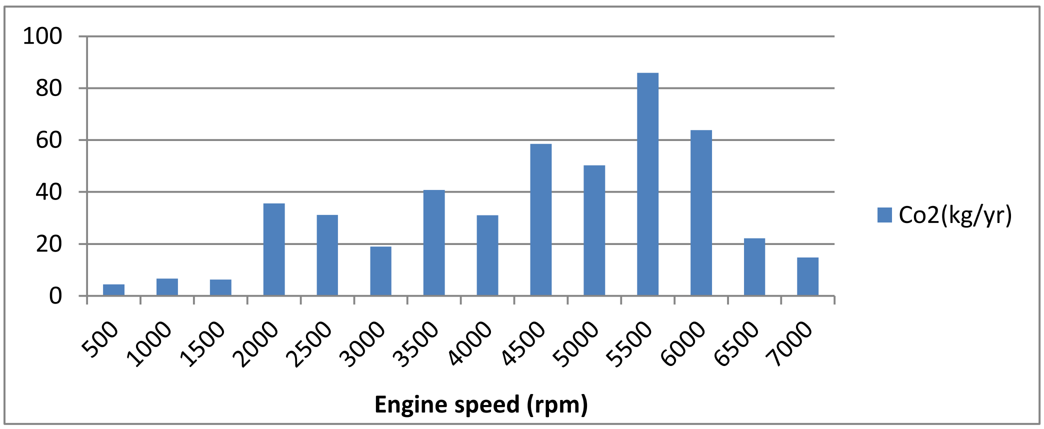

Figure 4.36 Annual Co_2 emission reductions

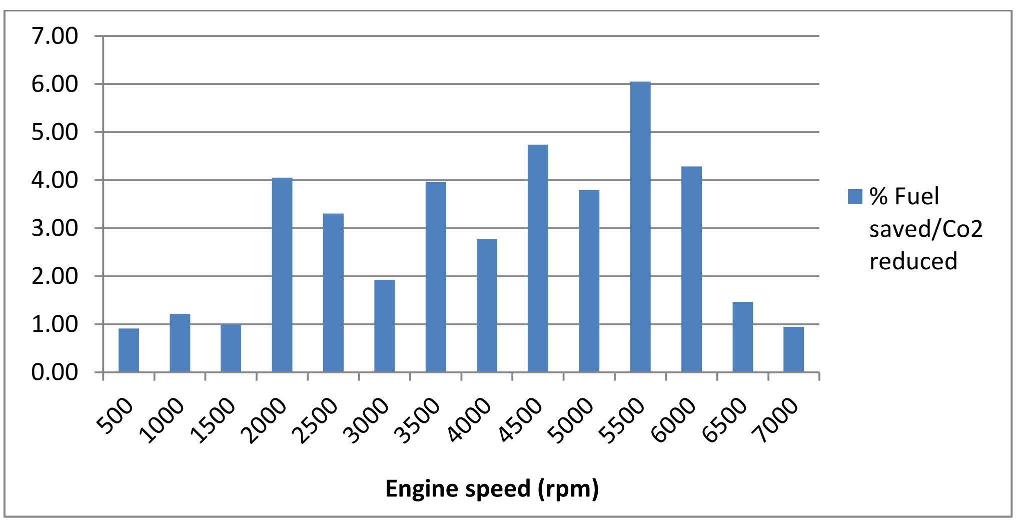

Figure 4.37 Percentage of fuel saving and Co2 reduction

Chapter Five

DESIGNING OF CVVT CAM MODEL

5.1. 3D modeling

In the previous section, three optimum cam profiles for each inlet and exhaust valves needed to construct the CVVT camshaft have been identified and summarized in table. Using these values the camshaft will be modeled using SOLIDWORKS. The Method used in drawing the cam profiles is shown in figure 5.1 using the second cam profile for intake cam (IC2).

	obtdc	cabdc	lift
IC1	15	6	12
IC2	40	38	13.846
IC3	17	75	15
	obbdc	catdc	lift
EC1	24	10	11.5
EC2	36	23	12.846
EC3	65	21	14

As shown in the table, valve opens at 40^0 before TDC in crankshaft angle which means 20^0 for camshaft angle. Exhaust valve opening is also shown to be 38^0 after BDC in crankshaft angles, which is 19^0 in camshaft angles. From specification, camshaft diameter is 28mm and cam base diameter is 34mm.

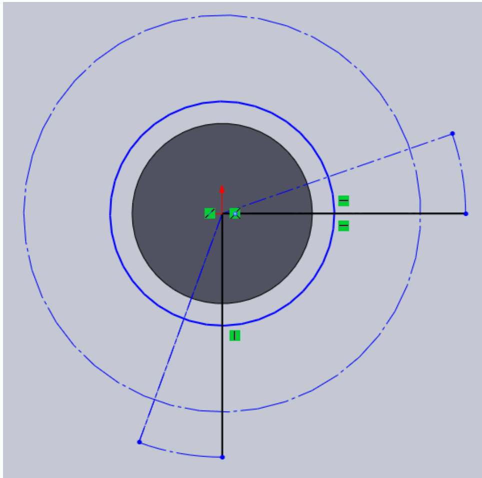

Figure 5.1 Base circle, opening and closing angles

The dark shaded solid circle is the camshaft and the solid blue circle is base circle of the cam lobe. The outer dashed circle represents the limit of lift for this cam profile. The black vertical line is drawn to indicate camshaft position where piston is at TDC and the horizontal line to indicate Camshaft position where piston will be at BDC. The arc connecting the vertical line and the blue dashed line indicates the valve opening angle of 20^0 before TDC while the arc connecting the horizontal line to the blue dashed line indicates valve closing angle of 19^0 after BDC as the camshaft rotates clockwise.

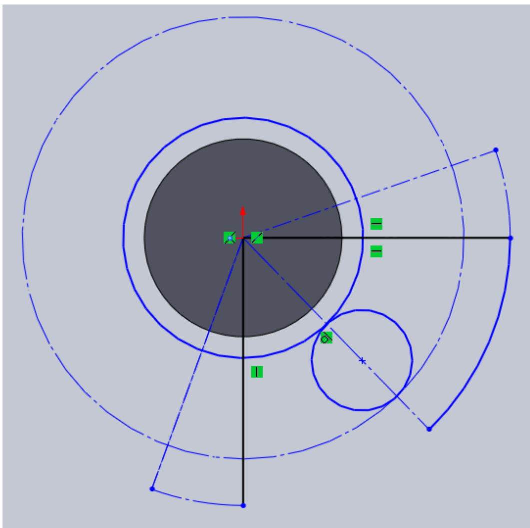

Figure 5.2 Base circle, opening and closing angles and lift

In figure 5.2, the arc extending down from the black horizontal line indicates the position of the centerline, which for this case is 45.5^0. This 0.5^0 difference is because the opening and closing angles before TDC and after BDC are not equal. The blue solid circle tangent to the cam base circle is drawn using the centerline as a locator and using the lift circle as a limiter. Two arcs tangent to the blue solid circles are drawn as shown in figure 5.3.

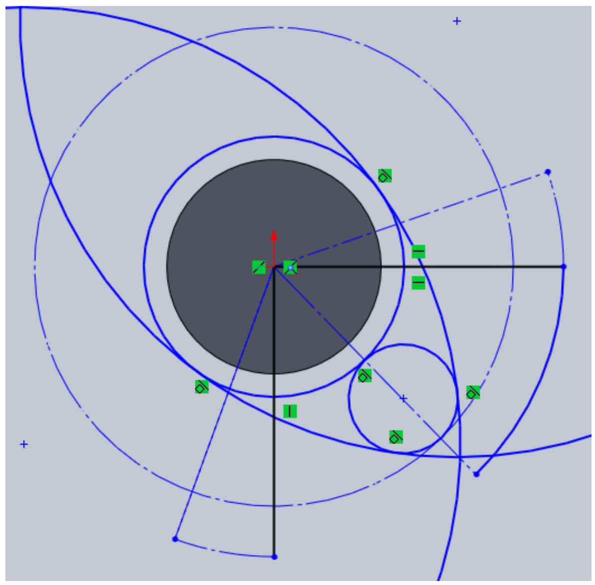

Figure 5.3 Opening and closing angles with circular arc

The two arcs drawn are lift profiles and are given enough gap to assure definite opening and closing at opening and closing points. Now that the cam profile is already in place, all unnecessary parts are removed and the final profile is shown in figure 5.4.

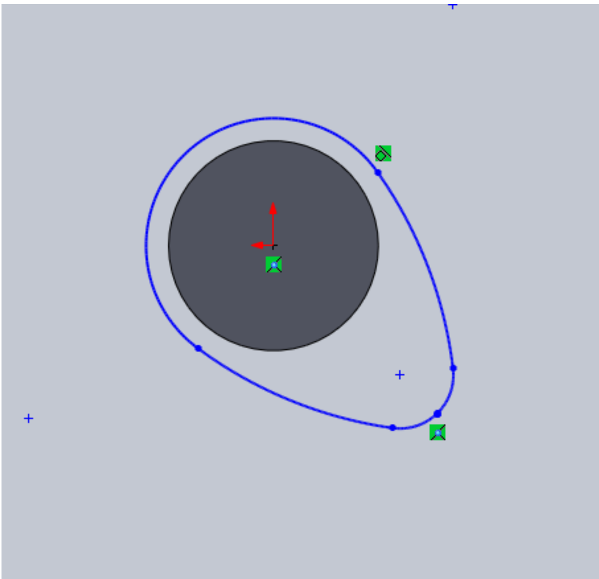

Figure 5.4 Complete cam profile

In this manner, the two cam profiles are also drawn and arranged in their right order of IC1, IC2 and IC3. Then a surface connecting these profiles is constructed, which represents the optimized CVVT cam lobe shown in figure 5.5.

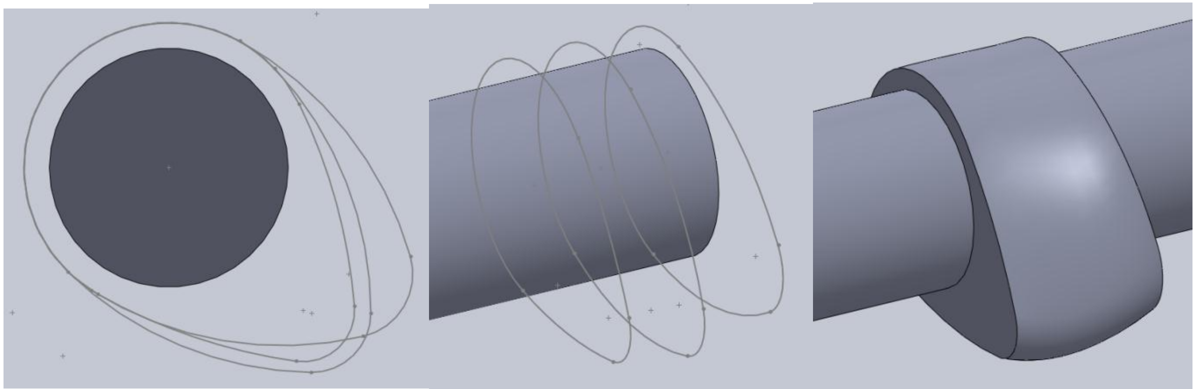

Figure 5.5 Complete cam lobe

The same procedure is applied while constructing the exhaust cam lobe. In figure 5.6, both intake and exhaust cam lobes are shown on the same camshaft.

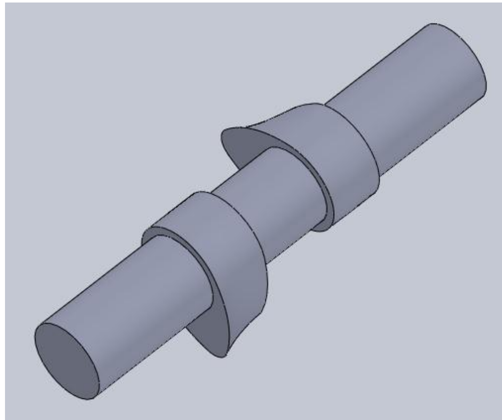

Figure 5.6 Single cylinder camshaft

The distance between these cam profiles is found by dividing the cam lobe thickness by thirteen, which is the number of intervals between the fourteen sample speeds and multiplying by the number of intervals until the cam profile of interest. Considering IC2, it is the cam profile at 4500 rpm which is the ninth sample speed, and the number of intervals at this speed is 8. Taking a cam lobe thickness of 30mm the axial distance of this cam profile to the first one (IC1) is calculated as shown below.

$$t_{i1,2} = t_i \times \frac{8}{13} = 30mm \times 0.615 = \boldsymbol{18.46mm}$$

This method is only applicable where the camshaft movement is linearly related to change in engine speed.

5.1.1. Cylinder head assembly

Since the center to center distance between intake and exhaust valves is 34mm, with an axially moving camshaft of 30mm lobe thickness is impractical since the intake cam touches the exhaust valve follower at low engine speeds and exhaust cam touches the intake valve follower at high engine speeds as shown in figure 5.7. Also the clearance between the intake and exhaust cam lobes is too small. As a result a mechanism that widens the gap between the contact points of the followers is needed.

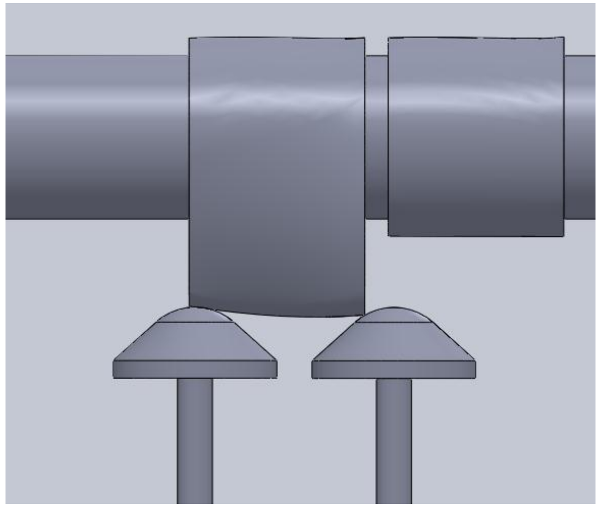

Figure 5.7 Center valve follower

To solve this problem, a roller follower with a contact point offset of 7.5mm from valve axis is used. The total distance between the contact points of intake and exhaust followers will be 49mm. As shown in figure 5.8, there is no contact between intake cam and exhaust valve follower, or exhaust cam and intake valve follower.

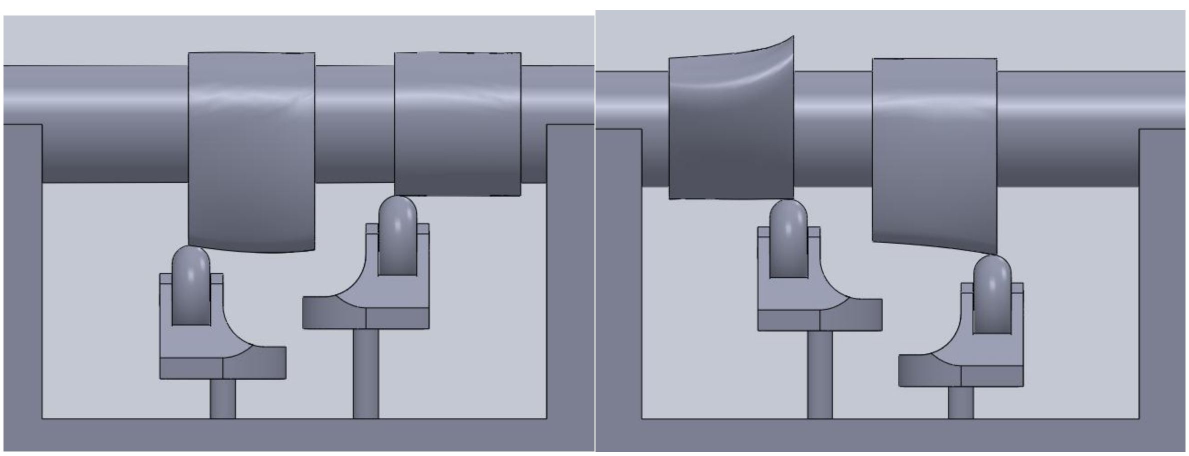

Figure 5.8 Offset valve follower

The arrangement shown in figure 5.8 only works for an engine with two valves per cylinder. If four valves per cylinder is a must, a similar follower of a bridge type can be applied to operate two valves with a single cam as shown in figure 5.9. In this case, the two intake or exhaust valves will not be arranged in a direction parallel to the axis of the camshaft, but in a perpendicular direction to the camshaft axis. This also requires a different intake and exhaust port design.

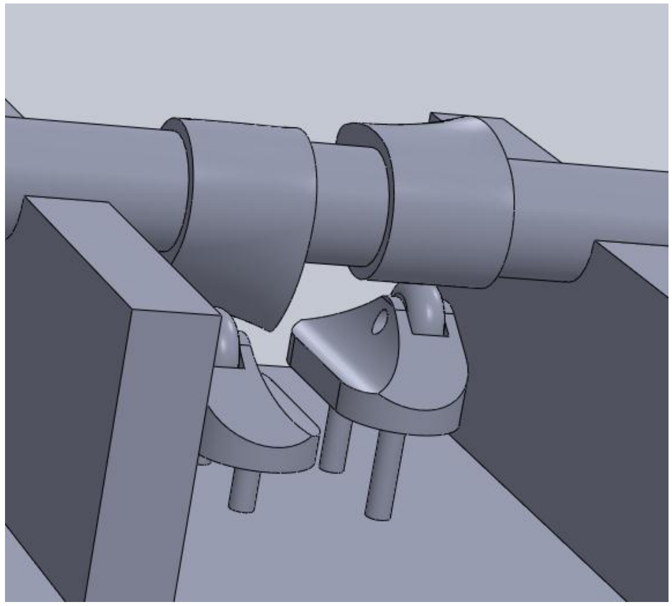

Figure 5.9 Offset valve follower in four valves per cylinder

Another option to apply this camshaft on an engine with four valves per cylinder is using double overhead camshaft (DOCS). This requires separate actuating cylinders for both intake and exhaust camshaft, but no modification is needed on the conventional port design.

5.1.2. Camshaft actuation system

A mechanism to operate the camshaft needs to control two types of motion, rotation at half the rotational speed of crankshaft and axial motion based on engine speed. The rotation can be easily controlled using a chain and sprocket system or a timing belt system with twice the number of teeth of crankshaft gear or sprocket at the camshaft.

However for the axial motion, a hydraulic cylinder needs to be used to move the camshaft 30mm back and forth. Also splined joints are needed to transmit rotation of camshaft gear to the camshaft. In figure 5.10, the whole cylinder head assembly is shown.

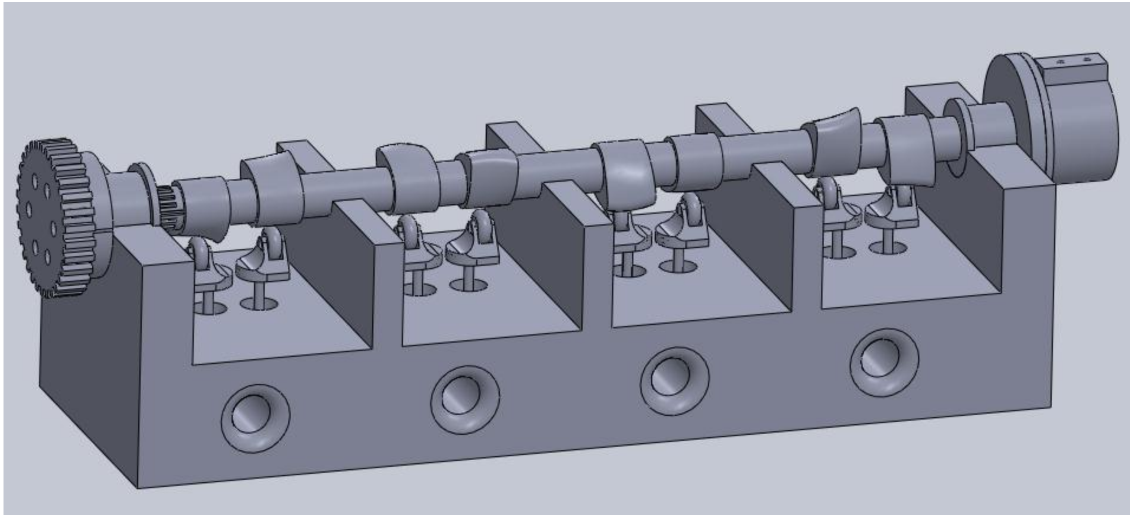

Figure 5.10 Cylinder head assembly

At the left end, the camshaft gear is shown bolted to a freely rotating member that transfers rotary motion to the camshaft by a spline connection. This member will be referred to as gear mount for discussion in this paper. The camshaft now will rotate with the gear mount and also at the same time can have axial movement.

On the right side of the figure, the cylinder assembly is shown. The cylinder assembly has mainly two components, the cylinder and the cylinder cover. Figure 5.11 shows the cylinder cover fixed to the head with bolted joint and the cylinder is fixed to the cover the same way.

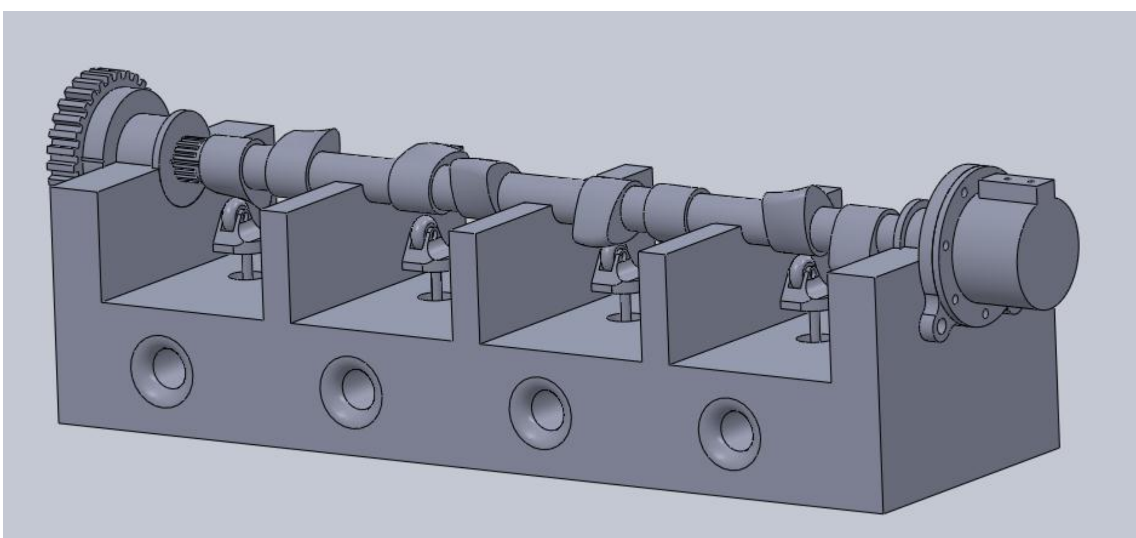

Figure 5.11 Cylinder head assembly

Two fluid passages holes are shown at the top of the cylinder each for forward and backward movement of the piston. The piston is directly joined to the camshaft and secured using a nut. Figure 5.12 shows exploded view of camshaft assembly. First the camshaft is inserted into cylinder cover, and then the piston and nut are fitted on the camshaft.

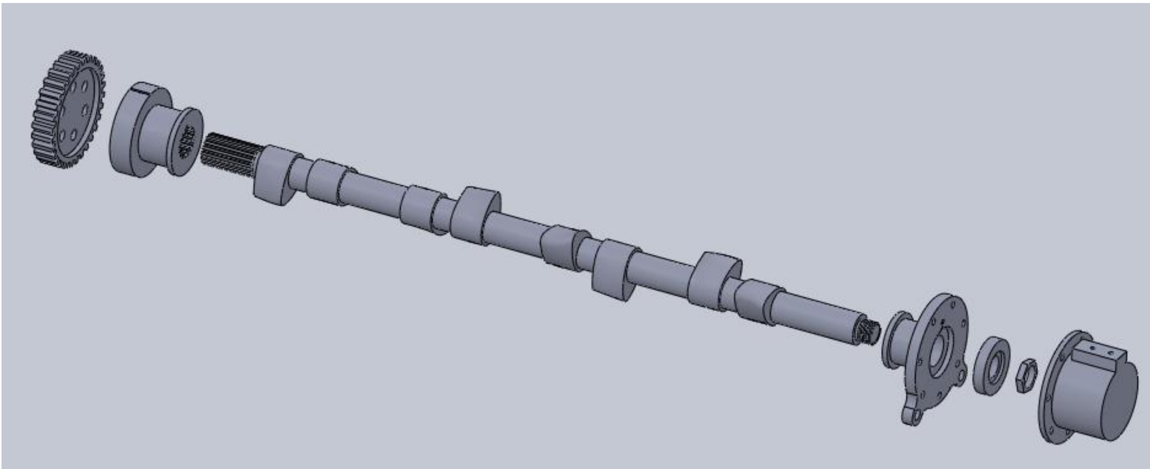

Figure 5.12 CVVT camshaft components

Figure 5.13 shows sectioned view of the cylinder assembly and the two fluid lines can clearly be seen. The retraction line passes through the cylinder to the cover before reaching the retraction camber.

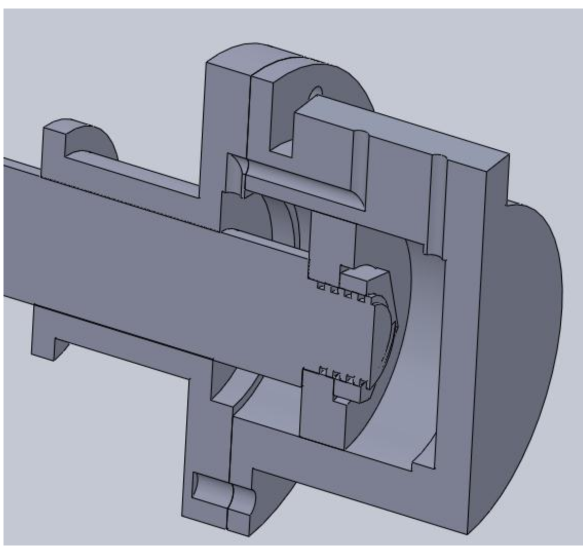

Figure 5.13 Actuating cylinder assembly

At both ends of the cylinder small volumes are preserved with smaller diameter than the piston to help develop enough actuation force. The cylinder provides the 30 mm of movement required.

5.2. Actuation force and fluid pressure

During operation of the camshaft, certain resistance forces are expected. These forces need to be overcome in order to effectively use the system. The resistance forces arise due to friction in the spline joint, camshaft journal bearings, and friction between cam lobe and follower rollers. However the most significant resistance force arises due to the spring force and inclined contact between the cam lobe and follower. These inclined contact faces create forces in the direction parallel to the camshaft axis.

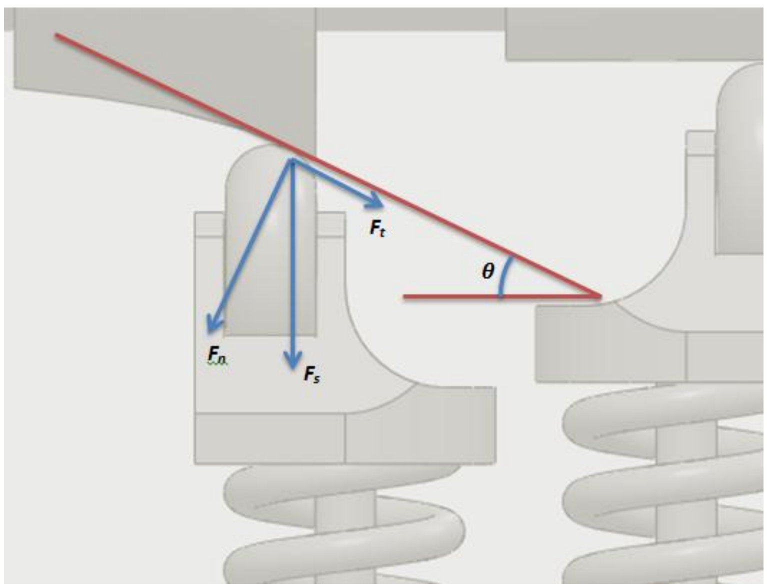

Figure 5.14 Camshaft forces

As shown in figure 5.14, the upward spring force is reacted by a force F_s of the cam lobe. The force F_s has a normal component F_n and a tangential component F_t. the tangential component F_t can be further divided into a force in the x direction F_x and a force in the y direction F_y. Force in the y direction is the maximum spring resistance the hydraulic fluid must overcome in order to move the camshaft in the axial direction.

The total cam follower resistance is the sum of the maximum spring resistance and friction force between roller and cam lobe. This friction force is product of the normal force F_n and the friction coefficient *f*. figure above shows the position of maximum contact surface inclination angle θwhich is measured to be 30^0.

Spring force Fs is calculated as

$$F_s = K \times x$$

where K is the spring constant and x is the spring deflection

$$k = \frac{G.d}{8C^3 n}$$

Where G is modulus of rigidity, d is wire diameter, C is ratio of coil diameter to wire diameter and n is effective number of turns.

$$k = \frac{80GPa \times 0.004m}{8 \times 125 \times 6} = 53.35KN/m$$

$$F_s = 53.35KN/m \times 0.015m = \mathbf{800N}$$

The tangential force Ft is calculated as

$$F_t = F_s \sin\theta$$

$$F_t = 800N \times \sin 30^0 = \mathbf{400N}$$

The normal force Fn is calculated as

$$F_n = F_s \cos\theta$$

$$F_n = 800N \times \cos 30^0 = \mathbf{692N}$$

Friction force between cam lobe and follower is calculated as

$$F_f = F_n \times f$$

$$F_f = 692N \times 0.13 = \mathbf{90N}$$

Without considering friction due to journal bearings and spline connection, the maximum resistive force is calculated as

$$F_R = F_f + F_t$$

$$F_R = 90N + 400N = \mathbf{490N}$$

Now, in order for the cylinder to effectively move the camshaft, the tangential component of the force applied should at least be equal to F_R.

$$F_c \cos\theta = F_R$$

$$F_c = \frac{F_R}{\cos\theta} = \frac{490N}{\cos 30^0} = \mathbf{565N}$$

The diameter of the piston is 50mm, and the fluid pressure required is calculated as

$$F_c = P_c \times A_p$$

$$P_c = \frac{F_c}{A_p} = \frac{565N}{0.00196m^2} = \mathbf{289KPa}$$

This much pressure is required to actuate the camshaft for single cam lobe in this position, and it can be clearly seen in figure 5.12 that only two cam lobes are in this position at the same time. Thus, the total actuation force required is twice the above calculated value.

$$P_c = 2 \times 289KPa = 578Ka = 5.78\ bar \approx \mathbf{6\ bar}$$

5.3. Dimension relationships

Major dimensions to sufficiently represent the size and shape of the camshaft are expressed as factors of cylinder diameter (bore) for reference. The camshaft diameter and cam base diameter are taken from previously conducted design project, and are also expressed as factors of bore.

Figure 5.15 shows the terms selected to represent the major camshaft and lobe variables of intake on the left and exhaust on the right.

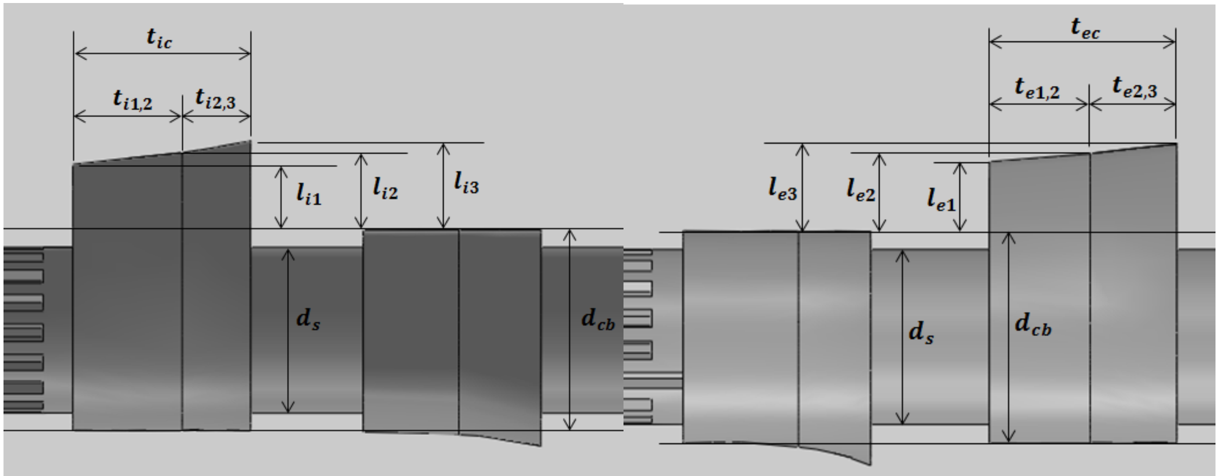

Figure 5.15 Axial cam lobe variables and lift

$$\boldsymbol{d_s} = camshaft\ diameter$$

$$\boldsymbol{d_{cb}} = cam\ base\ diameter$$

$$\boldsymbol{t_c} = \boldsymbol{t_{ic}} = \boldsymbol{t_{ec}} = thickness\ of\ cam$$

$$\boldsymbol{t_{i1,2}} = axial\ distance\ between\ intake\ cam\ profiles\ 1\ and\ 2$$

$$\boldsymbol{t_{i2,3}} = axial\ distance\ between\ intake\ cam\ profiles\ 2\ and\ 3$$

$$\boldsymbol{l_{i1}} = lift\ of\ intake\ cam\ profile\ 1$$

$$\boldsymbol{l_{i2}} = lift\ of\ intake\ cam\ profile\ 2$$

$$\boldsymbol{l_{i3}} = lift\ of\ intake\ cam\ profile\ 3$$

$$\boldsymbol{t_{e1,2}} = axial\ distance\ between\ exhaust\ cam\ profiles\ 1\ and\ 2$$

$$\boldsymbol{t_{e2,3}} = axial\ distance\ between\ exhaust\ cam\ profiles\ 2\ and\ 3$$

$$\boldsymbol{l_{e1}} = lift\ of\ exhaust\ cam\ profile\ 1$$

$$\boldsymbol{l_{e2}} = lift\ of\ exhaust\ cam\ profile\ 2$$

$$\boldsymbol{l_{e3}} = lift\ of\ exhaust\ cam\ profile\ 3$$

Thickness of cam is decided to be 30mm to prevent surfaces with large slope and at the same time save space for axial movement. If thickness is smaller, the resistance to movement will increase, and if thickness is larger, less space will be left for movement, which demands increased distance between cylinders. This will cause the size of the engine to increase.

All 14 cam profiles are linearly distributed on the specified cam thickness. For intake cam IC2 is the 9thcam profile and there are 8 intervals up to this cam profile. Total number of intervals is 13. To calculate$\boldsymbol{t_{i1,2}}$ (distance between IC1 and IC2), the cam thickness is divided by 13 and multiplied by 8.

$$t_{i1,2} = \frac{8}{13} \times t = 18.46mm$$

$$t_{i2,3} = t - t_{i1,2} = 11.54mm$$

The middle exhaust cam profile EC2 is the 8th cam profile with 7 intervals from EC1. $\boldsymbol{t_{e1,2}}$is found using similar calculation as above.

$$t_{e1,2} = \frac{7}{13} \times t = 16.15mm$$

$$t_{e2,3} = t - t_{e1,2} = 13.85mm$$

Lift values are for the six cam profiles of intake and exhaust cams are

$$l_{i1} = 12mm$$

$$l_{i2} = 13.84mm$$

$$l_{i3} = 15mm$$

$$l_{e1} = 11.5mm$$

$$l_{e2} = 12.84mm$$

$$l_{e3} = 14mm$$

Figure 5.16 shows terms assigned to express the angular arrangement of the cam profiles for intake on the left and exhaust on the right.

$$\theta_{id} = dwell\ angle\ (opening\ duration) of\ intake\ cam$$

$$\theta_{ic} = angle\ between\ centerline\ and\ TDC\ of\ intake\ cam$$

$$\theta_{ed} = dwell\ angle\ (opening\ duration) of\ exhaust\ cam$$

$$\theta_{ec} = angle\ between\ centerline\ and\ BDC\ of\ exhaust\ cam$$

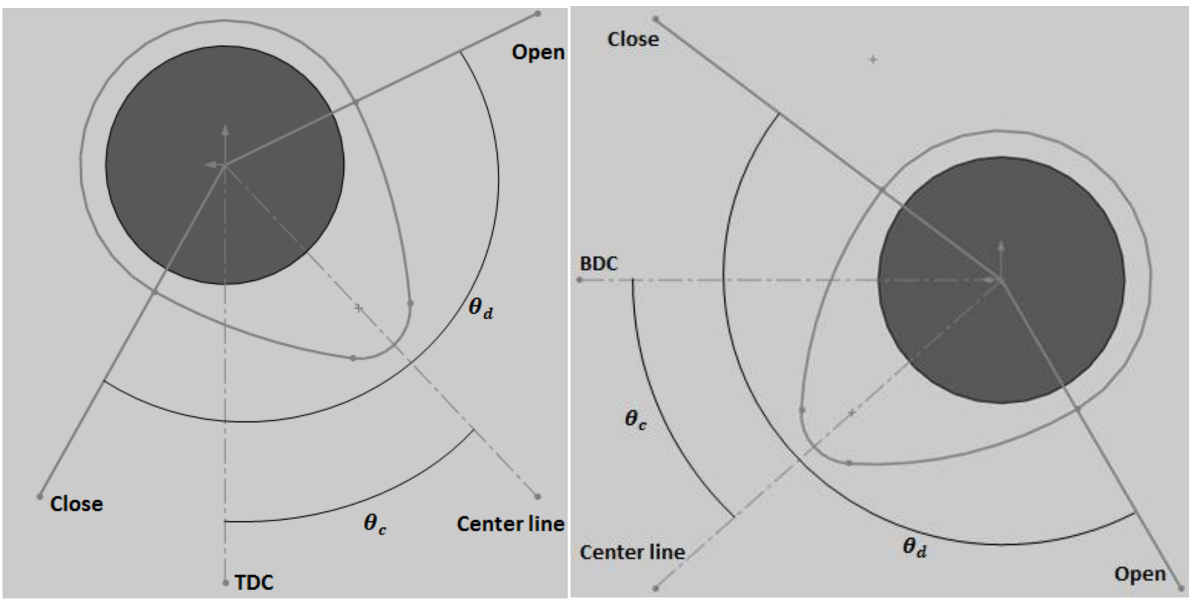

Figure 5.16 Angular cam lobe variables

For intake cam profile 1 (IC1), opening angle is 7.5^0 camshaft before TDC and closing angle is 3^0 of camshaft angle after BDC. The resultant gives 3.5^0 and dividing by two gives a centerline shift of 1.75^0 towards TDC.

Dwell angle of intake cam profile 1

$$\boldsymbol{\theta_{id1}} = 90^0 + 7.5^0 + 3^0 = \mathbf{100.5^0}$$

Center line angle from TDC of intake cam profile 1

$$\boldsymbol{\theta_{ic1}} = 45^0 - 1.75^0 = \mathbf{43.25^0}$$

Dwell angle of intake cam profile 2

$$\boldsymbol{\theta_{id2}} = 90^0 + 20^0 + 19^0 = \mathbf{129^0}$$

Center line angle from TDC of intake cam profile 2

$$\boldsymbol{\theta_{ic2}} = 45^0 - 0.5^0 = \mathbf{44.5^0}$$

Dwell angle of intake cam profile 3

$$\boldsymbol{\theta_{id3}} = 90^0 + 8.5^0 + 37.5^0 = \mathbf{136^0}$$

Center line angle from TDC of intake cam profile 3

$$\boldsymbol{\theta_{ic3}} = 45^0 + 14.5^0 = \mathbf{59.5^0}$$

Dwell angle of exhaust cam profile 1

$$\boldsymbol{\theta_{ed1}} = 90^0 + 12^0 + 5^0 = \mathbf{107^0}$$

Center line angle from TDC of exhaust cam profile 1

$$\boldsymbol{\theta_{ec1}} = 45^0 - 3.5^0 = \mathbf{41.5^0}$$

Dwell angle of exhaust cam profile 2

$$\boldsymbol{\theta_{ed2}} = 90^0 + 18^0 + 11.5^0 = \mathbf{119.5^0}$$

Center line angle from TDC of exhaust cam profile 2

$$\boldsymbol{\theta_{ec2}} = 45^0 - 3.25^0 = \mathbf{41.75^0}$$

Dwell angle of exhaust cam profile 3

$$\boldsymbol{\theta_{ed3}} = 90^0 + 32.5^0 + 10.5^0 = \mathbf{133^0}$$

Center line angle from TDC of exhaust cam profile 3

$$\boldsymbol{\theta_{ec3}} = 45^0 - 11^0 = \mathbf{34^0}$$

To express the above calculated variables as fractions of bore ***(B)***, all values are divided by the cylinder diameter of 84mm.

- **Thickness of cam**

$$t_c = 0.357 \times B$$

- **Camshaft diameter**

$$d_s = 0.333 \times B$$

- **Cam base diameter**

$$d_{cb} = 0.405 \times B$$

- **Axial distance between intake cam profiles 1 and 2**

$$t_{i1,2} = 0.22 \times B$$

- **Axial distance between intake cam profiles 2 and 3**

$$t_{i2,3} = 0.137 \times B$$

- **Lift of intake cam profile 1**

$$l_{i1} = 0.143 \times B$$

- **Lift of intake cam profile 2**

$$l_{i2} = 0.165 \times B$$

- **Lift of intake cam profile 3**

$$l_{i3} = 0.178 \times B$$

- **Axial distance between exhaust cam profiles 1 and 2**

$$t_{e1,2} = 0.192 \times B$$

- **Axial distance between exhaust cam profiles 2 and 3**

$$t_{e2,3} = 0.165 \times B$$

- **Lift of exhaust cam profile 1**

$$\boldsymbol{l_{e1} = 0.137 \times B}$$

- **Lift of exhaust cam profile 2**

$$\boldsymbol{l_{e2} = 0.153 \times B}$$

- **Lift of exhaust cam profile 3**

$$\boldsymbol{l_{e3} = 0.167 \times B}$$

Chapter Six

CONCLUSION, RECOMMENDATION AND FUTURE WORK

6.1. Conclusion

After stating the limitations of currently utilized variable valve timing systems, a new type of continuous variable valve timing system which is a slightly modified version of the three dimensional cam was proposed and analyzed for performance in terms of volumetric efficiency power torque and BSFC at selected engine speeds.

The analysis process was mainly focused on selecting optimum valve timing parameter values; namely, opening angles, closing angles and lift for both intake and exhaust valves by testing different variations. Then these values were optimized in order to simplify manufacturing and operation of the proposed camshaft. Another consideration taken on the optimization process is that the optimized values as much as possible should have an improved performance when compared to the assumed original camshaft.

The results have shown a maximum volumetric efficiency improvement of 19% and an average of improvement of ~5%. Maximum percent improvement for brake torque is seen to be 30.82% and percent improvements for brake power are exactly the same as brake torque with negligible differences at some engine speeds. Also a maximum and an average improvement of respectively of 8.5% and ~3% are seen for BSFC.

As for yearly fuel saving and Co_2 emission reduction, a maximum fuel saving of 96.47kg/yr is achieved at 5500 rpm, and a maximum Co_2 emission reduction of 85.9kg/yr at a similar engine speed of 5500 rpm. This may not seem quite high as it is only calculated for a single vehicle. The reason for low fuel saving and Co_2 reduction while power is improved by larger rate is that with more power, the vehicle should go faster, but aerodynamic and rolling resistances grow higher at high speeds. In that case, speed will fall to increase as it would for lower speeds for the same increment of power.

6.2. Recommendation and Future Work

As seen from the simulation and calculated results, maximum fuel savings are obtained in the speed range of 4500 rpm to 6000 rpm. These suggests for better fuel economy and Co_2 reduction, it is recommended to operate the engine in these speed range.

The valve timing system in this study is intended only for naturally aspirated and carbureted gasoline engines, and will not be suitable for other engine types. For other engine types, the cam profiles should be tuned as required to obtain optimum performance. This leaves huge space for additional work that considers more possible engine assemblies and formulates more general data.

Also, the three dimensional cam system was set aside by manufacturers due to considerable friction on the cam follower mechanism. Although one follower mechanism to reduce friction has been suggested in this study, there is very huge space for improvement as well including strength and fatigue analysis.

REFERENCES

[1]. Cosic Ivan, "Development and testing of a variable valve timing system (VVT) for twin cam system", *FTS thesis* 629.252 COS

[2]. YihuiQiu, David J. Perreault, Thomas A. Keim, & John G. Kassakian, "Optimal Cam Design and System Control for an Electromechanical Engine Valve Drive", *International Conference on Industrial Technology*, March 2010

[3]. Wilhelm Hannibal (Prof. Dr. Ing), "Variable Valve Timing Systems on Modern Spark Ignition Engines in Series Production and under Development", *Lecture at the Budapest University of Technology and Economics*, September, 2009

[4]. https://www.mechadyne-int.com**"**The Impact of Variable Valve Actuation on Engine Performance and Emissions" *Accessed Date: March 2, 2017*

[5]. Budynas-Nisbett, "Shigley's Mechanical Engineering Design, Eighth Edition", *McGraw-Hill Primis*, ISBN: 0-390-76487-6, 2008

[6]. Wilson N., Dobson C. and Mudell G., "Active Valve Train", Automotive Engineering Vol.18, 1993

[7]. Hosaka T. and Hamazaki M., "Development of the Variable Valve Timing and Lift (VTEC) Engine for the Honda NSX", SAE 910008, 1991

[8]. Bassett M.D., Blakey S.C. and Foss P.W., "A Simple Two-State Late Intake Valve Closing Mechanism", Proc. I. Mech. Vol. 211, 1997

[9]. John B. Heywood, "Internal Combustion Engine Fundamentals", *McGraw-Hill, ISBN 0-07-028637-X*

[10]. Herrin R. and Pozniak D., "A Lost-Motion, Variable Valve Timing System for Automotive Piston Engines", *SAE 840335*, 1984

[11]. Schechter, M. and Llevin M., "Camless Engine", SAE 960581, 1996

[12]. Mohammad Pournazeri, "Development of a New Fully Flexible Hydraulic Variable Valve Actuation System", *A thesis presented to the University of Waterloo,* Waterloo, Ontario, Canada, 2012

[13]. http://www.globalspec.com/reference/45865/203279/1-9-valve-timing-diagrams"Valve timing diagrams" *Accessed Date: June 2, 2017*

[14]. Jefry Bin DediEfendi, "Valve Timing Study of a Single Cylinder Motorcycle Engine", *A dissertation submitted to the University of Malaysia Pahang*, November 2009

[15]. Willard W. Pulkrabek, "Engineering Fundamentals of the Internal Combustion Engine", *Prentice Hall – Upper Saddle River*, New Jersey 07458

[16]. António Emanuel Figueiredo Costa, "Computer Simulation of an Internal Combustion Engine", *Faculdade de Engenharia da Universidade do Porto and University of Maryland, Baltimore County*, 2008

[17]. Performance Trends, Inc., "Engine Analyzer Pro User's Manual Version 3.9 B", Livonia, MI 48153

[18]. Chul-Ho kim, "Streamlined Design of a High-speed Coach For Fuel Saving And Carbon-dioxide Reduction", International Journal of Automotive Engineering 2 101-107, 2011

[19]. http://highered.mheducation.com"Types of Cams and Terminologies" *Accessed Date: April 15, 2017*

[20]. R.S. Khurmi and J.K. Gupta, "A Textbook of Machine Design - 14th Edition", *Eurasia Publishing House (Pvt.) Ltd.*, Ram Nagar, New Delhi-110 055, 2005

[21]. Kaj Madsen & Hans Bruun Nielsen, "Introduction to Optimization and Data Fitting", *DTU Informatics – IMM Richard PetersensPlads*, DK-2800 Kgs. Lyngby

[22]. https://en.m.wikipedia.org/wiki/Volumetric_efficiency "Volumetric efficiency" *Accessed Date: October7, 2017*

[23]. Ashish Jain, Dr S SThipse&Dr E Porpatham, "Design and Optimization of 2-stage Variable Valve Actuation Mechanism for Diesel Engines", *International Journal of Engineering Trends and Technology (IJETT)* – Volume 28 Number 8 - October 2015

[24]. Bruce R. Munson, Donald F. Young, Theodore H. Okiishi and Wade W. Huebsch, "Fundamentals of Fluid Mechanics – Sixth Edition", *John Wiley & Sons, Inc*. ISBN 978-0470-26284-9, 2009

[25]. Chen Jai-dui, “Dynamic Simulation and Experiments of a Novel Variable Valve Timing System”, International Journal of Multimedia and Ubiquitous Engineering, Volume 9, Number 7 (2014)

[26]. Desantes J., Payri F. and Corberan J., “A Study of the Performance of a SI Engine Incorporating a Hydraulically controlled Variable Valve Timing System”, *SAE 880604*, 1988

[27]. Douglas E., “EVA Meet Demands for Performance and Economy”, *Southwest Research Institute*, 1997

[28]. H. Hirani and S. Dani, “Variable Valve Actuation Mechanism Using Magnetorheological Fluid”, *Proceedings of WTC2005 World Tribology Congress III*, September 2005, Washington, D.C., USA

[29]. J Suresh Kumar, V Ganesan, J M Mallikarjuna& S Govindarajan, “Design and optimization of a throttle body assembly by CFD analysis”, *Indian Journal of Engineering & Material Sciences*, Volume 20, October 2013

[30]. J. P. Holman, “Heat Transfer -Tenth Edition”, *McGraw-Hill Companies, Inc.* ISBN 978–0–07–352936–3, 2010

[31]. Jiadui Chen, Yongming Wu, YulingXu, Ziqin Wang &FengguoTian, “Adjustment Performance of a Novel Continuous Variable Valve Timing and Lift System” *Chemical Engineering Transactions Paper*, VOL. 51, 2016

[32]. K. Nagaya, H. Kobayashi & K. Koike, "Valve timing and valve lift control mechanism for engines", *Journal of Mechatronics, vol. 16*, pp. 121-129, September 2005.

[33]. Kota Sridhar, R.B.V.Murali, Sk.MohammadYounus&K.Mohan Lakshmi, “Computerized Simulation of Spark Ignition Internal Combustion Engine”,*IOSR Journal of Mechanical and Civil Engineering (IOSR-JMCE)*, Volume 5, Issue 3 (Jan. - Feb. 2013)

[34]. M. GalalRabie, “Fluid Power Engineering”, *McGraw-Hill Companies, Inc.* ISBN: 978-0-07-162606-4, 2009

[35]. Matt Dixon, “Variable Camshaft Timing/ Variable Valve Timing”, *ICAIA Conference* fall 2012

[36]. Michael J. Moran and Howard N. Shapiro "Fundamentals of Engineering Thermodynamics – Fifth Edition", John Wiley & Sons, Inc. ISBN-13 978-0-470-03037-0, 2006

[37]. Mrdjan Jankovic & Stephen W. Magner, "Variable Cam Timing: Consequences to Automotive Engine Control Design", *Ford Research Laboratory, Dearborn, MI 48121*, USA, *15th Triennial World Congress*, Barcelona, Spain, 2002

[38]. Oleg Vinogradov, "Fundamentals of Kinematics and Dynamics of Machines and Mechanisms", *CRC Press LLC*, ISBN 0-8493-0257-9, 2000

[39]. Osama H. M. Ghazal &Mohamad S. H. Dado, "Gear Drive Mechanism for Continuous Variable Valve Timing of IC Engines", *Scientific Research*, Engineering, 2013, 5, 245-250

[40]. P. Blair Shelton, "A Review of Variable Valve Timing Devices" *A thesis submitted to the University of Arkansas*, May 2008

[41]. SundeepRamachandran, "Rapid Thermodynamic Simulation Model of an Internal Combustion Engine on Alternate Fuels", *Proceedings of the International Multi Conference of Engineers and Computer Scientists*, Volume II, March 2009, Hong Kong

[42]. T. Kuhn, Dr. D. Mowll, Dr. F. Wirbeleit& J. Willand, "Optimization of the valve lift strategy during the acceleration of a diesel engine using WAVE and DOE", *DaimlerChrysler AG Research and Technology*, Stuttgart, Germany

[43]. V. Mallikarjuna, N. Jashuva, G. Nagaraju& B. Rama Bhupal Reddy, "Design Manufacturing and Cost Estimation of Camshaft Used In Two Wheeler", IOSR Journal of Mechanical and Civil Engineering (IOSR-JMCE), Volume 11, Issue 1 (Feb. 2014)

[44]. Yunus A. Cengel, "Heat Transfer A Practical Approach – 2nd Edition", McGraw-Hill, 2006.

APPENDIX

Appendix A Simulation Tables

Appendix A1 Tuning process table at different engine speeds

500 rpm test result					
	degree	VE(%)	Tb(Nm)	Pb(Kw)	bsfc(g/Kwhr)
ivo/btdc(deg)	10	79.3	151.43	7.93	0.316
	12	79.2	151.26	7.92	0.316
	8	79.4	151.34	7.93	0.317
	6	79.4	151.42	7.93	0.317
	14	79.2	151.04	7.91	0.317
ivc/abdc(deg)	10	79.3	151.43	7.93	0.316
	12	79.3	151.23	7.92	0.317
	8	79.3	151.46	7.93	0.316
	6	79.3	151.32	7.93	0.317
evo/bbdc(deg)	25	79.3	151.43	7.93	0.316
	27	79.3	151.32	7.93	0.317
	23	79.4	151.49	7.93	0.316
	21	79.3	151.32	7.93	0.317
evc/atdc(deg)	5	79.4	151.49	7.93	0.316
	7	79.3	151.55	7.93	0.316
	9	79.3	151.47	7.93	0.316
	3	79.2	151.17	7.92	0.317
ivo/btdc(deg)	10	79.4	151.49	7.93	0.316
	11	79.3	151.39	7.93	0.316
	9	79.4	151.5	7.93	0.316
	8	79.4	151.57	7.93	0.317
ivc/abdc(deg)	8	79.4	151.5	7.93	0.316
	9	79.3	151.26	7.92	0.317
	7	79.4	151.47	7.92	0.317
evo/bbdc(deg)	23	79.4	151.5	7.93	0.316
	24	79.4	151.54	7.93	0.316
	25	79.4	151.43	7.93	0.317
evc/atdc(deg)	5	79.4	151.54	7.93	0.316
	6	79.4	151.53	7.93	0.316
	4	79.3	151.4	7.93	0.316
ivl(mm)	10	79.4	151.54	7.93	0.316
	11	79.4	151.61	7.94	0.316
	12	79.5	151.42	7.93	0.318
	11.5	79.5	151.63	7.94	0.317
evl(mm)	10	79.4	151.61	7.94	0.316

	11	79.4	151.62	7.94	0.316
	12	79.4	151.53	7.93	0.317
	11.5	79.4	151.59	7.93	0.317

1000 rpm test result					
	degree	VE(%)	Tb(Nm)	Pb(Kw)	bsfc(g/Kwhr)
ivo/btdc(deg)	10	81.6	180.41	18.9	0.273
	12	81.6	180.69	18.93	0.273
	14	81.8	180.92	18.95	0.273
	16	81.9	181.11	18.96	0.273
	18	82	181.48	19.01	0.274
ivc/abdc(deg)	10	81.9	181.11	18.96	0.273
	12	81.89	180.96	18.95	0.274
	8	81.87	181.12	18.97	0.273
evo/bbdc(deg)	25	81.9	181.11	18.96	0.273
	27	81.87	180.89	18.94	0.273
	23	81.77	181.12	18.97	0.273
evc/atdc(deg)	5	81.9	181.11	18.96	0.273
	7	81.9	181.35	18.99	0.273
	9	82.25	181.91	19.05	0.273
	11	82.51	182.37	19.1	0.273
	13	82.23	179.89	18.84	0.273
ivo/btdc(deg)	16	82.51	182.37	19.1	0.273
	17	82.66	183.02	19.16	0.273
	18	82.71	182.9	19.15	0.273
	19	82.88	183.18	19.19	0.273
	20	83.09	183.52	19.22	0.274
ivc/abdc(deg)	8	82.88	183.18	19.19	0.273
	9	82.9	183.23	19.19	0.273
	10	82.89	183.18	19.19	0.273
evo/bbdc(deg)	25	82.9	183.23	19.19	0.273
	26	83.05	183.37	19.2	0.274
	24	82.98	183.39	19.2	0.273
	23	82.78	183.12	19.18	0.273
evc/atdc(deg)	11	82.98	183.39	19.2	0.273
	12	83.08	183.75	19.24	0.273
	13	83.36	184.16	19.28	0.274
ivl(mm)	11	83.08	183.75	19.28	0.273
	12	83.24	184.01	19.27	0.273
	13	81.06	179.29	18.78	0.273
	12.5	83.28	184.07	19.28	0.273

evl(mm)	11	83.28	184.07	19.28	0.273
	11.5	83.38	184.11	19.28	0.274
	12	83.33	184.07	19.28	0.274

1500 rpm test result					
	degree	VE(%)	Tb(Nm)	Pb(Kw)	bsfc(g/Kwhr)
ivo/btdc(deg)	20	84.85	201.34	31.63	0.255
	22	85.28	201.98	31.73	0.255
	24	85.66	202.38	31.79	0.255
	26	86.03	203.21	31.92	0.256
ivc/abdc(deg)	10	86.66	202.38	31.79	0.255
	12	86.08	203.12	31.91	0.256
	14	86.01	203.07	31.9	0.256
evo/bbdc(deg)	30	85.66	202.38	31.79	0.255
	32	85.97	202.91	31.87	0.256
	28	86.16	203.32	31.94	0.256
	26	86.11	203.36	31.95	0.256
evc/atdc(deg)	15	86.16	203.32	31.94	0.256
	17	86.49	203.79	32.01	0.257
	13	85.8	203.24	31.92	0.255
ivo/btdc(deg)	26	86.16	203.32	31.94	0.256
	25	84.06	199.94	31.41	0.254
	24	85.49	202.34	31.78	0.255
	27	86.51	203.7	32	0.257
ivc/abdc(deg)	10	86.16	203.32	31.94	0.256
	11	86.27	203.43	31.95	0.256
	12	86.13	203.31	31.94	0.256
evo/bbdc(deg)	28	86.27	203.43	31.95	0.256
	29	86.2	203.28	31.93	0.256
	27	86.14	203.56	31.98	0.255
evc/atdc(deg)	15	86.27	203.43	31.95	0.256
	16	86.42	203.68	32	0.256
	17	86.41	203.97	32.04	0.256
ivl(mm)	12.5	86.42	203.68	32	0.256
	13	86.51	203.6	31.98	0.257
	13.5	86.48	203.85	32.02	0.256
evl(mm)	12	86.51	203.6	31.95	0.257
	12.5	86.45	203.81	32.01	0.256
	13	84.64	203.85	32.02	0.257

2000 rpm test result					
	degree	VE(%)	Tb(Nm)	Pb(Kw)	bsfc(g/Kwhr)
ivo/btdc(deg)	26	98.9	236.58	49.6	0.252
	28	99.47	237.57	49.75	0.253
	30	100.23	238.57	49.97	0.254
	24	98.25	235.89	49.4	0.252
ivc/abdc(deg)	11	99.47	237.37	49.75	0.253
	13	99.28	237.32	49.71	0.253
	9	99.77	238.07	49.86	0.253
	7	99.83	238.18	49.89	0.254
evo/bbdc(deg)	28	99.77	238.07	49.86	0.253
	30	99.79	237.92	49.83	0.254
	26	99.79	237.88	49.82	0.254
evc/atdc(deg)	16	99.77	238.07	49.86	0.253
	18	100.43	238.68	49.99	0.254
	14	99.02	237.04	49.65	0.252
ivo/btdc(deg)	28	99.77	238.07	49.86	0.253
	29	99.25	237.47	49.74	0.252
	27	98.57	236.31	49.49	0.252
ivc/abdc(deg)	9	99.77	238.07	49.86	0.253
	10	98.85	236.69	49.37	0.252
	8	98.89	237.11	49.66	0.252
evo/bbdc(deg)	28	99.77	238.07	49.86	0.253
	29	99.04	236.91	49.63	0.252
	27	99.02	237	49.63	0.252
evc/atdc(deg)	14	99.77	238.07	49.86	0.253
	15	99.38	237.61	49.77	0.252
	13	98.66	236.36	49.51	0.252
ivl(mm)	13	99.77	238.07	49.86	0.253
	14	99.25	237.43	49.73	0.252
	13.5	99.18	237.36	49.72	0.252
	12.5	98.86	236.82	49.6	0.252
evl(mm)	13	99.77	238.07	49.86	0.253
	13.5	99.18	237.28	49.69	0.252
	14	99.29	237.5	49.74	0.252
	12.5	99.93	236.81	49.6	0.252

2500 rpm test result					
	degree	VE(%)	Tb(Nm)	Pb(Kw)	bsfc(g/Kwhr)
ivo/btdc(deg)	28	103.63	243.55	63.76	0.257
	30	104.47	244.26	36.95	0.259

	32	104.85	244.12	63.91	0.26
	26	103.16	243.1	63.65	0.257
ivc/abdc(deg)	20	103.63	243.55	63.76	0.257
	22	103.93	243.71	63.8	0.258
	18	103.57	243.41	63.73	0.257
evo/bbdc(deg)	34	103.63	243.55	63.76	0.257
	32	103.49	243.25	63.68	0.257
	36	103.68	243.64	63.79	0.257
	38	103.48	243.23	63.68	0.257
evc/atdc(deg)	28	103.68	243.64	63.79	0.257
	26	102.98	242.65	63.53	0.257
	30	104.32	243.86	63.84	0.259
ivo/btdc(deg)	28	103.68	243.64	63.79	0.257
	27	103.38	243.4	63.72	0.257
	29	104	243.57	63.77	0.258
ivc/abdc(deg)	20	103.68	243.64	63.79	0.257
	21	103.71	243.41	63.73	0.257
	22	103.96	243.76	63.82	0.258
evo/bbdc(deg)	36	103.71	243.41	63.73	0.257
	35	103.48	243.26	63.68	0.257
	37	103.6	243.1	63.65	0.257
evc/atdc(deg)	28	103.71	243.41	63.73	0.257
	29	103.84	243.75	63.82	0.257
	30	103.35	246.83	63.84	0.259
ivl(mm)	13	103.84	243.75	63.82	0.257
	13.5	103.95	243.67	63.79	0.258
evl(mm)	12.5	103.84	243.75	63.82	0.257
	13	104.03	243.97	63.87	0.258
	13.5	104.23	244.02	63.88	0.258

3000 rpm test result					
	degree	VE(%)	Tb(Nm)	Pb(Kw)	bsfc(g/Kwhr)
ivo/btdc(deg)	28	90.89	213.45	67.06	0.257
	30	91.41	214.54	67.4	0.257
	32	91.87	215.34	67.65	0.258
ivc/abdc(deg)	21	91.41	214.54	67.4	0.257
	23	92.13	216.63	68.06	0.257
	25	92.99	218.92	68.78	0.257
	27	93.81	220.94	69.42	0.257
	29	94.64	223.05	70.07	0.256
	31	95.38	224.61	70.57	0.257

evo/bbdc(deg)	36	94.64	223.05	70.07	0.256
	38	94.66	222.72	69.97	0.257
	34	94.62	222.88	70.02	0.257
evc/atdc(deg)	29	94.64	223.05	70.07	0.256
	30	94.6	222.4	69.86	0.257
	28	94.71	222.8	70.02	0.257
ivo/btdc(deg)	30	94.64	223.05	70.07	0.256
	31	94.93	223.63	70.26	0.257
	32	95.26	223.62	70.25	0.258
ivc/abdc(deg)	29	94.93	223.63	70.26	0.257
	30	95.31	224.05	70.39	0.257
	31	96.25	226.22	71.07	0.257
	32	96.08	225.93	70.98	0.257
evo/bbdc(deg)	36	96.25	226.22	71.07	0.257
	37	96.26	226.35	71.11	0.257
	38	96.24	226.26	71.08	0.257
evc/atdc(deg)	29	96.26	226.35	71.11	0.257
	30	96.67	226.38	71.12	0.257
	31	96.24	226.37	71.12	0.257
ivl(mm)	13.5	96.67	226.38	71.12	0.257
	14	96.27	226.41	71.13	0.257
	13	96.18	226.3	71.1	0.257
evl(mm)	13.5	96.67	226.38	71.12	0.257
	14	96.21	226.42	71.13	0.257
	13	96.17	226.37	71.12	0.257

3500 rpm test result					
	degree	VE(%)	Tb(Nm)	Pb(Kw)	bsfc(g/Kwhr)
ivo/btdc(deg)	31	86.34	197.6	72.43	0.264
	33	86.33	197.52	72.39	0.264
	35	86.22	197.31	72.33	0.264
	29	86.14	197.03	72.21	0.264
ivc/abdc(deg)	31	86.34	197.6	72.43	0.264
	33	86.57	198.52	72.77	0.263
	35	86.62	198.57	72.78	0.263
	37	86.82	198.99	72.94	0.264
evo/bbdc(deg)	37	86.62	198.57	72.78	0.263
	39	86.56	198.51	72.76	0.263
	35	86.7	198.84	72.88	0.263
	33	86.76	198.8	72.87	0.264
evc/atdc(deg)	30	86.7	198.84	72.88	0.263

	32	86.3	197.66	72.45	0.264
	28	87.06	199.69	73.19	0.263
	26	87.39	200.5	73.49	0.263
	24	87.7	201.26	73.76	0.263
	22	87.9	201.61	73.89	0.264
ivo/btdc(deg)	31	87.7	201.26	73.76	0.263
	32	87.7	201.49	73.85	0.263
	33	87.75	201.5	73.85	0.263
	34	87.82	201.6	73.89	0.263
	35	87.86	201.88	74	0.264
ivc/abdc(deg)	35	87.82	201.6	73.89	0.263
	37	88.04	202.14	74.09	0.263
	39	88.5	203.7	74.66	0.263
	41	88.71	204.21	74.8	0.262
	43	88.7	203.96	74.7	0.263
evo/bbdc(deg)	35	88.71	204.21	74.85	0.262
	37	88.59	203.94	74.76	0.263
	33	88.81	204.35	74.9	0.263
	31	88.97	204.61	75	0.263
evc/atdc(deg)	24	88.71	204.21	74.85	0.262
	25	88.56	203.7	74.66	0.262
	23	88.82	204.46	74.94	0.263
ivl(mm)	13	88.71	204.21	74.85	0.262
	13.5	88.74	204.17	74.84	0.263
	12.5	88.65	204	74.77	0.263
evl(mm)	13	88.71	204.21	74.85	0.262
	13.5	88.67	204.05	74.79	0.263
	12.5	88.73	204.23	74.85	0.263

4000 rpm test result					
	degree	VE(%)	Tb(Nm)	Pb(Kw)	bsfc(g/Kwhr)
ivo/btdc(deg)	35	85.93	192.58	80.67	0.269
	37	85.47	191.71	80.3	0.269
	33	86.26	193.25	80.95	0.269
	31	86.52	194.02	81.27	0.269
	29	87.47	197.07	82.55	0.268
	27	87.83	197.6	82.77	0.269
ivc/abdc(deg)	27	87.47	197.07	82.55	0.268
	29	87.73	197.38	82.68	0.269
	31	87.39	196.21	82.19	0.269
evo/bbdc(deg)	38	87.73	197.38	83.68	0.269

	36	88.12	198.21	83.03	0.269
	34	88.32	199.01	83.36	0.268
	32	88.72	199.93	83.75	0.268
	30	89.26	201.15	84.26	0.268
	28	89.74	201.8	84.53	0.269
evc/atdc(deg)	30	89.26	201.15	84.26	0.268
	32	88.85	200.04	83.79	0.268
	28	89.55	201.98	84.61	0.268
	26	89.81	202.33	84.76	0.268
	24	89.93	203.03	85.05	0.268
	22	90.14	203.45	85.23	0.268
	20	90.05	203.51	85.25	0.268
ivo/btdc(deg)	29	90.14	203.45	85.23	0.268
	30	90.09	203.4	85.2	0.268
	28	90.08	203.81	85.11	0.268
ivc/abdc(deg)	29	90.14	203.45	85.23	0.268
	30	89.98	203.18	85.11	0.268
	28	90.2	203.66	85.31	0.268
	27	90.43	204	85.45	0.268
	26	90.54	204.77	85.78	0.267
	25	90.68	204.95	85.84	0.268
evo/bbdc(deg)	30	90.54	204.77	85.78	0.267
	31	90.39	204.28	85.58	0.268
	29	90.7	204.91	85.83	0.268
evc/atdc(deg)	22	90.54	204.77	85.78	0.267
	23	90.46	204.86	85.82	0.267
	21	90.56	204.8	85.79	0.267
	20	90.51	204.7	85.75	0.267
ivl(mm)	13	90.56	204.8	85.79	0.267
	13.5	90.73	204.96	85.85	0.268
	12.5	90.6	204.7	85.75	0.268
evl(mm)	13	90.56	204.8	85.79	0.267
	13.5	50.58	204.61	85.7	0.268

4500 rpm test result					
	degree	VE(%)	Tb(Nm)	Pb(Kw)	bsfc(g/Kwhr)
ivo/btdc(deg)	35	89.32	196.84	92.76	0.274
	37	89.36	197	92.83	0.274
	39	89.38	197.2	92.93	0.274
	41	89.5	197.33	92.99	0.274
	43	89.6	197.98	93.3	0.274

	45	89.15	196.25	92.49	0.274
ivc/abdc(deg)	35	89.6	197.98	93.3	0.274
	37	89.29	197.91	92.79	0.274
	33	89.23	197.95	92.81	0.274
evo/bbdc(deg)	40	89.6	197.98	93.3	0.274
	42	89.35	196.93	92.8	0.274
	38	89.68	198.25	93.43	0.273
	36	89.09	196.36	92.53	0.274
evc/atdc(deg)	30	89.68	198.25	93.43	0.273
	32	89.51	197.52	93.08	0.274
	28	89.59	197.26	92.96	0.274
ivo/btdc(deg)	43	89.6	198.25	93.43	0.273
	44	89.01	196.12	92.42	0.274
	42	89.23	196.46	92.56	0.274
ivc/abdc(deg)	35	89.6	198.25	93.43	0.273
	36	89.83	198.38	93.49	0.274
	37	89.21	196.46	92.58	0.274
evo/bbdc(deg)	36	89.6	198.25	93.43	0.273
	37	89.14	196.55	92.62	0.274
	35	89.06	195.86	92.3	0.275
evc/atdc(deg)	30	89.6	198.25	93.43	0.273
	28	89.59	197.26	92.96	0.274
	26	90.29	199.77	94.14	0.273
	24	90.59	200.44	94.46	0.273
	22	90.8	201.2	94.82	0.273
	21	92.15	203.62	95.9	0.274
ivl(mm)	11	90.8	201.1	94.82	0.273
	13	90.94	201.19	94.81	0.273
	13.5	90.95	201.1	94.76	0.273
	14	90.91	201.26	94.26	0.273
	14.5	90.92	201.22	94.82	0.273
evl(mm)	11	90.91	201.26	94.26	0.273
	13.5	90.7	200.4	94.44	0.274
	13	90.74	200.59	94.52	0.273
	12	30.77	200.43	94.45	0.274

5000 rpm test result					
	degree	VE(%)	Tb(Nm)	Pb(Kw)	bsfc(g/Kwhr)
ivo/btdc(deg)	40	90.91	196.91	103.1	0.279
	38	91.13	197.29	103.29	0.279
	36	91.84	199.09	104.24	0.279

	34	91.58	198.38	103.88	0.279
ivc/abdc(deg)	35	91.84	199.09	104.24	0.279
	37	92	199.31	104.35	0.279
	39	92.29	199.33	104.38	0.278
evo/bbdc(deg)	36	92	199.31	104.35	0.279
	38	92.13	199.98	104.71	0.279
	40	92.39	200.13	104.79	0.279
	42	92.35	200.76	105.12	0.278
	44	92.46	201.2	105.35	0.278
	46	92.82	201.75	105.64	0.277
	48	92.58	201.9	105.71	0.277
	50	92.57	201.6	105.56	0.277
evc/atdc(deg)	25	92.58	201.9	105.71	0.277
	27	92.13	201.01	105.26	0.277
	23	92.86	203.35	106.47	0.276
	21	93.09	203.56	106.58	0.276
	19	93.33	203.75	106.69	0.277
ivo/btdc(deg)	36	93.09	203.56	106.58	0.276
	37	93.94	203.33	106.47	0.276
	38	92.85	203.09	106.34	0.276
ivc/abdc(deg)	37	93.94	203.33	106.47	0.276
	38	93.13	203.25	106.43	0.277
	36	93.88	203.01	106.3	0.277
evo/bbdc(deg)	48	93.94	203.33	106.47	0.276
	49	93.03	203.01	106.29	0.277
	47	92.92	202.9	106.24	0.277
evc/atdc(deg)	21	93.94	203.33	106.47	0.276
	22	92.82	202.52	106.04	0.277
	20	92.19	203.12	106.35	0.277
ivl(mm)	14	93.94	203.33	106.47	0.276
	15	93.12	202.16	106.37	0.277
	14.5	93.14	202.97	106.28	0.277
	13.5	93.06	202.83	106.2	0.277
evl(mm)	13	93.94	203.33	106.47	0.276
	13.5	92.98	202.86	106.22	0.277
	12.5	93.08	202.83	106.2	0.277

5500 rpm test result					
	degree	VE(%)	Tb(Nm)	Pb(Kw)	bsfc(g/Kwhr)
ivo/btdc(deg)	40	91	191.86	110.51	0.286
	42	90.75	191.35	110.21	0.286

	38	91.35	192.66	110.97	0.286
	36	91.52	193.3	111.33	0.286
	34	91.56	193.34	111.36	0.286
	32	91.67	193.62	111.52	0.286
	30	91.67	193.61	111.51	0.286
ivc/abdc(deg)	37	91.67	193.62	111.52	0.286
	39	92.1	194.63	112.1	0.286
	41	92.52	195.58	113.65	0.286
	45	92.88	196.85	113.38	0.285
	47	92.98	196.93	113.43	0.285
	49	93.04	197.04	113.49	0.285
	51	93.05	196.97	113.45	0.285
evo/bbdc(deg)	48	93.04	197.04	113.49	0.285
	50	93.06	197.42	113.71	0.285
	52	93.08	197.69	113.86	0.285
	54	93.14	197.79	113.92	0.285
	56	93.16	198.29	114.21	0.284
	58	93.17	198.25	114.18	0.284
evc/atdc(deg)	30	93.16	198.29	114.21	0.284
	28	93.31	198.42	114.29	0.284
	26	93.37	198.68	114.44	0.284
	24	93.41	198.45	114.3	0.284
ivo/btdc(deg)	32	93.37	198.68	114.44	0.284
	33	93.35	198.75	114.47	0.284
	34	93.31	198.09	114.09	0.285
	31	93.42	198.3	114.21	0.285
ivc/abdc(deg)	49	93.37	198.68	114.44	0.284
	50	93.39	198.65	114.42	0.284
	51	93.41	198.44	114.29	0.285
evo/bbdc(deg)	56	93.37	198.68	114.44	0.284
	57	93.38	198.34	114.23	0.285
	55	93.4	198.57	114.38	0.284
	54	93.31	198.18	114.14	0.285
evc/atdc(deg)	26	93.4	198.57	114.38	0.284
	27	93.34	197.92	114	0.285
	25	93.401	198.52	114.34	0.284
	24	93.402	198.45	114.3	0.285
ivl(mm)	14	93.4	198.57	114.38	0.284
	14.5	93.405	198.53	114.35	0.284
	15	93.43	198.7	114.44	0.284
	15.5	93.48	198.48	114.32	0.285

evl(mm)	12.5	93.43	198.7	114.44	0.284
	13	93.47	198.8	114.5	0.284
	13.5	93.51	198.41	114.28	0.285

6000 rpm test result					
	degree	VE(%)	Tb(Nm)	Pb(Kw)	bsfc(g/Kwhr)
ivo/btdc(deg)	32	92.82	192.59	121.01	0.291
	30	93.04	193.34	121.48	0.291
	28	93.22	193.94	121.85	0.291
	26	92.47	192.13	120.72	0.291
ivc/abdc(deg)	49	93.22	193.94	121.85	0.291
	51	92.73	192.8	121.14	0.291
	53	92.95	193.03	121.28	0.291
	55	94.3	196.49	123.46	0.29
	57	94.5	197.15	123.85	0.29
	59	94.65	197.94	124.37	0.289
	60	94.72	197.68	124.21	0.29
evo/bbdc(deg)	55	94.65	197.94	124.37	0.289
	57	94.65	197.85	124.32	0.289
	59	94.68	197.98	124.4	0.289
	61	94.683	198.32	124.61	0.288
	63	94.67	198.42	124.67	0.288
	65	94.65	198.3	124.6	0.288
evc/atdc(deg)	26	94.67	198.42	124.67	0.288
	28	94.56	197.66	124.2	0.289
	24	94.71	198.51	124.73	0.288
	22	94.76	198.82	124.92	0.288
	20	94.68	198.37	124.64	0.288
ivo/btdc(deg)	28	94.76	198.82	124.92	0.288
	29	94.51	198.18	124.52	0.288
	27	94.81	198.36	124.63	0.289
ivc/abdc(deg)	59	94.76	198.82	124.92	0.288
	60	94.76	198.61	124.8	0.288
	58	94.68	198.03	124.43	0.289
evo/bbdc(deg)	63	94.76	198.82	124.92	0.288
	64	94.72	198.53	124.74	0.288
	62	94.62	198.38	124.65	0.288
evc/atdc(deg)	22	94.76	198.82	124.92	0.288
	23	94.73	198.33	124.62	0.289
	21	94.71	198.64	124.82	0.288
ivl(mm)	14	94.76	198.28	124.92	0.288

	14.5	94.77	198.64	124.82	0.288
	15	94.81	198.28	124.58	0.289
evl(mm)	13	94.77	198.64	124.82	0.288
	13.5	94.81	198.91	124.98	0.288
	14	94.85	198.76	124.89	0.288

6500 rpm test result					
	degree	VE(%)	Tb(Nm)	Pb(Kw)	bsfc(g/Kwhr)
ivo/btdc(deg)	35	84.66	166.87	113.59	0.307
	33	85.05	167.55	114.05	0.307
	31	85.38	168.62	114.78	0.306
	29	84.98	167.84	114.24	0.306
	27	85.89	170.16	115.82	0.305
	25	86.19	171.01	116.4	0.305
	23	85.72	170.02	115.73	0.305
ivc/abdc(deg)	50	86.19	171.01	116.4	0.305
	52	86.06	170.63	116.14	0.305
	54	86.78	172.01	117.09	0.305
	56	87.9	175.23	119.27	0.303
	57	88.2	175.04	119.83	0.303
	59	88.63	176.72	120.3	0.303
	61	88.42	176.41	120.07	0.303
	63	89.44	179.1	121.91	0.302
	65	89.71	179.63	122.28	0.302
	67	89.92	180.23	122.68	0.302
	70	90.04	180.47	122.85	0.302
	72	90.09	180.65	122.97	0.301
	75	90.03	180.38	122.78	0.302
evo/bbdc(deg)	55	90.09	180.65	122.97	0.301
	57	90.12	180.6	122.93	0.302
	59	90.19	181.44	123.5	0.3
	61	90.23	181.6	123.61	0.3
	63	90.15	181.87	123.79	0.299
	65	90.17	181.58	123.61	0.3
	67	90.15	181.95	123.85	0.299
evc/atdc(deg)	35	90.23	181.6	123.61	0.3
	33	90.53	182.22	124.04	0.3
	31	90.76	182.94	124.53	0.3
	29	90.99	183.61	124.98	0.299
	27	91.2	183.92	125.19	0.3
	25	91.34	184.41	125.52	0.299

	23	91.46	184.72	125.73	0.299
	21	91.56	185.22	126.08	0.299
	19	91.68	185.15	126.03	0.299
	17	91.66	185.08	125.99	0.299
ivo/btdc(deg)	25	91.68	185.15	126.03	0.299
	26	91.56	185.07	125.98	0.299
	24	91.73	185.57	126.32	0.299
	23	91.8	185.73	126.43	0.299
	21	91.92	185.68	126.39	0.299
	20	91.5	186.38	126.87	0.298
	19	92	186.13	126.69	0.299
ivc/abdc(deg)	72	91.95	186.38	126.87	0.298
	71	91.98	186.14	126.71	0.299
	70	91.96	186.24	126.77	0.299
	73	91.9	185.87	126.52	0.299
evo/bbdc(deg)	61	91.95	186.38	126.87	0.298
	60	91.92	185.92	126.56	0.299
	62	91.97	186.4	126.88	0.298
	63	91.98	185.73	126.43	0.299
evc/atdc(deg)	19	91.97	184.4	126.88	0.298
	20	91.88	185.88	126.53	0.299
	18	91.95	186.37	126.87	0.298
ivl(mm)	14.5	91.97	186.4	126.88	0.298
	15	91.96	185.22	126.76	0.299
	14	91.91	186.36	126.86	0.298
evl(mm)	14	91.97	186.4	126.88	0.298
	14.5	91.954	186.26	126.78	0.298
	13.5	91.95	185.86	126.52	0.299
	15	91.95	185.64	126.37	0.299

7000 rpm test result					
	degree	VE(%)	Tb(Nm)	Pb(Kw)	bsfc(g/Kwhr)
ivo/btdc(deg)	20	88.56	170.65	125.12	0.313
	22	88.54	170.6	125.06	0.314
	18	88.62	171.08	125.41	0.313
	16	88.65	171.21	125.5	0.313
	14	88.64	171.01	125.35	0.313
ivc/abdc(deg)	72	88.65	171.21	125.5	0.313
	70	88.46	170.7	125.14	0.313
	74	88.77	171.29	125.57	0.313
	76	88.79	171.13	125.45	0.313

	78	88.78	171.38	125.62	0.313
evo/bbdc(deg)	62	88.7	171.13	125.45	0.313
	60	88.82	170.47	125.33	0.314
	64	88.76	171.62	125.81	0.313
	58	88.8	170.82	125.22	0.314
evc/atdc(deg)	19	88.82	170.97	125.33	0.314
	21	88.85	170.98	125.34	0.314
	23	88.79	171.33	125.6	0.313
ivo/btdc(deg)	16	88.85	170.98	125.34	0.314
	17	88.82	170.91	125.29	0.314
	15	88.82	171.28	125.28	0.313
ivc/abdc(deg)	76	88.85	170.98	125.34	0.314
	75	88.8	170.04	125.37	0.314
	77	88.86	171.28	125.56	0.313
	78	88.8	171.23	125.52	0.313
evo/bbdc(deg)	60	88.85	170.98	125.34	0.314
	61	88.83	171.35	125.61	0.313
	62	88.84	171.59	125.79	0.313
	63	88.81	171.65	125.83	0.313
	59	88.86	171.06	125.4	0.314
	58	88.81	170.79	125.2	0.314
evc/atdc(deg)	21	88.86	171.06	125.4	0.314
	22	88.84	171.02	125.37	0.314
	20	88.84	171.06	152.4	0.314
ivl(mm)	11	88.86	171.06	125.4	0.314
	13	89.07	171.38	125.62	0.314
	14	89.15	171.52	125.74	0.314
	15	89.14	171.44	125.67	0.314
	14.5	89.15	171.51	125.73	0.314
evl(mm)	11	89.15	171.51	125.73	0.314
	13	89.2	171.92	126.02	0.313
	14	89.18	171.95	126.05	0.313
	13.5	89.17	172.22	126.24	0.313

Appendix A2 Error values for second order polynomial curve fittings

rpm	ivo	ivo-poly	error	ivc	ivc-poly	error	evo	evo-poly	error	evc	evc-poly	error	ivl	ivl-poly	error	evl	evl-poly	error
500	9	10.46	0.163	8	7.82	0.022	24	24.34	0.014	5	7.14	0.428	11	11.74	0.067	11	11.19	0.017
1000	19	17.21	0.094	9	9.72	0.080	24	25.46	0.061	12	10.59	0.117	12.5	12.11	0.031	11	11.62	0.057
1500	26	22.96	0.117	11	12.12	0.102	28	26.94	0.038	16	13.64	0.147	13	12.46	0.041	12.5	12.01	0.039
2000	28	27.71	0.010	9	15.02	0.669	28	28.76	0.027	14	16.29	0.164	13	12.79	0.016	13	12.35	0.050
2500	28	31.46	0.124	21	18.42	0.123	36	30.94	0.141	20	18.54	0.073	13	13.10	0.008	12.5	12.65	0.012
3000	31	34.21	0.104	31	22.32	0.280	37	33.46	0.096	19	20.39	0.073	13.5	13.39	0.008	13.5	12.90	0.044
3500	34	35.96	0.058	41	26.72	0.348	35	36.34	0.038	24	21.84	0.090	13	13.66	0.051	13	13.11	0.009
4000	29	36.71	0.266	26	31.62	0.216	30	39.56	0.319	21	22.89	0.090	13	13.91	0.070	13	13.27	0.021
4500	42	36.46	0.132	35	37.02	0.058	36	43.14	0.198	22	23.54	0.070	14	14.14	0.010	13	13.39	0.030
5000	37	35.21	0.048	37	42.92	0.160	48	47.06	0.020	21	23.79	0.133	14	14.35	0.025	13	13.46	0.036
5500	32	32.96	0.030	49	49.32	0.007	55	51.34	0.067	26	23.64	0.091	15	14.54	0.031	13	13.49	0.038
6000	28	29.71	0.061	59	56.22	0.047	63	55.96	0.112	22	23.09	0.050	14.5	14.71	0.015	13.5	13.47	0.002
6500	20	25.46	0.273	72	63.62	0.116	62	60.94	0.017	19	22.14	0.165	14.5	14.86	0.025	14	13.41	0.042
7000	16	20.21	0.263	76	71.52	0.059	59	66.26	0.123	21	20.79	0.010	14.5	14.99	0.034	13	13.30	0.023
average			0.124			0.163			0.091			0.122			0.031			0.030

Appendix A3Error values for linear data fittings

rpm	ivo	ivo-linear	error	ivc	ivc-linear	error	evo	evo-linear	error	evc	evc-linear	error	ivl	ivl-linear	error	evl	evl-linear	error
500	9	15.00	0.667	8	6.00	0.250	24	24.00	0.000	5	10.00	1.000	11	12.00	0.091	11	11.50	0.045
1000	19	18.13	0.046	9	10.00	0.111	24	25.71	0.071	12	11.86	0.012	12.5	12.23	0.022	11	11.69	0.063
1500	26	21.25	0.183	11	14.00	0.273	28	27.43	0.020	16	13.71	0.143	13	12.46	0.041	12.5	11.88	0.049
2000	28	24.38	0.129	9	18.00	1.000	28	29.14	0.041	14	15.57	0.112	13	12.69	0.024	13	12.08	0.071
2500	28	27.50	0.018	21	22.00	0.048	36	30.86	0.143	20	17.43	0.129	13	12.92	0.006	12.5	12.27	0.018
3000	31	30.63	0.012	31	26.00	0.161	37	32.57	0.120	19	19.29	0.015	13.5	13.15	0.026	13.5	12.46	0.077
3500	34	33.75	0.007	41	30.00	0.268	35	34.29	0.020	24	21.14	0.119	13	13.38	0.030	13	12.65	0.027
4000	29	36.88	0.272	26	34.00	0.308	30	36.00	0.200	21	23.00	0.095	13	13.61	0.047	13	12.85	0.012
4500	42	40.00	0.048	35	38.00	0.086	36	40.83	0.134	22	22.67	0.030	14	13.85	0.011	13	13.04	0.003
5000	37	35.40	0.043	37	45.40	0.227	48	45.67	0.049	21	22.33	0.064	14	14.08	0.005	13	13.23	0.018
5500	32	30.80	0.038	49	52.80	0.078	55	50.50	0.082	26	22.00	0.154	15	14.31	0.046	13	13.42	0.033
6000	28	26.20	0.064	59	60.20	0.020	63	55.33	0.122	22	21.67	0.015	14.5	14.54	0.003	13.5	13.62	0.009
6500	20	21.60	0.080	72	67.60	0.061	62	60.17	0.030	19	21.34	0.123	14.5	14.77	0.019	14	13.81	0.014
7000	16	17.00	0.063	76	75.00	0.013	59	65.00	0.102	21	21.00	0.000	14.5	15.00	0.034	13	14.00	0.077
average			0.119			0.207			0.081			0.144			0.029			0.037

Appendix A4 Volumetric efficiency (%) table for all optimum cam profiles

Engine RPM	C1	C2	C3	C4	C5	C6	C7	C8	C9	C10	C11	C12	C13	C14
500	79.423	76.789	72.351	72.612	67.236	69.232	69.956	68.02	83.961	83.879	81.254	78.356	71.188	66.963
1000	81.293	81.017	80.175	80.714	79.45	79.974	79.931	79.077	88.566	88.683	85.529	80.081	71.35	68.454
1500	83.311	83.671	84.127	84.58	83.647	84.248	83.017	83.454	87.68	87.099	83.78	79.358	72.899	70.533
2000	92.65	94.709	97.975	98.375	101.269	100.48	95.054	97.763	101.099	97.664	92.477	84.941	76.117	73.483
2500	94.9	96.216	98.602	98.197	103.68	104.938	101.606	101.237	104.807	102.273	98.874	92.604	84.52	81.926
3000	86.896	87.743	89.265	88.925	90.868	96.275	99.029	93.352	98.96	96.139	96.575	94.305	89.361	87.62
3500	84.774	84.888	85.167	84.977	85.43	86.283	88.671	86.953	88.309	87.395	87.034	86.128	85.904	84.894
4000	89.847	91.083	91.713	91.189	89.799	86.998	86.688	90.583	86.184	84.537	83.025	83.074	82.937	82.462
4500	87.157	88.541	89.267	88.552	89.801	90.166	90.883	91.747	91.084	90.606	86.095	83.944	80.994	79.655
5000	83.258	84.347	85.287	84.286	87.879	90.382	92.011	90.115	90.957	92.948	93.476	93.27	89.398	87.596
5500	80.591	82.041	83.194	82.215	86.017	89.871	92.798	88.824	91.411	91.917	93.512	93.079	90.366	88.946
6000	74.369	76.111	78.054	76.869	82.588	87.114	90.922	85.268	87.969	88.832	92.988	94.824	94.767	94.272
6500	67.159	70.852	72.862	71.429	75.674	79.382	84.233	79.097	80.869	82.112	86.828	90.351	91.954	91.861
7000	62.105	66.634	68.713	67.293	70.685	74.568	80.158	74.799	76.641	77.746	82.949	86.845	89.174	89.198

Appendix A5 BSFC (kg/kw.hr) table for all optimum cam profiles

Engine RPM	C1	C2	C3	C4	C5	C6	C7	C8	C9	C10	C11	C12	C13	C14
500	0.316	0.316	0.318	0.318	0.32	0.321	0.321	0.319	0.346	0.37	0.378	0.369	0.347	0.342
1000	0.273	0.273	0.273	0.273	0.274	0.276	0.276	0.274	0.29	0.293	0.295	0.293	0.288	0.287
1500	0.254	0.254	0.255	0.255	0.255	0.257	0.259	0.255	0.263	0.264	0.266	0.266	0.266	0.266
2000	0.25	0.25	0.252	0.252	0.258	0.262	0.259	0.254	0.265	0.261	0.263	0.263	0.265	0.265
2500	0.251	0.251	0.252	0.252	0.257	0.261	0.259	0.254	0.262	0.259	0.26	0.259	0.26	0.26
3000	0.26	0.26	0.259	0.259	0.257	0.257	0.257	0.257	0.26	0.257	0.257	0.259	0.26	0.26
3500	0.266	0.266	0.265	0.265	0.265	0.265	0.263	0.264	0.263	0.264	0.265	0.267	0.266	0.266
4000	0.268	0.268	0.267	0.266	0.267	0.269	0.269	0.266	0.269	0.271	0.274	0.274	0.275	0.274
4500	0.277	0.276	0.276	0.276	0.274	0.274	0.273	0.273	0.273	0.273	0.277	0.282	0.283	0.284
5000	0.287	0.286	0.285	0.285	0.282	0.28	0.279	0.281	0.28	0.276	0.277	0.277	0.28	0.282
5500	0.3	0.299	0.296	0.297	0.292	0.29	0.289	0.292	0.289	0.286	0.285	0.285	0.287	0.288
6000	0.319	0.318	0.314	0.315	0.307	0.301	0.298	0.306	0.3	0.296	0.291	0.288	0.288	0.289
6500	0.341	0.343	0.333	0.334	0.322	0.317	0.314	0.319	0.317	0.31	0.304	0.3	0.298	0.299
7000	0.414	0.435	0.406	0.409	0.359	0.343	0.333	0.347	0.336	0.33	0.325	0.314	0.313	0.314

Appendix A6 Brake Torque (Nm) table for all optimum cam profiles

Engine RPM	C1	C2	C3	C4	C5	C6	C7	C8	C9	C10	C11	C12	C13	C14
500	151.62	146.65	137.75	138.02	127.08	130.36	131.66	128.94	154.17	147.84	143.11	138.55	124.02	118.42
1000	179.92	179.31	177.26	178.4	174.96	175.57	175.02	174.64	184.59	175.2	158.74	165.25	149.66	144.11
1500	197.92	198.84	199.66	200.49	198.04	197.9	194.11	197.39	201.6	190.63	163.8	180.05	165.37	160.35
2000	224.14	229.12	235.19	235.87	237.16	232.2	221.85	232.1	230.83	212.35	166.18	194.74	173.72	167.97
2500	228.9	231.57	236.55	234.81	243.68	243.04	237.72	240.96	241.44	229.87	169.83	216.36	196.34	190.6
3000	202.26	204.36	208.51	207.66	213.84	226.15	232.35	219.67	229.92	226.56	177.46	220.08	207.35	203.24
3500	192.5	192.74	193.99	193.56	195.09	197.22	203.97	199.17	202.98	198.55	183.13	195.02	194.89	192.76
4000	202.22	205.31	207.55	206.64	203.1	195.1	194.22	205.28	193.34	183.36	180.28	182.97	182.3	181.76
4500	189.73	193.65	195.93	194.28	198.29	199.2	201.05	203.01	201.94	187.93	183.81	180.13	172.47	169.6
5000	175.13	178.2	181.03	179	188.65	195.05	199.41	193.72	196.63	204.11	192.51	203.1	192.57	187.79
5500	162.52	165.67	169.82	167.32	177.84	187.25	194.18	183.82	191.33	198.63	190.09	197.53	190.22	186.74
6000	140.84	144.82	150.21	147.45	162.73	174.7	184.41	168.31	177.23	193.43	190.95	198.94	198.52	197.05
6500	118.99	124.88	132.27	129.24	142.18	151.38	162.06	149.67	154.16	172.8	172.79	182.17	186.3	185.71
7000	90.76	92.63	102.13	99.37	118.8	131.42	145.18	130.12	137.82	154.41	155.2	166.74	172.34	171.76

Appendix A7 Brake Power (KW) table for all optimum cam profiles

Engine RPM	C1	C2	C3	C4	C5	C6	C7	C8	C9	C10	C11	C12	C13	C14
500	7.94	7.68	7.21	7.23	6.65	6.82	6.9	6.75	8.08	8.1	7.74	7.26	6.5	6.2
1000	18.84	18.78	18.56	18.68	18.32	18.39	18.33	18.29	19.33	19.15	18.34	17.31	15.67	15.09
1500	31.09	31.24	31.36	31.49	31.11	31.09	30.49	31.01	31.67	31.33	29.95	28.28	25.98	25.19
2000	46.95	47.99	49.26	49.4	49.67	48.63	46.46	48.61	48.34	47.37	44.47	40.79	36.38	35.18
2500	59.92	60.63	61.93	61.48	63.79	63.63	62.24	63.08	63.21	62.47	60.18	56.64	51.4	49.9
3000	63.55	64.2	65.51	65.23	67.18	71.05	73	69.01	72.24	70.92	71.18	69.14	65.14	63.85
3500	70.56	70.65	71.1	70.95	71.51	72.29	74.76	73	74.4	73.31	72.77	71.48	71.43	70.65
4000	84.71	86	86.94	86.55	85.08	81.73	81.36	85.99	80.99	78.98	76.81	76.64	76.37	76.14
4500	89.41	91.25	92.33	91.55	93.44	93.88	94.75	95.67	95.17	94.41	88.56	84.88	81.27	79.92
5000	91.71	93.31	94.79	93.73	98.78	102.13	104.41	101.43	102.96	106.48	106.87	106.35	100.83	98.33
5500	93.61	95.42	97.81	96.37	102.43	107.85	111.84	105.88	110.2	111.99	114.41	113.77	109.56	107.55
6000	88.5	90.99	94.38	92.65	102.25	109.77	115.87	105.76	111.36	114.1	121.54	125	124.73	123.81
6500	80.99	85.01	90.04	87.97	96.78	103.04	110.31	101.88	104.93	108.91	117.62	124	126.81	126.4
7000	66.54	67.9	74.87	72.84	87.08	96.34	106.43	95.38	101.03	104.48	113.19	122.23	126.33	125.9

Appendix B Prototype Manufacturing

Appendix B1 Cylinder Head made from wood

Appendix B2 Cam profiles cut out of 2mm thick plastic

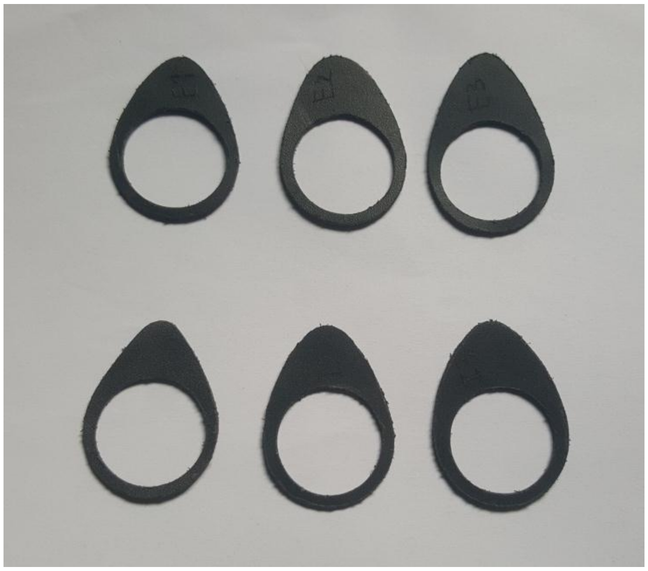

Appendix B3 Cam profiles arranged on a wooden shaft

Appendix B4 Cement formed between cam profiles